Technical Report Documentation Page

1. Report No.	2. Government Accession No.	3. Recipient's Catalog No.
FHWA/TX-04/0-1405-8		

4. Title and Subtitle	5. Report Date
Long-Term Post-Tensioned Column Exposure Test Specimens: Final Evaluation	October 2003
	6. Performing Organization Code
7. Author(s)	8. Performing Organization Report No.
R. M. Salas, J. S. West, A. J. Schokker, J. E. Breen, and M. E. Kreger	Research Report 0-1405-8
9. Performing Organization Name and Address	10. Work Unit No. (TRAIS)
Center for Transportation Research The University of Texas at Austin 3208 Red River, Suite 200 Austin, TX 78705-2650	11. Contract or Grant No. Research Study 0-1405
12. Sponsoring Agency Name and Address	13. Type of Report and Period Covered
Texas Department of Transportation Research and Technology Implementation Office P.O. Box 5080 Austin, TX 78763-5080	Research Report (9/93-8/03)
	14. Sponsoring Agency Code

15. Supplementary Notes

Project conducted in cooperation with the U.S. Department of Transportation, Federal Highway Administration, and the Texas Department of Transportation.

16. Abstract

Post-tensioned concrete piers or columns may be exposed to very severe environments affecting their long-term durability. Two main exposure conditions are of special interest: partially submerged structures in sea water and structures exposed to deicing salts. The durability study of post-tensioned columns or vertical concrete elements under these conditions has unique characteristics. In order to provide detailed observations to improve the durability design of columns under these exposure conditions, a research study was started with the dual intent to evaluate how to use post-tensioning to improve corrosion protection and how to protect the post-tensioning systems from corrosion damage.

This report is part of a comprehensive research program started in 1993, which has the objectives to examine the use of post-tensioning in bridge substructures, identify durability concerns and existing technology, develop and carry out an experimental testing program, and conclude with durability design guidelines. Three experimental programs were developed: A long-term macrocell corrosion test series, to investigate corrosion protection for internal tendons in precast segmental construction; a long-term beam corrosion test series, to examine the effects of post-tensioning on corrosion protection as affected by crack width; and, a long-term column corrosion test series, to examine corrosion protection in vertical elements.

This report documents the final evaluation, conclusions, recommendations and implementation measures from the long-term column exposure test specimens. A total of ten large-scale column specimens were designed, constructed and placed under exposure testing in July 1996. Comprehensive autopsies were performed in January 2003, after six and a half years of accelerated exposure.

After forensic examination, overall findings indicate negative durability effects due to the use of small concrete covers, galvanized steel ducts and rubber gaskets at the duct ends. Relying on epoxy and galvanized bar coating was also found inappropriate because of local attack. On the other hand, very positive effects were found with the use of fly ash concrete, post-tensioning through the column-foundation interface, sound epoxy filling at the joints and plastic ducts.

17. Key Words	18. Distribution Statement
corrosion, dry joints, epoxy joints, post-tensioned concrete columns, post-tensioning ducts, epoxy and galvanized bar coatings, fly ash concrete	No restrictions. This document is available to the public through the National Technical Information Service, Springfield, Virginia 22161.

19. Security Classif. (of report)	20. Security Classif. (of this page)	21. No. of pages	22. Price
Unclassified	Unclassified	113	

Form DOT F 1700.7 (8-72) Reproduction of completed page authorized

LONG-TERM POST-TENSIONED COLUMN EXPOSURE TEST SPECIMENS: FINAL EVALUATION

by

R. M. Salas, J. S. West, A. J. Schokker,
J. E. Breen, and M. E. Kreger

Research Report 0-1405-8

Research Project 0-1405

DURABILITY DESIGN OF POST-TENSIONED BRIDGE SUBSTRUCTURE ELEMENTS

conducted for the
Texas Department of Transportation

in cooperation with the
U.S. Department of Transportation
Federal Highway Administration

by the

CENTER FOR TRANSPORTATION RESEARCH
BUREAU OF ENGINEERING RESEARCH
THE UNIVERSITY OF TEXAS AT AUSTIN

October 2003

Research performed in cooperation with the Texas Department of Transportation and the U.S. Department of Transportation, Federal Highway Administration.

ACKNOWLEDGMENTS

We greatly appreciate the financial support from the Texas Department of Transportation that made this project possible. In particular, we would like to acknowledge the contributions of Rene Vignos who developed the initial concept of the test specimen and fabricated the specimens and the exposure testing devices. We are grateful for the active support of the project director, Bryan Hodges (TYL), and the support of program coordinator, Richard Wilkison, is also very much appreciated. We thank Project Monitoring Committee members, Gerald Lankes (CST), Ronnie VanPelt (BMT), and Tamer Ahmed (FHWA).

DISCLAIMER

J. E. Breen, P.E., TX #18479
M. E. Kreger, P.E., TX #65541

Research Supervisors

TABLE OF CONTENTS

LIST OF TABLES

LIST OF FIGURES

SUMMARY

Post-tensioned concrete piers or columns may be exposed to very severe environments affecting their long-term durability. Two main exposure conditions are of special interest: partially submerged structures in sea water and structures exposed to deicing salts. The durability study of post-tensioned columns or vertical concrete elements under these conditions has unique characteristics. In order to provide detailed observations to improve the durability design of columns under these exposure conditions, a research study was started with the dual intent to evaluate how to use post-tensioning to improve corrosion protection and how to protect the post-tensioning systems from corrosion damage.

This report is part of a comprehensive research program started in 1993, which has the objectives to examine the use of post-tensioning in bridge substructures, identify durability concerns and existing technology, develop and carry out an experimental testing program, and conclude with durability design guidelines. Three experimental programs were developed: A long-term macrocell corrosion test series, to investigate corrosion protection for internal tendons in precast segmental construction; a long-term beam corrosion test series, to examine the effects of post-tensioning on corrosion protection as affected by crack width; and, a long-term column corrosion test series, to examine corrosion protection in vertical elements.

This report documents the final evaluation, conclusions, recommendations and implementation measures from the long-term column exposure test specimens. A total of ten large-scale column specimens were designed, constructed and placed under exposure testing in July 1996. Comprehensive autopsies were performed in January 2003, after six and a half years of accelerated exposure.

After forensic examination, overall findings indicate negative durability effects due to the use of small concrete covers, galvanized steel ducts and rubber gaskets at the duct ends. Relying on epoxy and galvanized bar coating was also found inappropriate because of local attack. On the other hand, very positive effects were found with the use of fly ash concrete, post-tensioning through the column-foundation interface, sound epoxy filling at the joints and plastic ducts.

CHAPTER 1: INTRODUCTION

Post-tensioned concrete piers or columns may be exposed to very severe environments affecting their long-term durability. Two main exposure conditions are of special interest: partially submerged structures in sea water and structures exposed to deicing salts. The durability study of post-tensioned columns or vertical concrete elements under these conditions has unique characteristics. This report documents the procedures and results from long-term corrosion tests performed to large scale column specimens, and is a portion of the Texas Department of Transportation Research Project 0-1405: "Durability Design of Post-Tensioned Bridge Substructure Elements."

1.1 BRIDGE SUBSTRUCTURE DURABILITY

Columns or piers in sea water are exposed to a very severe environment. This is especially the case for columns in the tidal zone (region between low and high tides) with periodic wetting and drying. In addition, above the high tide zone, the "wicking effect" (or capillary rise) may take place, which combined with periodic splashing, provide the conditions for aggressive chloride exposure (see Figure 1.1) and subsequent corrosion damage (see Figure 1.2).

Bridge piers on columns and like members in parking garages or other structures, may be subject to deicing salts that are applied to roadways in cold (ice and snow) environments. Depending on the ability of the drainage systems to evacuate run off from the top slabs and decks, these chlorides combined with water may trickle down the structures along the concrete faces, providing unfavorable conditions of intermittent moisture and chlorides.

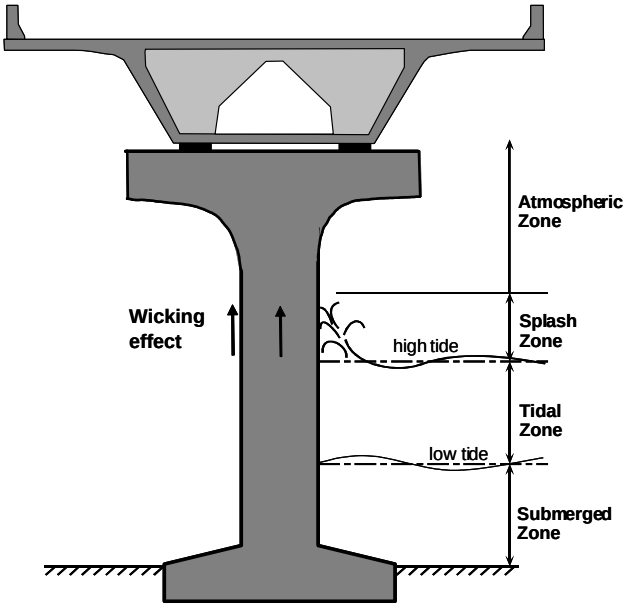

Figure 1.1 Exposure of Partially Submerged Column in Sea Water[1]

(a) Deicing Chemical Exposure "Attack from Above"

(b) Coastal Saltwater Exposure "Attack from Below"

Figure 1.2 Typical Corrosion Damage in Bridge Substructures[2]

1.2 PROBLEM STATEMENT

The research project 0-1405 is being performed at the Phil M. Ferguson Structural Engineering Laboratory and is sponsored by the Texas Department of Transportation and the Federal Highway Administration. The title of project involves two main aspects:

- Durability of Bridge Substructures, and
- Post-Tensioned Bridge Substructures.

The durability emphasis is in response to the deteriorating condition of bridge substructures in some areas of Texas. While considerable research and design effort has been given to bridge deck design to prevent corrosion damage, substructures had historically been more overlooked. Often superstructure drainage details result in substructures having a high exposure to aggressive agents such as, deicing salts, also substructures are often in direct contact with salt water and damaging soils.

The second aspect of the research is post-tensioned substructures. Relatively few post-tensioned substructures have been used in the past. There are many possible applications in bridge substructures where post-tensioning can provide structural and economical benefits, and can possibly improve durability. Post-tensioning is now being used in Texas bridge substructures, and it is reasonable to expect the use of post-tensioning to increase in the future as precasting of substructure components becomes more prevalent and as foundation sizes increase. This is expected, even though some problems have been encountered in post-tensioned bridges throughout the world.

The problem that bridge engineers face is that there are few comprehensive durability design guidelines for post-tensioned concrete structures. Durability design guidelines should provide information on how to identify possible durability problems, how to improve durability using post-tensioning, and how to ensure that the post-tensioning system does not introduce new durability problems.

A review of literature has indicated that while a few problems have been encountered in some bridges in Europe, Japan, and the U.S.A., damage has been limited to a very small percentage of post-tensioned bridges. In general, post-tensioning systems have been successfully used in bridge designs. However, as these bridges age and increase in cumulative exposure, more problems are being noted. New practices and materials are required to guarantee the safety and design life of these structures.

1.3 RESEARCH OBJECTIVES, SCOPE, AND REPORTS

1.3.1 Project Objectives

The overall research objectives for TXDOT Project 0-1405 are as follows:

1. To examine the use of post-tensioning in bridge substructures,
2. To identify durability concerns for bridge substructures in Texas,
3. To identify existing technology to ensure durability or improve durability,
4. To develop experimental testing programs to evaluate protection measures for improving the durability of post-tensioned bridge substructures, and
5. To develop durability design guidelines and recommendations for post-tensioned bridge substructures.

The specific research objectives for the large-scale column corrosion test series are as follows:

1. To investigate the effect of post-tensioning on concrete pier and column durability (corrosion protection) through precompression of the concrete and precompression of construction joints, and
2. To investigate the relative performance of various aspects of corrosion protection for post-tensioning, including concrete type, duct type, post-tensioning bar coatings and loading.

1.3.2 Project Scope

The subject of durability is extremely broad, and as a result a broad scope of research was developed for TXDOT Project 0-1405. Based on the project proposal and an initial review of relevant literature, the project scope and necessary work plan were defined. The main components of TXDOT Project 0-1405 are:

1. Extensive Literature Review
2. Survey of Existing Bridge Substructures Inspection Reports (BRINSAP)
3. Long-Term Corrosion Tests with Large-Scale Post-Tensioned Beam and Column Elements
4. Investigation of Corrosion Protection (near joints) for Internal Prestressing Tendons in Precast Segmental Bridges
5. Development of Improved Grouts for Post-Tensioning
6. Development of recommendations and design guidelines for durable bonded post-tensioned bridge substructures

Components 1 and 2 (literature review and survey of Brinsap report) were performed initially by West[2], Schokker[3], Koester[4] and Larosche[5] and findings up to 1998 were published in References 2 and 3. The literature review process was continued by Kotys[6] and Salas[1] and is published in References 6 and 1.

Component 3 was divided into Large Scale Beam Corrosion Tests and Large Scale Column Corrosion Tests. The beam tests were implemented in two phases: the first phase was implemented by West,[2] and exposure testing began in December 1997. The second phase was implemented by Schokker,[3] and exposure testing begun in December 1998. Comprehensive autopsies of around half of these specimens, at the end of their exposure testing period were performed in 2002 by Kotys[6] and Salas[1]. The column tests were started by Larosche[5] and West.[2] Column exposure testing began in July 1996. Full autopsies were performed by Salas[1] in 2003 and are reported herein.

Component 4 (corrosion protection at joints of segmental bridges) was developed and implemented by Vignos[7] under TxDOT Project 0-1264. This testing program was transferred to TxDOT Project 0-1405 in 1995 for long-term testing. Although this aspect of the research was developed under Project 0-1264 to address corrosion concerns for precast segmental bridge superstructures, the concepts and variables are equally applicable to precast segmental substructures, and the testing program fits well within the scope

of Project 0-1405. Half of the macrocell laboratory specimens were autopsied at four and a half years of exposure testing by West.[2] Final autopsies of the remaining specimens were performed by Kotys[6] and Salas,[1] and findings were reported in Reference 1.

Component 5 (Development of Improved Grouts for Post-Tensioning) was developed and implemented by Schokker[3] based on previous work published by Hamilton[8] and Koester[4]. The accelerated corrosion testing was performed and conclusions were drawn and published.[9, 3] Under this portion of the research, high-performance grouts for bonded post-tensioning were developed through a series of fresh property tests, accelerated corrosion tests, and large-scale field trials. These grouts have become widely used in practice.

Component 6 (Development of recommendations and design guidelines for durable bonded post-tensioned bridge substructures) refers to the most important implementation directed aspect of the research program. Interim design guidelines were developed and published by West and Schokker[10] based on research results up to 1999. Updated Guidelines based on final autopsy results from the macrocell, column, and beam tests are reported by Salas in Reference 1 and in CTR Report 1405-9.

The project scope is outlined in Figure 1.1. This figure shows the cooperative effort performed by all graduate research assistants during the length of the project. In Figure 1.1 the years in brackets show the actual or expected publication dates for each technical report, published under TxDOT Project 0-1405.

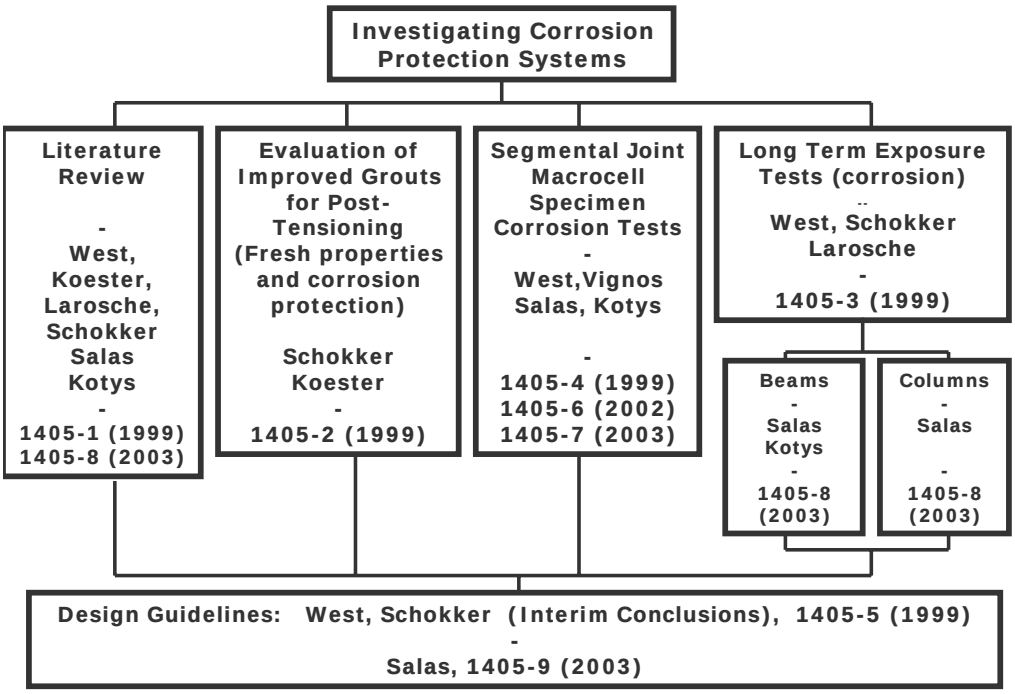

Figure 1.3 TxDOT Project 0-1405 Scope, Researchers and Technical Reports[1]

1.3.3 Project Reports

Nine reports are schedule to be developed from Project 0-1405 as listed in Table 1.1. This report is the eighth in this series.

Report 1405-1 provides a detailed background on the topic of durability design of post-tensioned bridge substructures. The report contains an extensive literature review on various aspects of the durability of

post-tensioned bridge substructures and a detailed analysis of bridge substructure condition rating data in the State of Texas.

Report 1405-2 presents a detailed study of improved and high-performance grouts for bonded post-tensioned structures. Three testing phases were employed in the testing program: fresh property tests, accelerated corrosion tests and large-scale pumping tests. The testing process followed a progression of the three phases. A large number of variables were first investigated for fresh properties. Suitable mixtures then proceeded to accelerated corrosion tests. Finally, the most promising mixtures from the first two phases were tested in the large-scale pumping tests. The variables investigated included water-cement ratio, superplasticizer, antibleed admixture, expanding admixture, corrosion inhibitor, silica fume and fly ash. Two optimized grouts were recommended depending on the particular post-tensioning application.

Report 1405-3 describes the development of two long-term, large-scale exposure testing programs, one with beam elements, and one with columns. A detailed discussion of the design of the test specimens and selection of variables is presented. Preliminary experimental data is presented and analyzed, including cracking behavior, chloride penetration, half-cell potential measurements and corrosion rate measurements. Preliminary conclusions are presented.

Report 1405-4 describes a series of macrocell corrosion specimens developed to examine corrosion protection for internal prestressing tendons in precast segmental bridges. This report briefly describes the test specimens and variables, and presents and discusses four and a half years of exposure test data. One-half (nineteen of thirty-eight) of the macrocell specimens were subjected to a forensic examination after four and a half years of testing. A detailed description of the autopsy process and findings is included. Conclusions based on the exposure testing and forensic examination are presented.

Report 1405-5 contains a summary of the conclusions and recommendations from the first four reports from Project 0-1405. The findings of the literature review and experimental work were used to develop preliminary durability design guidelines for post-tensioned bridge substructures. The durability design process is described, and guidance is provided for assessing the durability risk and for ensuring protection against freeze-thaw damage, sulfate attack and corrosion of steel reinforcement. These guidelines were refined and expanded as more experimental data became available and will be reported in Report 1405-9.

Report 1405-6 describes a series of macrocell corrosion specimens developed to examine corrosion protection for internal prestressing tendons in precast segmental bridges. This report briefly describes the test specimens and variables, and presents and discusses eight years of exposure test data. One-half (nineteen of thirty-eight) of the macrocell specimens were subjected to a forensic examination after four and a half years of testing, and were reported in Report 1405-4. A detailed description of the autopsy process for the remaining macrocell specimens and findings is included. Final conclusions and recommendations based on the exposure testing and forensic examination are presented.

Report 1405-7 describes a series of beam corrosion specimens developed to examine corrosion protection for bonded internal prestressing tendons in linear flexural bridge elements. This report briefly describes the test specimens and variables, and presents and discusses the results after approximately one-half of the beam specimens were autopsied after three an a half years and four a half years of exposure testing. A detailed description of the autopsy process and findings is included. Final conclusions based on the exposure testing and forensic examination are presented. The report concludes with recommendations for materials and implementation measures.

Report 1405-8 (this document) describes a series of column corrosion specimens developed to examine the effect of post-tensioning on concrete pier and column durability (corrosion protection) through precompression of the concrete and precompression of construction joints, and to investigate the relative performance of various aspects of corrosion protection for post-tensioning, including concrete type, duct type, post-tensioning bar coatings and loading. A detailed description of the autopsy process and findings

is included. Final conclusions based on the exposure testing and forensic examination are presented. The report concludes with recommendations for materials and implementation measures.

Table 1.1 Proposed Project 0-1405 Reports

Number	Title	Estimated Completion
1405-1	State of the Art Durability of Post-Tensioned Bridge Substructures	1999
1405-2	Development of High-Performance Grouts for Bonded Post-Tensioned Structures	1999
1405-3	Long-term Post-Tensioned Beam and Column Exposure Test Specimens: Experimental Program	1999
1405-4	Corrosion Protection for Bonded Internal Tendons in Precast Segmental Construction	1999
1405-5	Interim Conclusions, Recommendations and Design Guidelines for Durability of Post-Tensioned Bridge Substructures	1999
1405-6	Final Evaluation of Corrosion Protection for Bonded Internal Tendons in Precast Segmental Construction	2002
1405-7	Long-term Post-Tensioned Beam Exposure Test Specimens: Final Evaluation	2003
1405-8	Long-term Post-Tensioned Column Exposure Test Specimens: Final Evaluation	2003
1405-9	Conclusions, Recommendations and Design Guidelines for Corrosion Protection of Post-Tensioned Bridges	2003
1405-S	Corrosion Protection of Post-Tensioned Bridge Elements	2003

Several dissertations and theses at The University of Texas at Austin were developed from the research from Project 0-1405. These documents may be valuable supplements to specific areas in the research and are listed in Table 1.2 for reference.

Table 1.2 Project 0-1405 Theses and Dissertations, The University of Texas at Austin

Title	Author	Date
Master's Theses		
Evaluation of Cement Grouts for Strand Protection Using Accelerated Corrosion Tests"	Bradley D. Koester	12/95
"Durability Examination of Bonded Tendons in Concrete Beams under Aggressive Corrosive Environment"	Andrea L. Kotys	5/03
"Test Method for Evaluating Corrosion Mechanisms in Standard Bridge Columns"	Carl J. Larosche	8/99
"Test Method for Evaluating the Corrosion Protection of Internal Tendons Across Segmental Bridge Joints"	Rene P. Vignos	5/94
Ph.D. Dissertations		
"Accelerated Corrosion Testing, Evaluation and Durability Design of Bonded Post-Tensioned Concrete Tendons"	Ruben M. Salas	8/03
"Improving Corrosion Resistance of Post-Tensioned Substructures Emphasizing High-Performance Grouts"	Andrea J. Schokker	5/99
"Durability Design of Post-Tensioned Bridge Substructures"	Jeffrey S. West	5/99

CHAPTER 2: EXPERIMENTAL PROGRAM

A total of ten large-scale column specimens were designed, constructed and placed under exposure testing by West and Larosche.[11] Exposure testing began in July 1996 and was performed by West, Larosche and Schokker until April 1999. Exposure testing was maintained by other graduate research assistants until August 2000, when Kotys and Salas took over responsibility for the exposure testing. Continued exposure testing was carried out until Salas performed full autopsies, which began in January 2003, after six and a half years of accelerated exposure.

2.1 TEST SPECIMEN

Test specimens are circular cast-in place columns. The columns were patterned after standard Texas Department of Transportation (TxDOT) multicolumn substructures (see Figure 2.1). The column dimensions and details were selected such that covers, reinforcement sizes and post-tensioning hardware were of similar order of magnitude as in practical applications, with consideration for construction and loading of the specimens. A reduced nominal column diameter of 18 in. and reduced height of 6 ft were selected for the actual test specimens.

2.1.1 Design Loading

Typical bridge column reinforcement is based on minimum reinforcement requirements, and the nominal capacity of the column is usually well in excess of the design loading dictated by analysis of the bridge. Thus, it was decided to obtain design loading for a typical TxDOT multicolumn bridge substructure (see Figure 2.1), proportion the test specimen to meet minimum requirements and compare the column capacity against the design loading. During testing, the columns would be subjected to the design loading, which would provide a more realistic representation of the typical case.

The prototype bridge substructure carried two lanes of traffic and one shoulder. The bent was skewed to the roadway alignment at 45 degrees. The superstructure consisted of five Type C precast, pretensioned bridge girders with a 75 ft span and an 8-in. thick cast-in-place concrete deck.

The three-column frame bent was analyzed using a plane frame analysis program. AASHTO LRFD was used for design loading on the bridge.

The bent cap was divided into several segments and the analysis was performed to refine the end moments of inertia, either using the gross transformed moment of inertia or elastic cracked section moment of inertia (positive or negative bending). The frame was re-analyzed and the various combinations of axial load and moment for the columns were determined. The calculated forces for the outside columns are shown in Table 2.1. Loading on the substructure was not symmetric due to the shoulder. The critical combination was taken at the top of column 3, with the largest eccentricity.

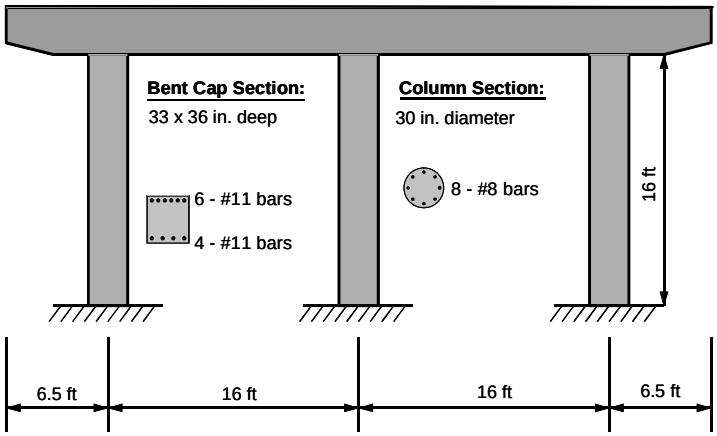

Figure 2.1 Prototype Multicolumn Substructure[2]

Table 2.1 Calculated column forces for Prototype Substructure (unfactored)[2]

Location	Data	Column 1		Column 3	
Column Base	N_{max}	1781 kN	(400.4 kips)	994 kN	(223.4 kips)
	M_{max}	55.8 kN-m	(494.4 k-in.)	74.6 kN-m	(660.0 k-in.)
	e = M/N	30.5 mm	(1.2 in.)	76.2 mm	(3.0 in.)
Column Top	N_{max}	1716 kN	(385.7 kips)	**928 kN**	**(208.7 kips)**
	M_{max}	144.8 kN-m	(1281.6 k-in.)	**118.0 kN-m**	**(1044.0 k-in.)**
	e = M/N	83.8 mm	(3.3 in.)	**127 mm**	**(5.0 in.)**

The design loading from the prototype analysis was scaled for use with the column specimens. Axial forces are scaled by the square of the ratio of column diameters, following Equation 1. Bending moments are scaled by the cube of the ratio of column diameters, following Equation 2.

$$N_{specimen} = \left(\frac{D_{specimen}}{D_{prototype}}\right)^2 \times N_{prototype} = 75.2 \text{ kips} \qquad \textbf{Eq. 1}$$

$$M_{specimen} = \left(\frac{D_{specimen}}{D_{prototype}}\right)^3 \times M_{prototype} = 225 \text{ kip in.} \qquad \textbf{Eq. 2}$$

Assuming an average load factor of 1.5, the factored design forces are:

N_f = 112.6 kips, M_f = 338.6 kip in

2.1.2 Reinforced Concrete Design

The smallest circular column used by TxDOT is 18 in. diameter. This column was selected as the nonprestressed or reinforced concrete design in the research program. The reinforced concrete section is shown in Figure 2.2.

Figure 2.2 Reinforced Concrete Column Section Details[2]

The reinforced concrete (3600 psi) section was analyzed using a layer-by-layer strain compatibility section analysis technique to produce axial force-moment interaction diagrams, as shown in Figure 2.3. The factored resistance is well in excess of the factored loading.

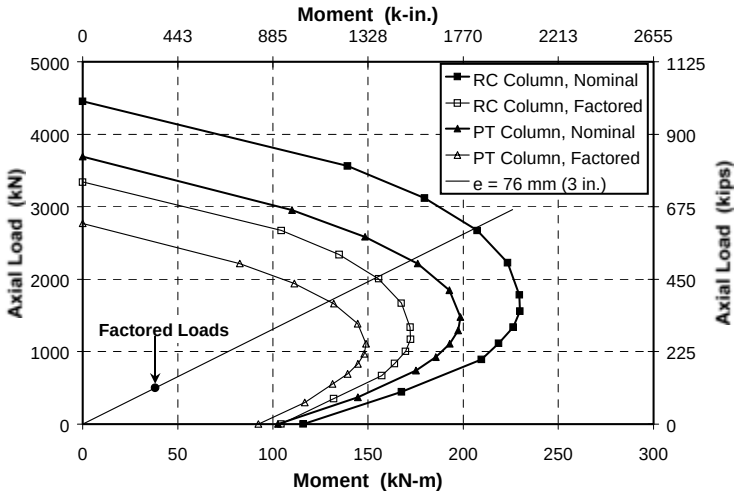

Figure 2.3 Column Interaction Diagrams[2]

The elastic decompression moment for the column was calculated for the design service loading, and was equal to 169 kip in. The service load moment of 225 kip in. exceeded the decompression moment.

2.1.3 Post-Tensioned Column Design

The design of the post-tensioned columns kept the same mild steel reinforcement (due to the need for confinement and concerns for creep) as the reinforced column design, and added four threaded prestressing bars (bars are often used instead of strands in columns). The four PT bars would provide continuity between the column and foundation, effectively developing the flexural capacity about more than one axis, and would increase the decompression moment, which could improve durability at construction joints.

A minimum effective prestress of 60% of ultimate (fpe =0.6 fpu) was used for design and analysis purposes. The column section details are shown in Figure 2.4.

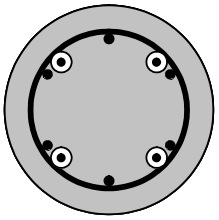

Main Reinforcement:
6 - #6 bars
4 – 5/8 in. PT bars
$f_{pe} = 0.6f_{pu}$

Spiral:
#3 at 6 in. pitch

Column Diameter: 18 in.
Clear Cover to Spiral: 2 in.

** Only PT bars provide continuity to foundation

Figure 2.4 Post-Tensioned Column Section Details[2]

The decompression moment was calculated as 406 kip in., which exceeded the applied service moment of 225 kip in. by a considerable margin.

The post-tensioned column section was analyzed using the layer-by-layer strain compatibility analysis technique. A detailed description of the procedure is included in Reference 2. The calculated moment diagrams are also shown in Figure 2.3. The lower nominal capacity of the post-tensioned columns illustrates the effect of post-tensioning on the axial load carrying capacity of these elements. However, even with this reduction, the factored resistance of the post-tensioned columns far exceeded the factored loads.

Long-term prestress losses were calculated for periods of 500, 1000 and 1500 days, see details in Reference 2. Table 2.2 summarizes the results. Losses are not uniform in the loaded case due to the eccentric loading. The calculated losses indicate that with an initial prestress of 0.68 fpu the effective prestress in the columns will meet or exceed the design value for an experiment duration longer than 1500 days. The average initial prestress in the gross column section was about 500 psi.

Table 2.2 Long-Term Prestress Losses[2]

Time Period (days)	Prestress Loss ΔF_{p1}	Prestress Loss ΔF_{p2}
Case 1: Loaded, $f_{pi} = 0.68f_{pu}$		
500	10.7%	8.8%
1000	11.5%	9.6%
1500	11.9%	9.9%
Case 2: Unloaded, $f_{pi} = 0.68f_{pu}$		
500	7.8%	7.8%
1000	8.4%	8.4%
1500	8.8%	8.8%

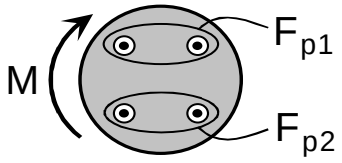

2.2 VARIABLES

Variables selected for exploration fall into five main categories: column to foundation joint, loading, concrete type, post-tensioning duct types and prestressing bar coatings.

2.2.1 Control Variables

Standard variables based on typical current TxDOT practice were defined to represent control cases. Table 2.3 summarizes the control variables used for the research study.

Table 2.3 Control Variables Based on TxDOT Practice[2]

Variable	Typical mix or material used
Concrete	Based on TxDOT Specification Item 421, Tx DOT Class C concrete for bridge substructures, Maximum w/c ratio = 0.533, Maximum coarse aggregate size = 3/4 in., Retarder, Rheocrete 300-R, Entrained air admixture, 2 in. clear cover to main steel.
Cement Grout	Based on TxDOT Specification Item 426.3.4a w/c ratio = 0.44 Type I cement
PT Duct	Rigid galvanized steel duct.

2.2.2 Column to Foundation Connection

The construction joint between the column and foundation presents a possible weak link in corrosion protection since it represents a pre-formed crack that could open under loading. This problem is aggravated by the potential exposure conditions at the column foundation interface, since the cold joint could be directly exposed to moisture and chlorides in coastal and deicing chemical exposures. Selected configurations are shown in Figure 2.5. In this figure, reinforcing cages (mild steel) consisting on 6#6 longitudinal bars and #3 bar spiral at 6 in. pitch are shown. A two-inch cover was left at the base of the column and the reinforcing cage. Only dowels or post-tensioned bars crossed the joint.

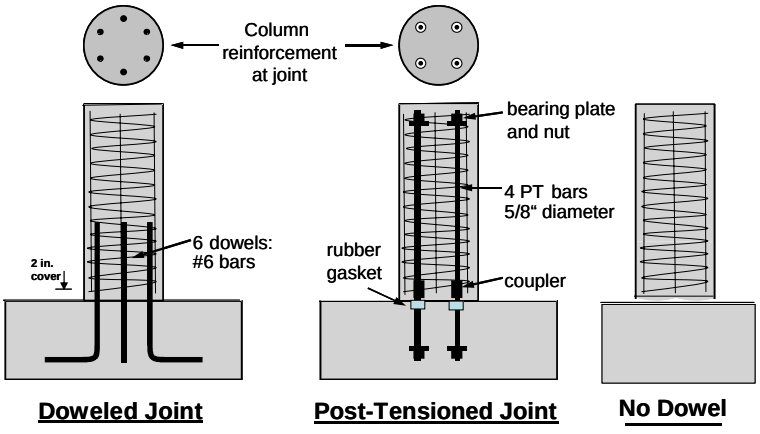

Figure 2.5 Column-Foundation Joint Configurations[2]

2.2.3 Loading

Two loading conditions were considered: unloaded and service load. The columns were subjected to the combined axial load and moment conditions obtained from the prototype substructure analysis for the service load condition:

$$N_{service} = 75.2 \text{ kips}, \quad M_{service} = 225 \text{ kip in.}$$

The unloaded case was included since it could represent a worse case condition for allowing moisture and chloride penetration at the construction joint.

2.2.4 Concrete Type

TxDOT standard concrete mix was used in eight specimens. In two columns, 35% of cement by volume (31% replacement by weight) was replaced with fly ash (ASTM Class C), with no other significant changes to the concrete mix.

2.2.5 Post-Tensioning Ducts

Impermeable plastic ducts are compared directly within individual specimens to standard galvanized steel ducts, without duct splices, as shown in Figure 2.6. Uncoated post-tensioning bars were used in columns where duct type was evaluated.

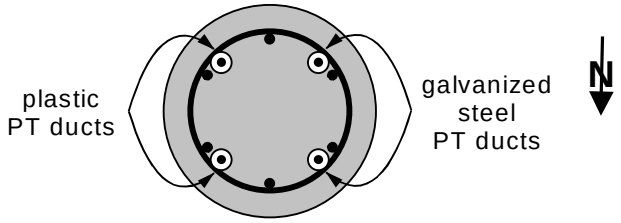

Note: PT bars are uncoated

Figure 2.6 Comparison of Ducts Types for Post-Tensioning[2]

A rubber gasket was placed around the protruding PT-bars in the top of the foundation to seal the dead ends of the ducts as shown in Figure 2.14. As is discussed in Chapter 5, it was a serious error in the specimen definition not to splice ducts at this location.

2.2.6 Prestressing Bar Coating

Two prestressing bar coatings are investigated: Epoxy coated (according to ASTM A775-97) and zinc galvanized prestressing bars. The coated bars were compared directly to uncoated bars within individual specimens (see Figure 2.7). In both cases, anchorage hardware was either epoxy coated or galvanized. Nuts and couplers are proportioned to limit damage in epoxy coating or zinc coating.

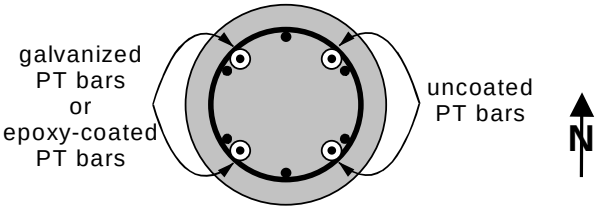

Note: all ducts are galvanized steel

Figure 2.7 Comparison of Prestressing Bar Coatings[2]

2.3 SPECIMEN TYPES

Ten specimens were used to address all selected variables, using the notation shown in Table 2.4. The complete experimental program is listed in Table 2.5.

Table 2.4 Specimen Notation[2]

Connection Type	Loading	Concrete type	PT Protection
DJ: Doweled Joint	**N:** No Load	**TC:** TxDOT Class C	**PD:** Plastic Duct
PT: Post-Tensioned Joint			**EB:** Epoxy-Coated PT Bar**
NJ: No dowel	**S:**Service Load	**FA:** 35% Fly Ash	**GB:** Galvanized PT Bar**
			Blank: Not applicable (i.e., no PT)
Example: PT-TC-S-PD			

* plastic ducts used for bars 1 and 2, galvanized steel ducts used for bars 3 and 4

** epoxy-coated or galvanized bars used for bars 3 and 4, uncoated bars used for bars 1 and 2

Table 2.5 Column Specimen Types and Variables[2]

Specimen	Foundation Connection	Concrete Type	Loading	PT Protection
1 DJ-TC-N	Doweled	Class C	Unloaded	n/a
2 PT-TC-N-PD	Post-tensioned	Class C	Unloaded	Plastic Duct
3 NJ-TC-N	No dowel	Class C	Unloaded	n/a
4 DJ-TC-S	Doweled	Class C	Service	n/a
5 PT-TC-S-PD	Post-tensioned	Class C	Service	Plastic Duct
6 NJ-TC-S	No dowel	Class C	Service	n/a
7 PT-TC-S-EB	Post-tensioned	Class C	Service	Epoxy-coated PT Bar
8 PT-TC-S-GB	Post-tensioned	Class C	Service	Galvanized PT Bar
9 DJ-FA-S	Doweled	35% Fly Ash	Service	n/a
10 PT-FA-S-PD	Post-tensioned	35% Fly Ash	Service	Plastic Duct

2.4 MATERIALS

The materials used in the column corrosion tests are summarized in Table 2.6.

Table 2.6 Column Construction Material Details[2]

Item	Description		
<u>Column Concrete:</u> Texas DOT Class C Concrete for Bridge Substructures	• w/c = 0.45 (based on slump, max. allowable w/c = 0.53) • f'c = 3600 psi minimum allowable • batch proportions: (per 1 yd^3) Coarse Aggregate (3/4 in.) Fine Aggregate Type I/II Cement Water Set retarder Entrained Air Admixture • cylinder strengths: (average)	 7-day 14-day 28-day	 1877 lbs 1186 lbs 564 lbs 254 lbs 24 oz 4 oz 4358 psi 5250 psi 5284 psi
<u>Column Concrete:</u> Texas DOT Class C Concrete with 31% Fly Ash by Weight	• w/(c +p) = 0.42 • f'c = 3600 psi minimum allowable • batch proportions: (per 1 yd^3) Coarse Aggregate (3/4 in.) Fine Aggregate Type I/II Cement Class C Fly Ash Water Set retarder Entrained Air Admixture • cylinder strengths: (average)	 7-day 28-day	 1855 lbs 1245 lbs 362 lbs 162 lbs 220 lbs 20.0 oz 3.5 oz 4447 psi 6473 psi
Foundation Concrete Mix 1 (for RC Columns, Capitol Aggregates Mix 241)	• w/(c + p) = 0.39 • f'c = 8000 psi design strength • batch proportions: (per 1 yd^3) Coarse Aggregate (3/4 in.) Fine Aggregate Type I/II Cement Class C Fly Ash Water Set Retarder • avg. cylinder strengths:	 28-day	 1790 lbs 1131 lbs 525 lbs 225 lbs 295 lbs 22.5 oz 6220 psi

Table 2.6 (Continued) Column Construction Material Details[2]

Item	Description		
Foundation Concrete Mix 2 (for PT Columns, Capitol Aggregates Mix 246)	• w/(c + p) = 0.25		
	• f'c = 14,000 psi design strength		
	• batch proportions: (per 0.764 m^3 (1 yd^3))		
	Coarse Aggregate (0.5 in.)		1665 lbs
	Fine Aggregate		1371 lbs
	Type I/II Cement		714 lbs
	Class C Fly Ash		254 lbs
	Water		240 lbs
	Superplasticizer		160 oz
	• cylinder strengths:	7-day	5102 psi
	(average)	14-day	7536 psi
		28-day	8478 psi
TxDOT Grout for Post-Tensioning	• w/c = 0.44		
	• batch proportions: (per 1 ft^3)		
	Type I Cement		82.4 lbs
	Water		36.2 lbs
Threaded Prestressing Bars	• 5/8 in. diameter high strength threaded prestressing bar		
	• Grade 157 (157 ksi)		
	• Supplier: Dywidag Systems, Inc.		
Mild Steel Reinforcement	• ASTM A615, Grade 60 (60 ksi)		
Steel Duct	• Corrugated, semi-rigid, galvanized steel duct		
	• 1.575 in. outside diameter		
	• Supplier: Dywidag Systems, Inc.		
Plastic Duct	• Corrugated, flexible plastic duct		
	• 2 in. outside diameter		
	• Supplier: Dywidag Systems, Inc.		
Epoxy Bonding Agent	• Sikadur 32 High-Mod - Epoxy Bonding Adhesive		
	• Supplier: Sika		

Cylinder compressive strengths are included in Tables 2.7 and 2.8. Foundation concrete strengths did not reach their design values, but were deemed sufficient. Grout for post-tensioning was not sampled for strength testing, as such testing is not required by TxDOT specifications.

Table 2.7 TxDOT Class C Concrete Cylinder Strengths[2]

Column Numbers	Average Cylinder Strength		
	7 Day	14 Day	28 Day
1, 3, 4, 6	33.0 MPa (4791 psi)	42.6 MPa (6177 psi)	42.0 MPa (6091 psi)
2, 5, 9, 10	27.0 MPa (3924 psi)	29.8 MPa (4324 psi)	30.9 MPa (4478 psi)
Averages	30.0 MPa (4358 psi)	36.2 MPa (5250 psi)	36.4 MPa (5284 psi)

Table 2.8 FlyAsh (35%) Concrete Cylinder Strengths[2]

Column Numbers	Average Cylinder Strength		
	7 Day	14 Day	28 Day
7	35.2 MPa (5107 psi)	41.6 MPa (6028 psi)	46.2 MPa (6706 psi)
8	26.1 MPa (3788 psi)	n / a	43.0 MPa (6240 psi)
Averages	30.7 MPa (4447 psi)	n / a	44.6 MPa (6473 psi)

2.5 EXPERIMENTAL SETUP

The experimental setup was designed to meet the following requirements:

- Provide a realistic simulated foundation for the column specimens
- Permit loading of the columns
- Accommodate exposure conditions consisting of salt water continuously ponded around column base and regular application of saltwater to one face of columns (dripper system)

The experimental setup is shown in Figures 2.8 and 2.9. The dripper system is shown in Figure 2.10.

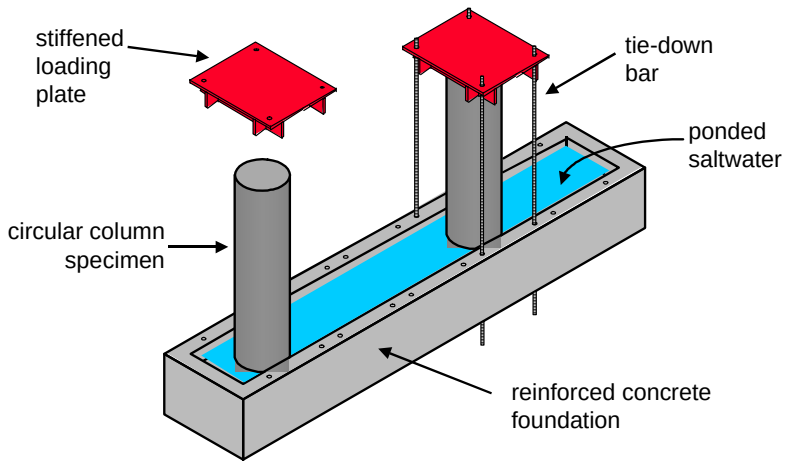

Figure 2.8 Column Corrosion Test Setup – Schematic[2]

The dimensions of the reinforced concrete foundation (designed using a strut and tie model) were 15.33 ft long, 36 in. wide and 18 in. high, with a 6 x 6 in. curb along the perimeter of the top surface to contain ponded saltwater. Loading was applied on the columns using a stiffened loading plate on top of the column and four-one inch threaded prestressing bars. The forces in the bars were adjusted to apply the desired moment and axial force.

Figure 2.9 Column Corrosion Test Setup[2]

All foundation reinforcement was epoxy-coated to prolong the life of the foundation. The top surface and curbs of the foundation were painted with swimming pool paint to improve water-tightness of the ponded area. Details of the foundation reinforcement and loading plates are included in Reference 2.

The loading system was treated as external prestressing in the column calculations, and loading force losses were estimated for various time periods. Loading force losses were small, 6.6% for post-tensioned columns and 3.6% for reinforced concrete columns, in the period of 500 days from first loading. For this reason, it was decided to simplify the loading system and not use springs, readjusting periodically the loading forces on the columns.

2.5.1 Exposure Conditions

Exposure testing consisted of saltwater based on ASTM G109 (3.5% NaCl in tap water), continuously ponded around the base of the columns to simulate a coastal exposure. To simulate deicing salts dripping from the superstructure or saltwater spray, a dripper system was placed on one face of each column, as shown in Figure 2.10. Saltwater was pumped for a period of six to eight hours every two weeks, controlling equal flow rates to each column.

2.5.2 Specimen Location

The specimen location on two foundations is shown in Figure 2.11. The mild steel bars and post-tensioning bars were numbered according to the scheme shown. The curved arrows in the figure indicate the direction of applied moment on each column. Columns without arrows were not loaded. The dripper was located on the tension side for the loaded columns.

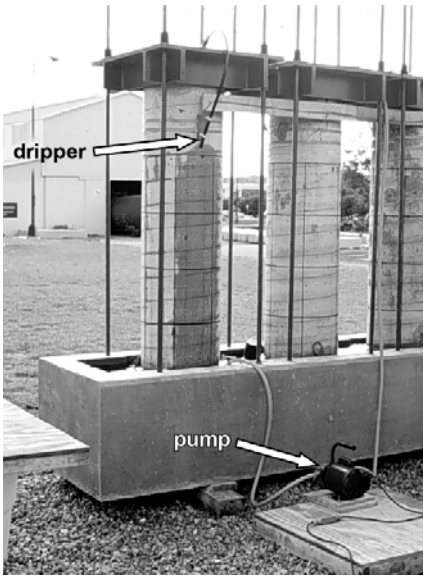

Figure 2.10 Column Dripper System[2]

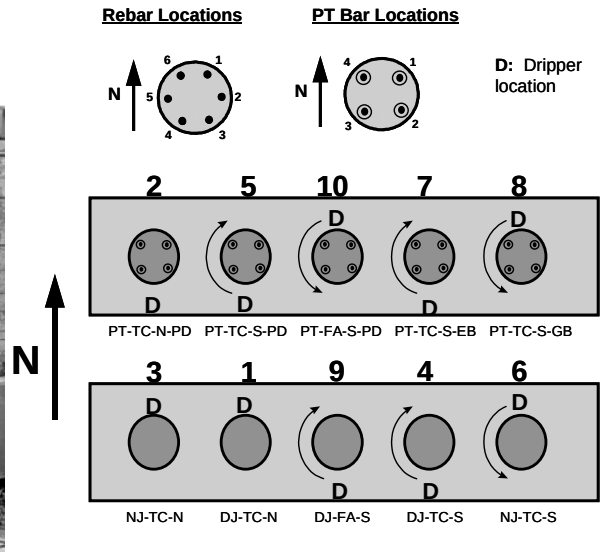

Figure 2.11 Specimen Location Specimen Details[2]

2.6 SPECIMEN FABRICATION

Column foundations were constructed inside the Ferguson Laboratory. Once the foundations had been cast, column reinforcement and post-tensioning hardware was assembled. Each foundation was then transported and placed in the final location and the columns were cast in place, post-tensioned and loaded. A detailed description of the construction process is included in Reference 11. Photos of foundation and column fabrication are shown in Figures 2.12 and 2.13.

As shown in Figure 2.14, short lengths of post-tensioning bar were cast into the foundation to provide anchorage for the column post-tensioning bars. Shallow, square pockets were formed around each bar to accommodate rubber gaskets to seal the "dead end" of the post-tensioning ducts. The column post-tensioning bars were coupled to the protruding bars prior to placement of the ducts. Ground clamps were used to attach ground wires for measurements of potentials to the post-tensioning bar ends prior to capping.

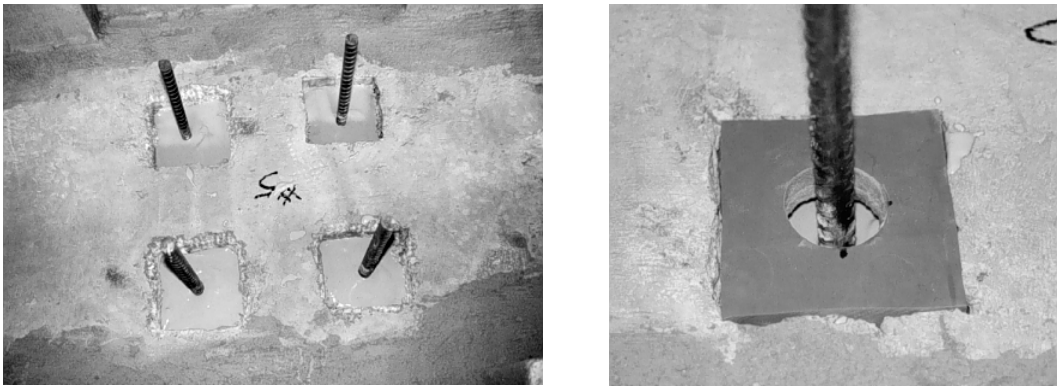

Top View ***End view***

Figure 2.12 Foundation Reinforcement[3]

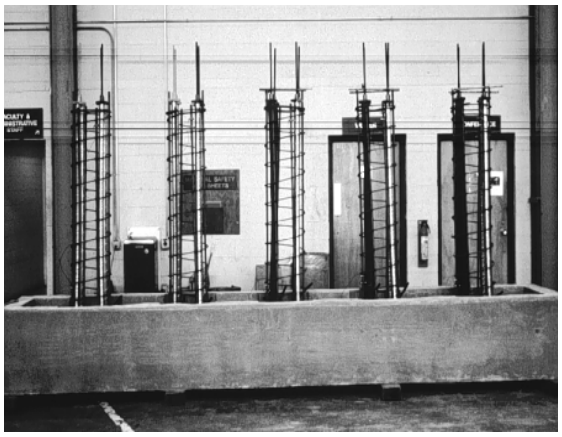

Column Reinforcement on Foundation ***Pouring Column Concrete***

Figure 2.13 Column Construction[3]

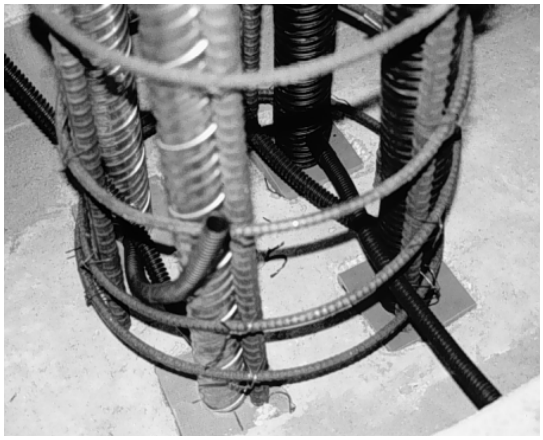

PT Bars Protruding from Foundation Reinforcement, Ducts and Grout Tubes

Gasket Around Post-Tensioning Bar Top of Column Prior to Capping

Figure 2.14 Column Post-Tensioning Details[3]

Losses during stressing were negligible. The post-tensioning jacking force, F_{pj}, was taken equal to the initial prestress force, F_{pi} ($0.68f_{pu}A_{pbar}$=30 kips). Each bar was post-tensioned individually, monitoring the post-tensioning force during stressing with a load cell and by a pressure gauge on the hydraulic pump (see Figure 2.15).

Grouting was done immediately after post-tensioning, all according to TxDOT Specifications. Grouts were mixed in large buckets using a paddle mixer mounted on a large hand held drill, and pumped immediately using an electric grout pump, until a continuous flow of grout was exiting the vent. Figure 2.16 shows the inlet and vent for grouting.

An important caution was suggested by West[2] after grouting: "…after the column grouting had been completed, the possibility of an error in the post-tensioning grout came to light. It is possible that incorrectly labeled cement barrels may have resulted in partial or complete cement replacement with Class F fly ash. The amount of fly ash, if any, is not certain. If the fly ash content is high, very little hydration will have occurred. The effect of this uncertainty on the experimental results is not certain. Persons performing

invasive inspections or autopsies on the columns should be aware of the possibility of fly ash in the grout. The most likely columns to contain fly ash grout are PT-TC-S-EB and PT-TC-S-GB."

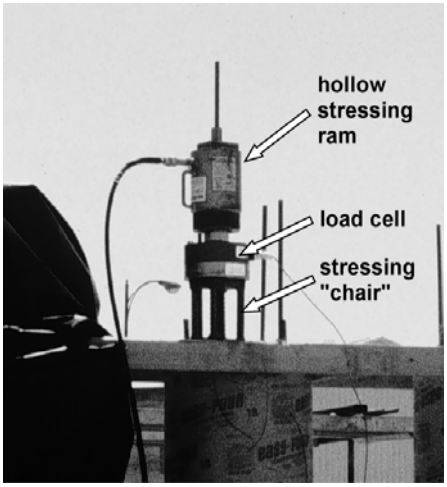

Figure 2.15 Column Post-Tensioning[2]

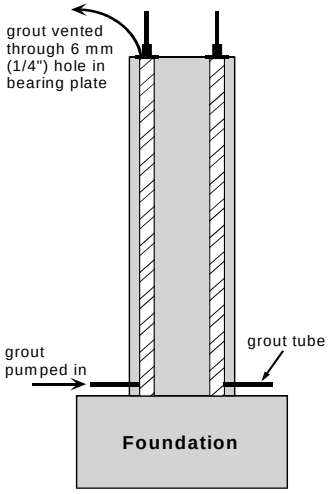

Figure 2.16 Inlet and Vent for Grouting[2]

2.7 SPECIMEN LOADING

Column loading was performed using the loading system shown in Figure 2.17. The applied forces are shown in Figure 2.18. A separate hydraulic pump was used for each ram, and the forces T_1 and T_2 were applied simultaneously in four increments of 22% and a final increment of 12%. Tie-down bar nuts were tightened to refusal using a large wrench once the desired forces had been attained.

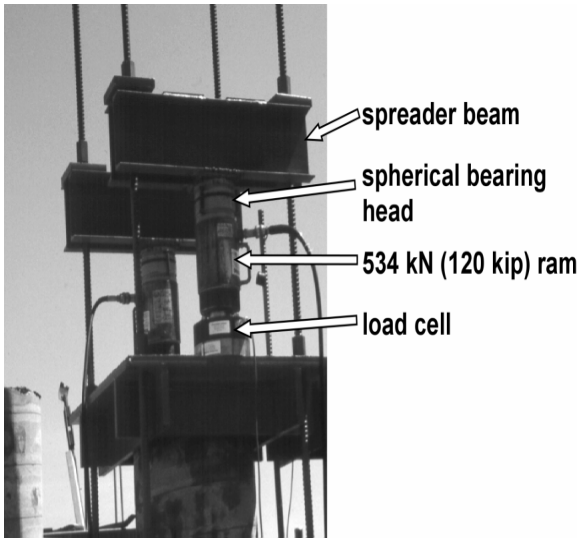

Figure 2.17 Loading System[2]

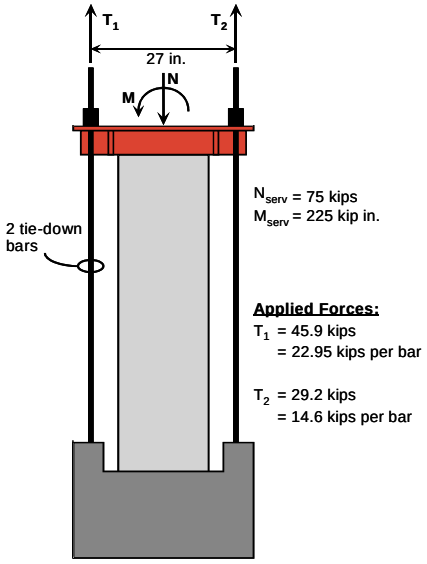

Figure 2.18 Column Loading Forces[2]

2.8 MEASUREMENTS DURING EXPOSURE TESTING

Specimen monitoring during exposure testing included half-cell potential measurements every four weeks, periodic visual inspection for signs of corrosion and distress, and chloride samples taken occasionally to monitor chloride ingress at various depths and heights.

2.8.1 Half-Cell Potential Readings

Half-Cell (HC) potentials were measured against a Saturated Calomel Electrode (SCE), once a month, according to ASTM C876.[12] The numerical significance of the HC potential readings for normal reinforcing is shown in Table 2.9. The voltmeter was connected to the reinforcing cage using a wire that was left attached to the reinforcing cage prior to concrete casting. Figure 2.19 shows the reinforcement placement, and level numbering for HC readings. The readings were taken on three out of six reinforcing bars (labeled 1, 3 and 6) and on all four post-tensioning bars at three different heights (labeled levels 1, 3 and 5) in the column.

Standard ASTM C876 was developed for uncoated reinforcement steel, and therefore, the values reported in Table 2.9 may not necessarily be appropriate for grouted prestressing bars (coated or uncoated) in concrete.

Table 2.9 Interpretation of Half Cell Potentials for Uncoated Reinforcing Steel[12]

Measured Potential (vs SCE)	Probability of Corrosion
more positive than –130 mV	less than 10% probability of corrosion
Between -130 mV and –280 mV	corrosion activity uncertain
more negative than –280 mV	greater than 90% probability of corrosion

2.8.2 Chloride Penetration

Chloride samples were taken periodically from specimens representing each concrete type, joint type, and load level. Powder samples were taken at three depths: 0.5 in, 1 in., and 2 in. The two-inch depth data represent the chloride concentration at the bar level. The chloride samples are also taken at three heights to investigate possible "wicking" effects: 3 in., 9 in., and 15 in., as shown in Figure 2.19. The three-inch height represents the constantly submerged concrete. Each sample is taken from two locations and the powder is combined to give a representative sample.

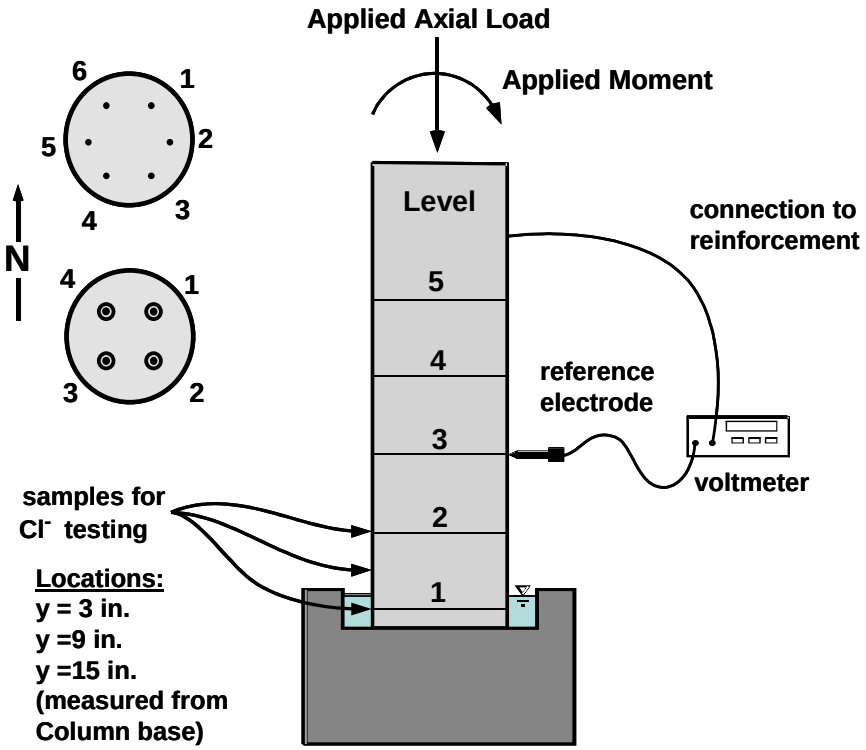

Figure 2.19 Numbering and Locations for Half-Cell Potential Measurements and Chloride Samples (adapted from Ref. 10)

CHAPTER 3: EXPOSURE TEST RESULTS

Exposure testing started in July 1996 and ended in January 2003, after 2367 days (six and a half years). During this period, half-cell potential measurements and chloride samples were taken periodically, except between 1361 days and 1648 days of testing when half-cell readings were interrupted. During this interruption, specimens remained continuously ponded around the column base, without the application of saltwater to the face of the columns (dripper system).

3.1 HALF-CELL POTENTIAL READINGS

Half-Cell (HC) potential plots were developed for all specimens. Two types of data are plotted for each non-prestressed specimen:

- All Half-Cell Potentials: Potentials measured for each reinforcing bar at each level (level 1 – bottom, level 2 – mid-height, level 3 – top). Figure 3.1 and Figure 3.2 show "all" Half-Cell Potentials for specimens NJ-TC-N and DJ-TC-N. Plots for the other non-prestressed specimens are included in Appendix A.
- Average Half-Cell Potentials: Average potentials for all bars at each level (level 1 – bottom, level 2 – mid-height, level 3 – top). "Average" half cell potentials are included in Appendix A.

For post-tensioned specimens, four types of data were plotted:

- All Half-Cell Potentials (**Rebar**): Potentials measured for each reinforcing bar at each level (level 1 – bottom, level 2 – mid-height, level 3 – top). Figure 3.3 shows "all" Half-Cell potentials for specimen PT-TC-N-PD. HC-Plots for other post-tensioned specimens are included in Appendix A.
- Average Half-Cell Potentials (**Rebar**): Average potentials for all reinforcing bars at each level (level 1 – bottom, level 2 – mid-height, level 3 – top). See HC Potential plots in Appendix A.
- All Half-Cell Potentials (**PT-Bars**): Potentials measured for each PT-Bar at each level (level 1 – bottom, level 2 – mid-height, level 3 – top). Figure 3.4 shows "all" Half-Cell Potentials for post-tensioning bars in specimen PT-TC-N-PD. Plots for all other post-tensioning specimens are included in Appendix A.
- Average Half-Cell Potentials (**PT-Bars**): Average potentials for PT-Bars #1 and #2, and Average potentials for PT-Bars #3 and #4. See plots in Appendix A.

Each post-tensioned specimen has two plain post-tensioning bars or ducts and two bars or ducts that investigate a protection variable. For these reason, average values were obtained in pairs (ducts #1 and #2, and ducts #3 and #4; or, PT-bar #1 and #2, and PT-bar #3 and #4). Each variable is clearly separated for each specimen in the plots.

Specimens are also compared relatively to each other on the same plot. Three types of comparison plots were constructed:

- Average Half-Cell Potentials (**Rebar**) at Level 1, Level 3 and Level 5 in Non-Prestressed Columns. See Figure 3.5 through Figure 3.7.
- Average Half-Cell Potentials (**Rebar**) at Level 1, Level 3 and Level 5 in Post-Tensioned Columns. See Figure 3.8 through Figure 3.10.
- Average Half-Cell Potentials (**PT Bars**) (grouped in pairs #1,#2 and #3,#4), at Level 1, Level 3 and Level 5 in Post-Tensioned Columns. See Figure 3.11 through Figure 3.13.

In these plots, ASTM C876[12] corrosion threshold values are shown for reference.

Table 3.1 shows a summary of the probability of corrosion for reinforcing bars in non-prestressed columns, at levels 1, 2 and 3. In a similar manner, Table 3.2 shows a summary of the probability of corrosion for reinforcing bars and post-tensioned bars in PT-columns, at the same three levels 1, 3 and 5.

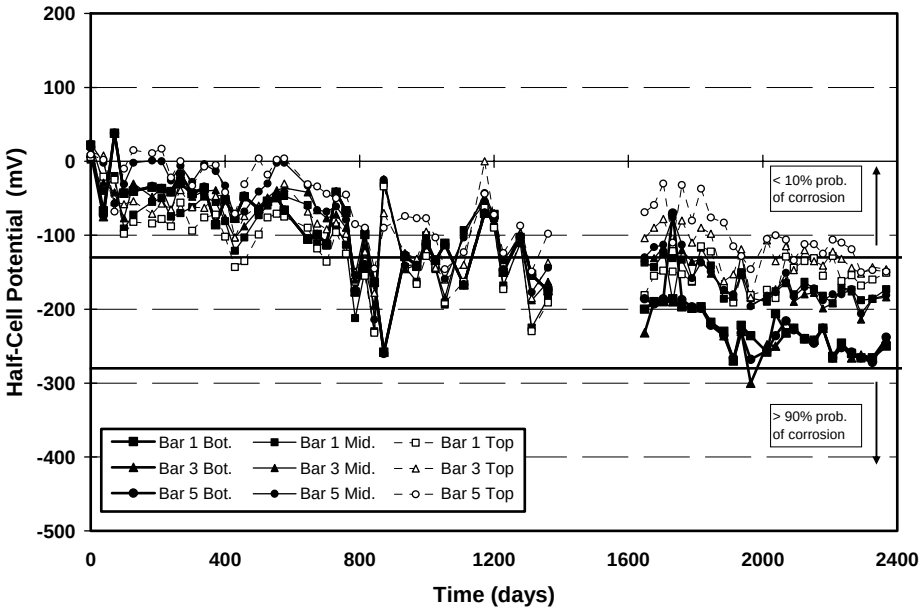

Figure 3.1 All Half-Cell Potential Readings: Column NJ-TC-N[1]

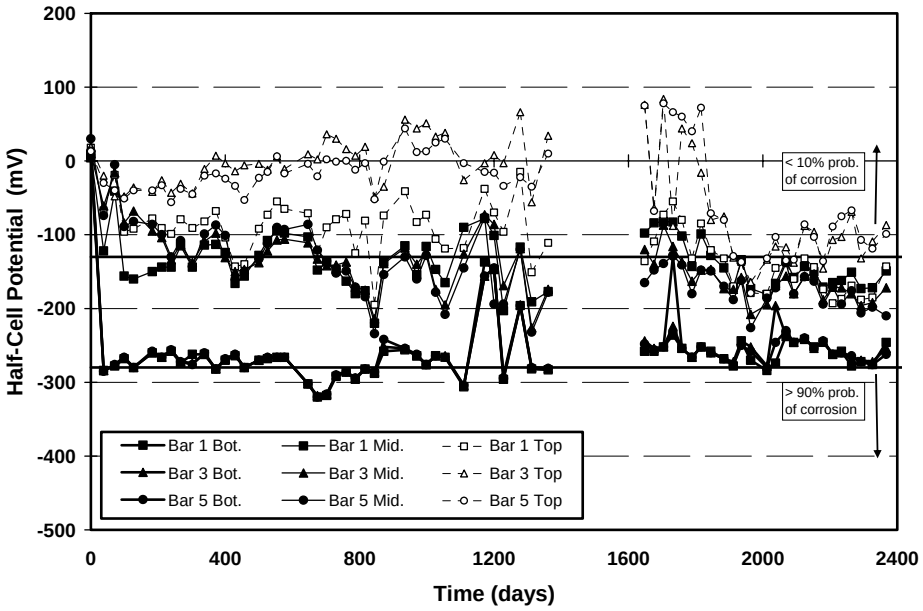

Figure 3.2 All Half-Cell Potential Readings: Column DJ-TC-N[1]

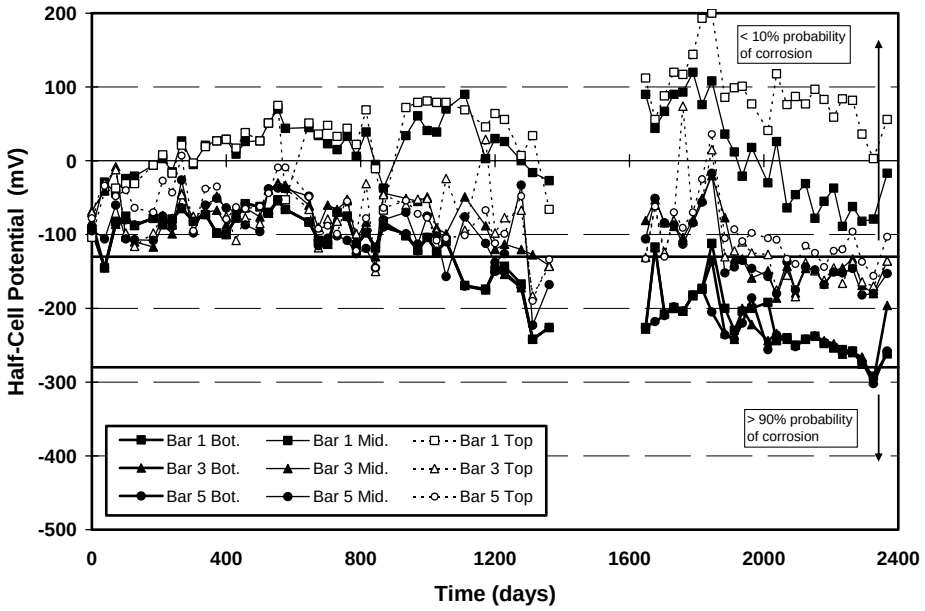

Figure 3.3 All Half-Cell Potential Readings: Column PT-TC-N-PD – Rebar[1]

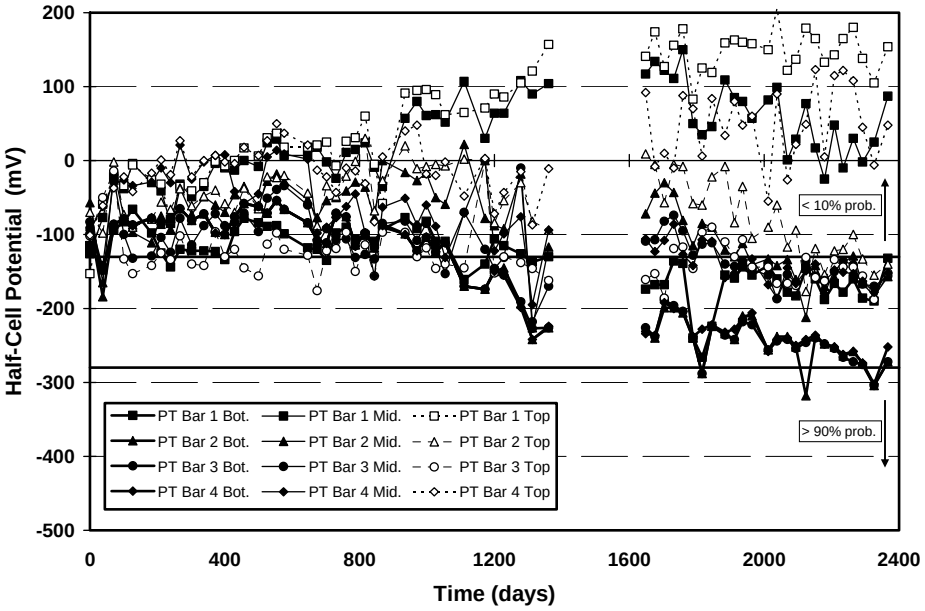

Figure 3.4 All Half-Cell Potential Readings: Column PT-TC-N-PD – PT Bars[1]

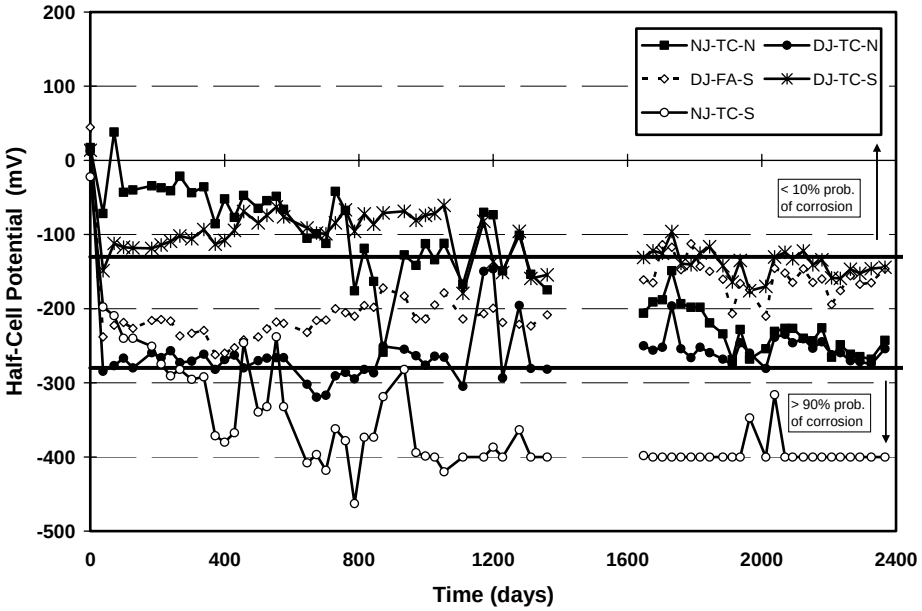

Figure 3.5 Average Half-Cell Potential Readings at Column Base (Level 1): Non-Prestressed Columns[1]

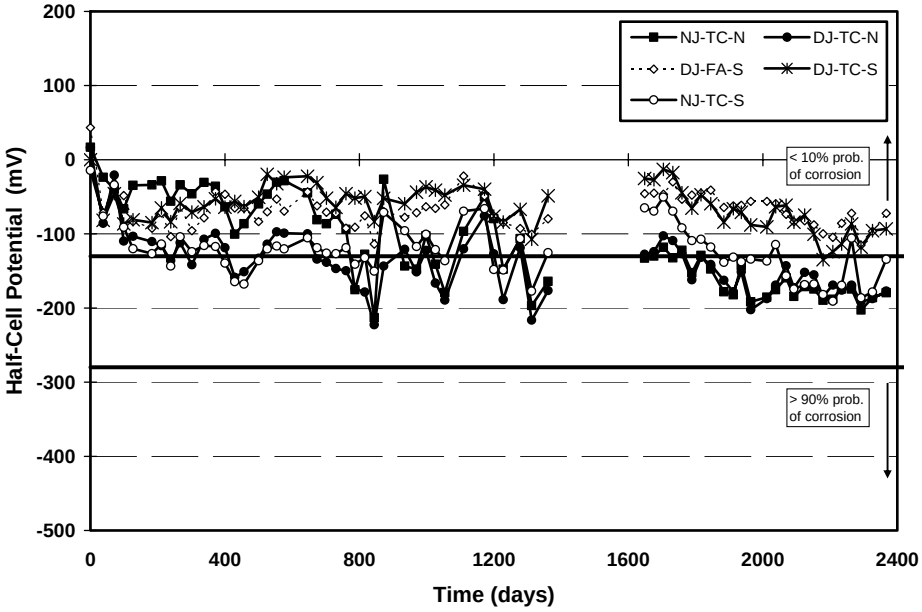

Figure 3.6 Average Half-Cell Potential Readings at Column Mid-height (Level 3): Non-Prestressed Columns[1]

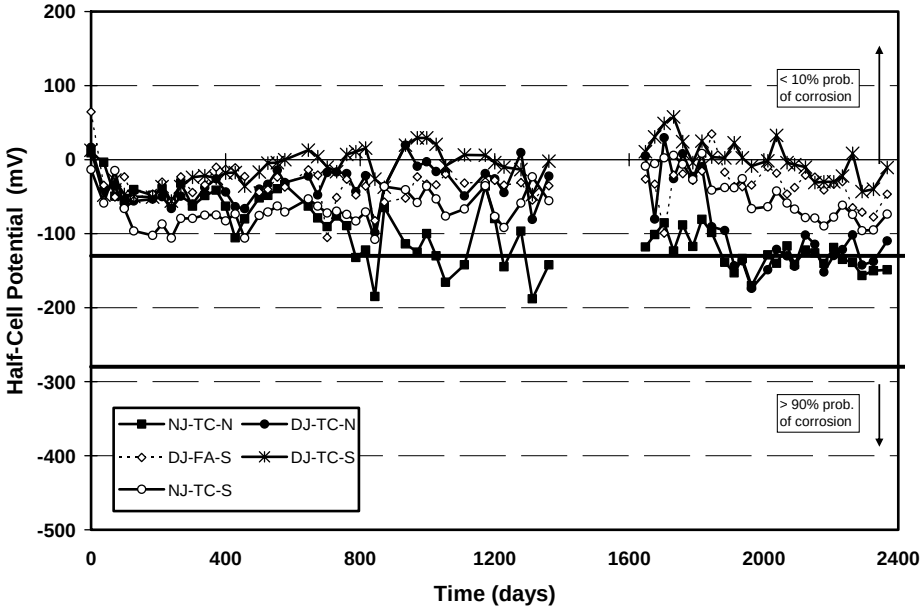

Figure 3.7 Average Half-Cell Potential Readings at Top of Column (Level 5): Non-Prestressed Columns[1]

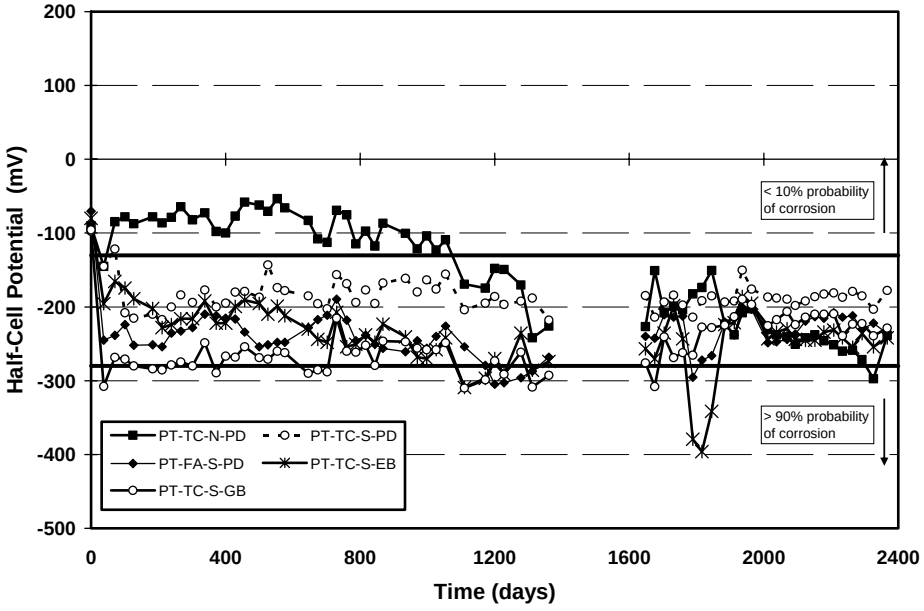

Figure 3.8 Average Half-Cell Potential Readings at Column Base (Level 1): PT Columns – Rebar[1]

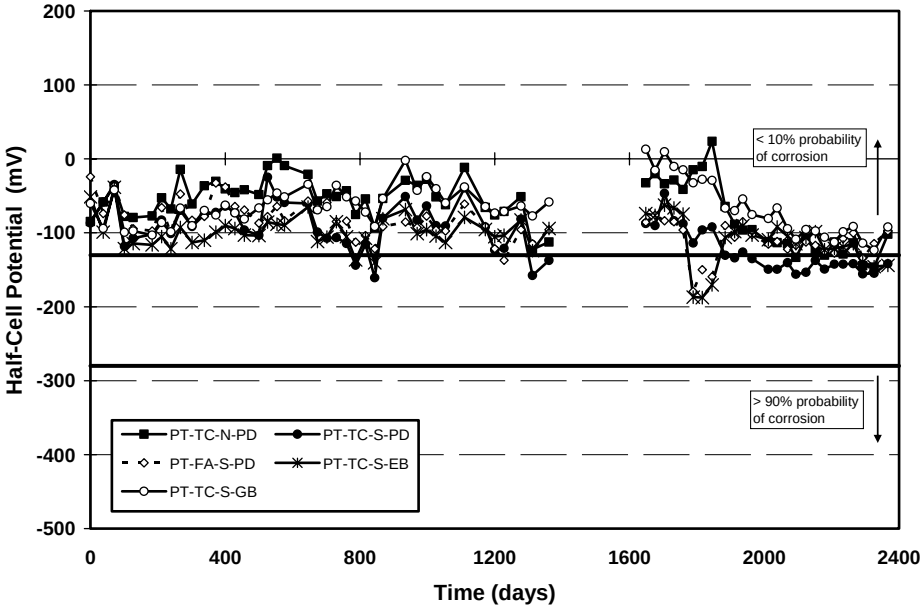

Figure 3.9 Average Half-Cell Potential Readings at Column Mid-Height (Level 3): PT Columns – Rebar[1]

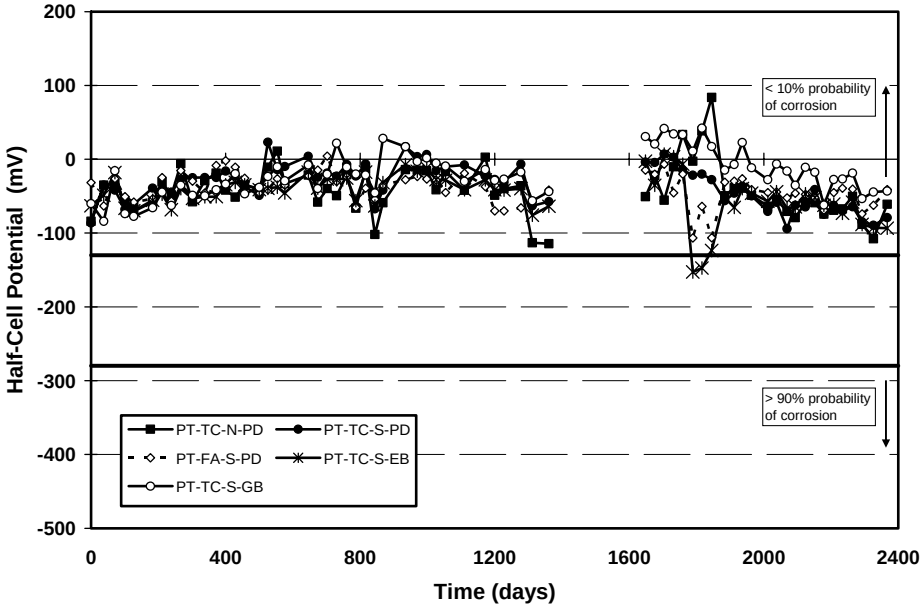

Figure 3.10 Average Half-Cell Potential Readings at Top of Column (Level 5): PT Columns – Rebar[1]

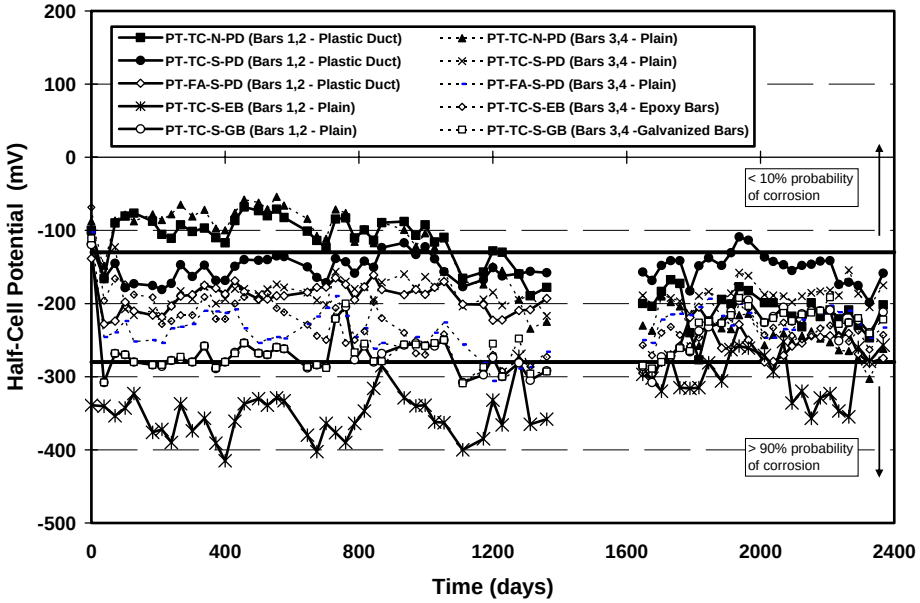

Figure 3.11 Average Half-Cell Potential Readings at Column Base (Level 1): PT Columns – PT Bars[1]

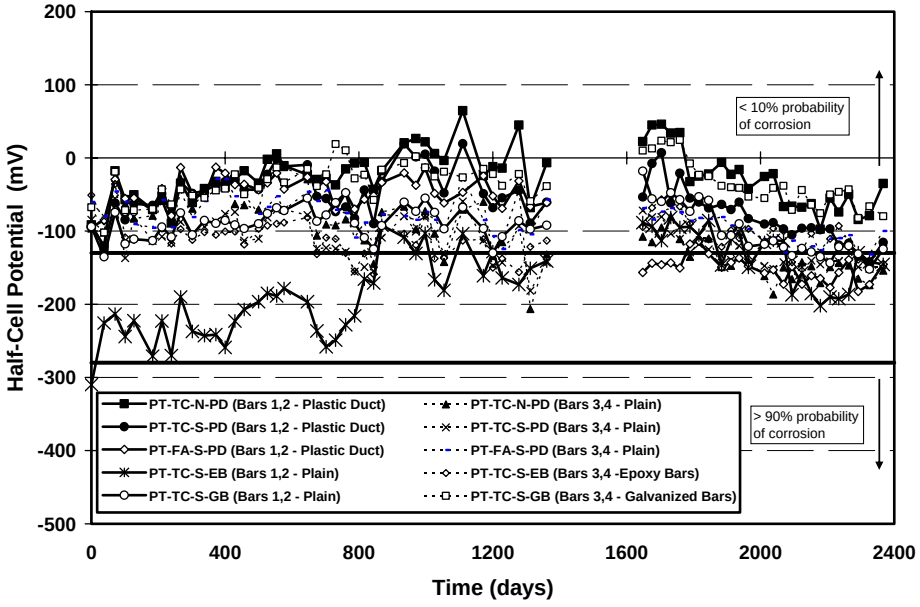

Figure 3.12 Average Half-Cell Potential Readings at Column Mid-Height (Level 3): PT Columns – PT Bars[1]

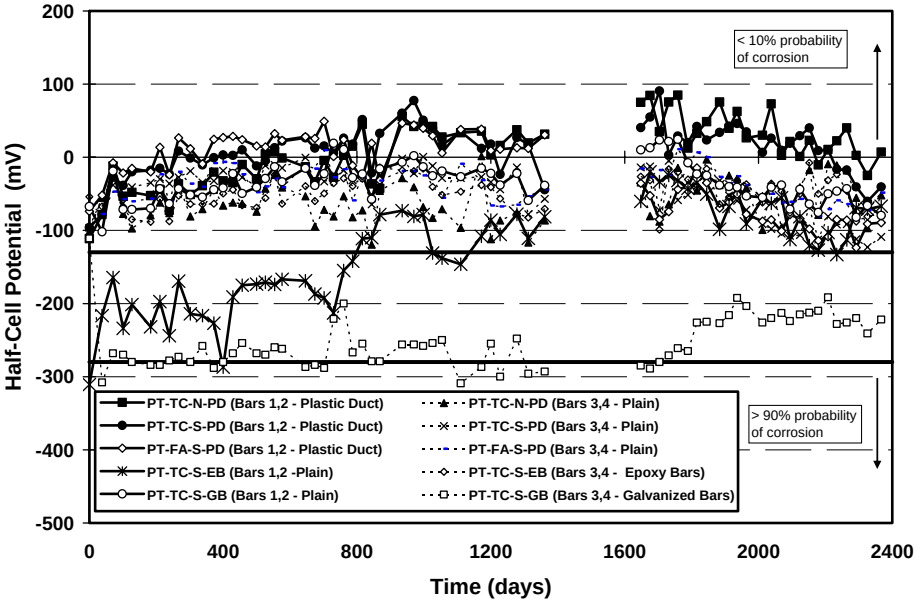

Figure 3.13 Average Half-Cell Potential Readings at Top of Column (Level 5): PT Columns – PT Bars[1]

Table 3.1 Nonprestressed Column Average Half-Cell Readings Summary

Specimen	*Level*	*Probability of Corrosion*
NJ-TC-N	**5**	uncertain
	3	uncertain
	1	uncertain
DJ-TC-N	**5**	low
	3	uncertain
	1	uncertain
DJ-FA-S	**5**	low
	3	low
	1	uncertain
DJ-TC-S	**5**	low
	3	low
	1	uncertain
NJ-TC-S	**5**	low
	3	uncertain
	1	high

Table 3.2 Post-Tensioned Column Average Half-Cell Readings Summary

Specimen	*Level*	*Rebar*	*Reading PT Bars (Plain)*	*PT Bars (Protected)*
PT-TC-N-PD	**5**	low	low	low
	3	low	low	low
	1	high	uncertain	uncertain
PT-TC-S-PD	**5**	low	low	low
	3	uncertain	low	low
	1	uncertain	uncertain	uncertain
PT-FA-S-PD	**5**	low	low	low
	3	low	low	low
	1	uncertain	uncertain	uncertain
PT-TC-S-EB	**5**	low	low	low
	3	low	uncertain	low
	1	uncertain	high	uncertain
PT-TC-S-GB	**5**	low	low	low
	3	low	low	low
	1	uncertain	uncertain	uncertain

Analysis of the non-prestressed specimen plots, indicates that higher HC potentials are observed at Level 1 corresponding to the continuously submerged zone. In general, the HC potential at this level was in the range between -130 mV and -280 mV (uncertain probability of corrosion as described in Table 2.9). The only specimen showing higher average HC-potentials at this level was specimen NJ-TC-S (No dowel - normal Type C concrete - service load), with readings more negative than -400 mV (>90% probability region). At Level 3 (column mid-height) three specimens showed potential values in the uncertain range (between 10% and 90% probability of corrosion): NJ-TC-N (No dowel – type C Concrete - unloaded), DJ-TC-N (doweled – type C concrete - unloaded) and NJ-TC-S (No dowel – type C concrete - service load). Specimens DJ-TC-S (doweled – Type C concrete - service load) and DJ-FA-S (doweled – fly ash concrete - service load) showed average potentials more positive than -130 mV, suggesting a very low probability of corrosion (<10%). At Level 5 (top level) all specimens showed low probability of corrosion, with slightly higher probability of corrosion in specimen NJ-TC-N (No dowel – type C concrete, unloaded), which showed values in the Low to Uncertain probability ranges (around -130 mV).

For post-tensioned specimens, a higher probability of rebar corrosion was found at the bottom level (Level 1). At this level specimen PT-TC-N-PD (type C concrete – unloaded – plastic ducts) showed the higher probability of corrosion, with readings in the order of -300 mV. Other post-tensioning specimens showed readings at Level 1 in the uncertain probability range, with readings between -130 mV and -280 mV. At levels 3 and 5, all post-tensioned specimens showed low probability of rebar corrosion (values more positive than -130 mV), with a slightly higher probability of corrosion at level 3 in specimen PT-TC-S-PD (type C concrete – service load – plastic duct).

The probability of corrosion for post-tensioned bars at level 1 was found in the uncertain probability range (between -130 mV and -280 mV) for all specimens, except for specimen PT-T-S-EB (type C concrete – service load – epoxy-coated bars) that showed a high probability of corrosion (above 90% probability) for the two non-protected PT-bars. At Levels 3 and 5, all specimens showed low probability of corrosion (below 10%), except again for specimen PT-TC-S-EB where a slightly higher probability of corrosion was found on the plain (non protected) PT-bars.

Very negative Half-Cell potentials at the three-inch level (Level 1) may not be the result of very high corrosion rates or severity; therefore, the results presented above must be evaluated with care. As

explained by West,[2] "…When the oxygen supply is restricted, as in the case of submerged concrete, the rate of cathodic reaction is reduced and the corroding system is said to be under diffusion control. A system under diffusion control is illustrated by mixed potential theory in Figure 3.14. Because the slope of the cathodic reaction becomes very steep, the corrosion potential at equilibrium is very negative and the corrosion rate is small. Thus, very negative half-cell potentials in submerged concrete should not necessarily be interpreted as an indication of significant corrosion activity."

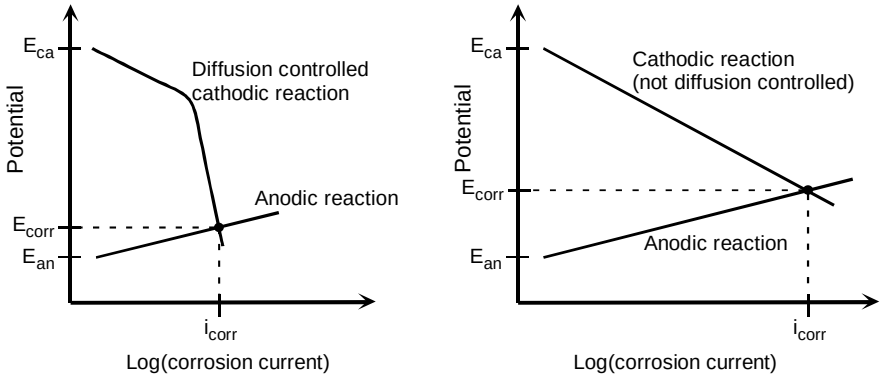

Figure 3.14 Effect of Diffusion Controlled Cathodic Polarization (Lack of Oxygen) on Corrosion Potential and Current[3]

Half-Cell potentials may also be misleading if absolute values at specific dates are used, instead of trends or changes of these values over time. Commonly, a well-defined transition between stable readings to more negative readings would define the onset of corrosion. Also, a continuing trend of more negative readings could be the indication of corrosion activity. However, if half-cell potential readings have been consistent with no significant deviations, this may be the indication that corrosion is not occurring in the element under consideration. With this concept, specimens NJ-TC-N, NJ-TC-S, PT-TC-N-PD (Rebar and PT Bars), PT-FA-S-PD (PT Bars), and PT-TC-S-EB (Rebar) showed some indication of corrosion activity over time; however, specimens DJ-TC-N, DJ-TC-N, DJ-FA-S, DJ-TC-S, PT-TC-S-PD (Rebar and PT Bars), PT-FA-S-PD (Rebar), PT-TC-S-EB (PT Bars), PT-TC-S-GB (Rebar and PT Bars), showed steady potentials, and therefore uncertain corrosion activity.

3.2 CHLORIDE CONTENT IN CONCRETE

Concrete chloride samples were taken directly from the column specimens after 20 months, 32 months and 78 months (end of testing). Acid-soluble chloride content results at 20 months and at 32 months were reported in reference 2. After 78 months (at the end of testing) powder samples were collected from the column specimens at 3 inches, 9 inches and 15 inches from the base of the specimens, on both the dripper and the non-dripper side. At each location, samples were taken at three different depths: 0.5 inches, 1.0 inch and 2.0 inches.

Figure 3.15 and Figure 3.16 show chloride penetration plots for column NJ-TC-N. Figure 3.17 and Figure 3.18 show chloride penetration plots for column PT-TC-N-PD. Plots for other specimens are included in Appendix A.

The relative specimen performance with respect to chloride penetration is compared in Figures 3.19 through 3.24. These plots have been constructed for all specimens at each depth in all sample locations, for both the dripper and non-dripper sides.

Chloride threshold value is indicated in the figures at 0.033%. This value, intended as a guide only, is based on the widely accepted chloride threshold value of 0.2% of the weight of cement.[13]

As can be observed from the figures, acid soluble chloride contents at a height of 3 inches (submerged zone) and at 9 inches, are in most specimens well in excess of the threshold value for corrosion. However, at 15 inches, most specimens show low chloride contents, below the threshold value, at all depths. Exceptions are fly ash specimens (DJ-FA-S and PT-FA-S-PD) that show chloride contents below the threshold value at 9 inches on the non-dripper side (at all depths), and on the dripper side (at 0.5 in. and 2 in.).

Typically, chloride contents at 2 in. depth are 20% to 80% lower than those chloride contents at 1 in. depth, with few exceptions (NJ-TC-N dripper side, DJ-TC-N non-dripper side, DJ-TC-S dripper side, PT-TC-S-PD non dripper side, PT-TC-S-EB dripper side). Additionally, all post-tensioned specimens, and non-prestressed specimens with fly ash concrete, show less chloride penetration than non-prestressed specimens with normal Type C concrete.

From these results, the wicking effect or upward migration of chlorides in the specimens is evident. Significant chloride contents were found at 9 inches from the column base, and much lower contents were found at 15 inches, suggesting that the chloride content is due to the wicking effect, and not to the trickle water coming from above.

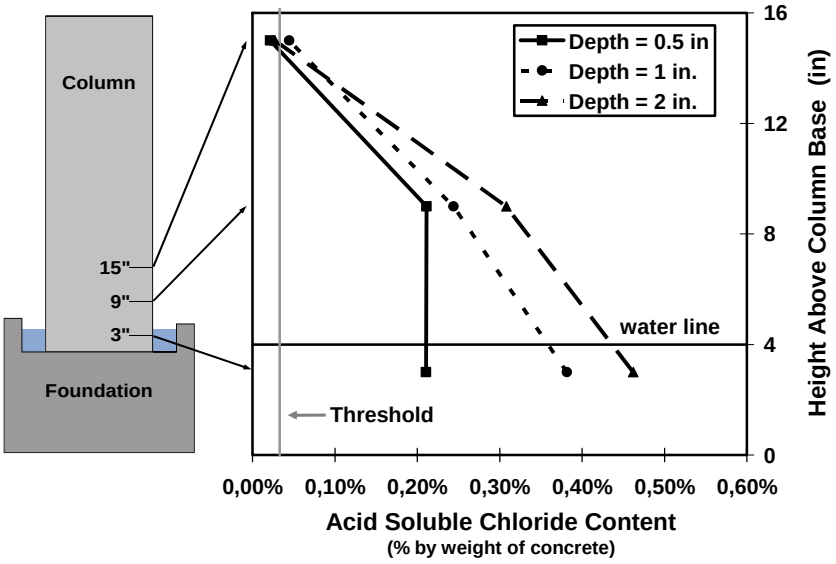

Figure 3.15 Concrete Chloride Penetration for Column NJ-TC-N in Non-Dripper Side at End of Testing[1]

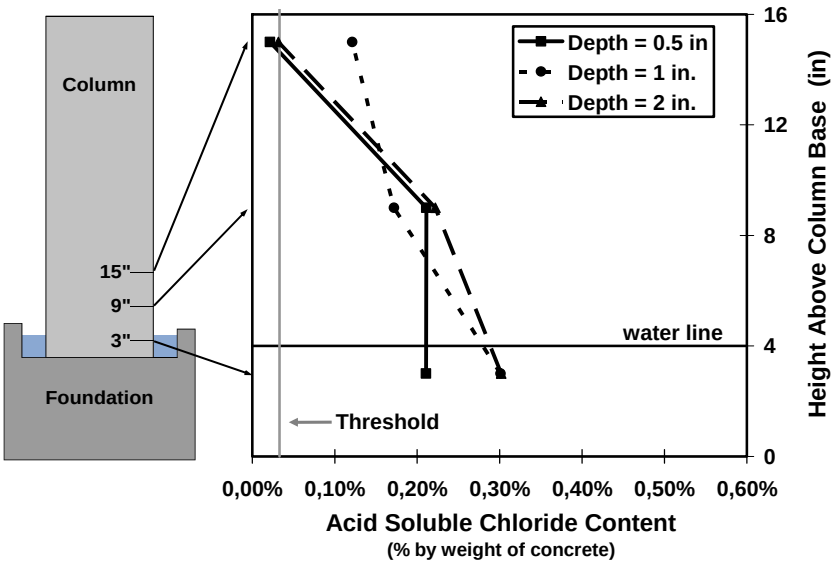

Figure 3.16 Concrete Chloride Penetration for Column NJ-TC-N in Dripper Side at End of Testing[1]

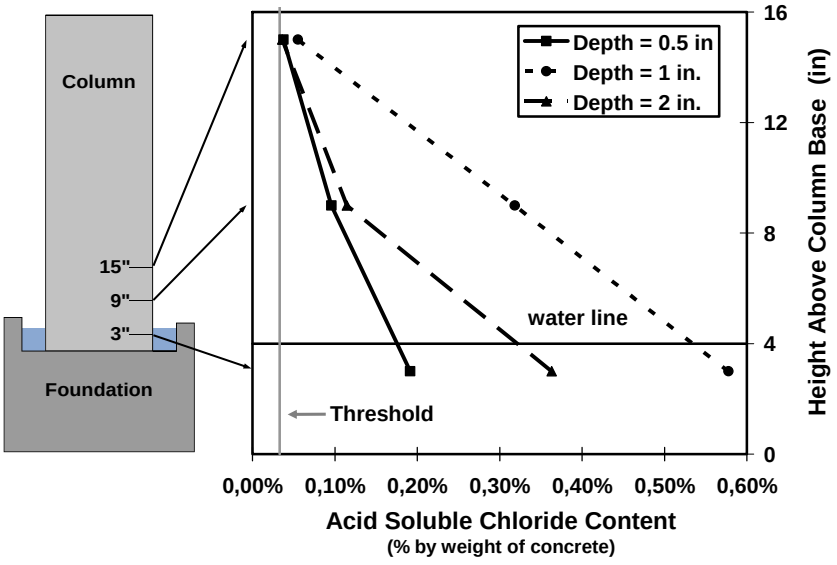

Figure 3.17 Concrete Chloride Penetration for Column PT-TC-N-PD in Non-Dripper side at End of Testing[1]

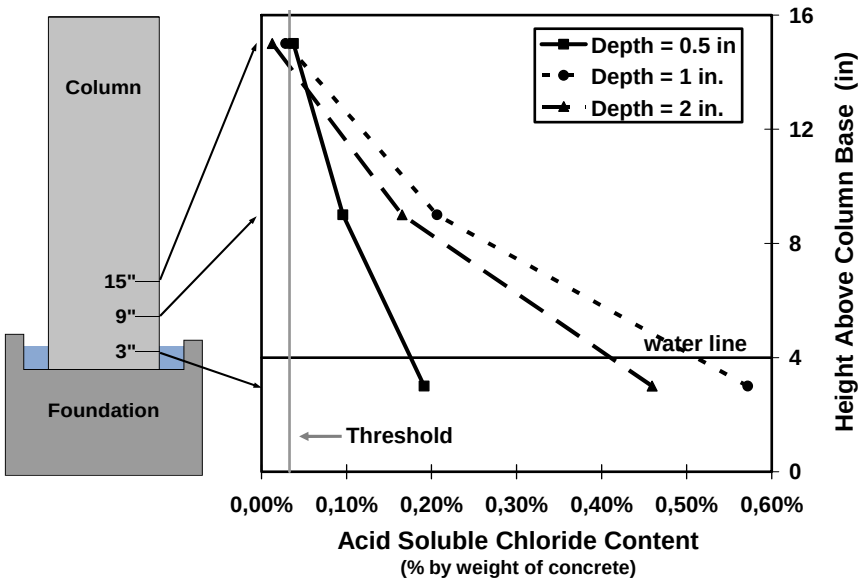

Figure 3.18 Concrete Chloride Penetration for Column PT-TC-N-PD in Dripper Side at End of Testing[1]

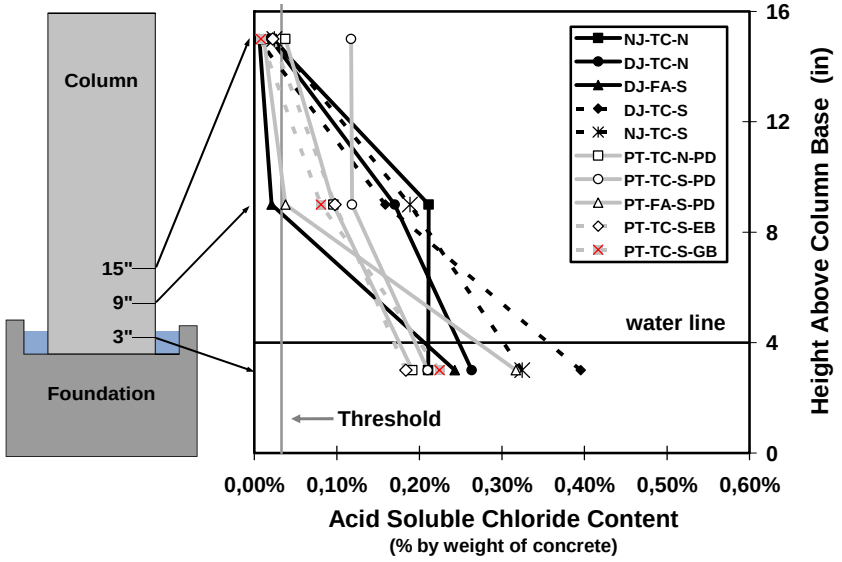

Figure 3.19 Concrete Chloride Penetration at 0.5 inches for All Columns in Non-Dripper Side at End of Testing[1]

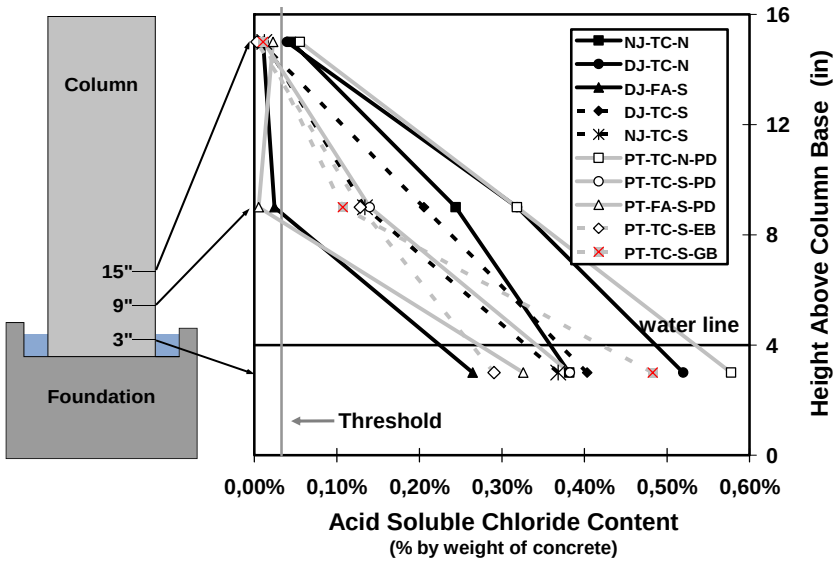

Figure 3.20 Concrete Chloride Penetration at 1.0 inch for All Columns in Non-Dripper Side at End of Testing[1]

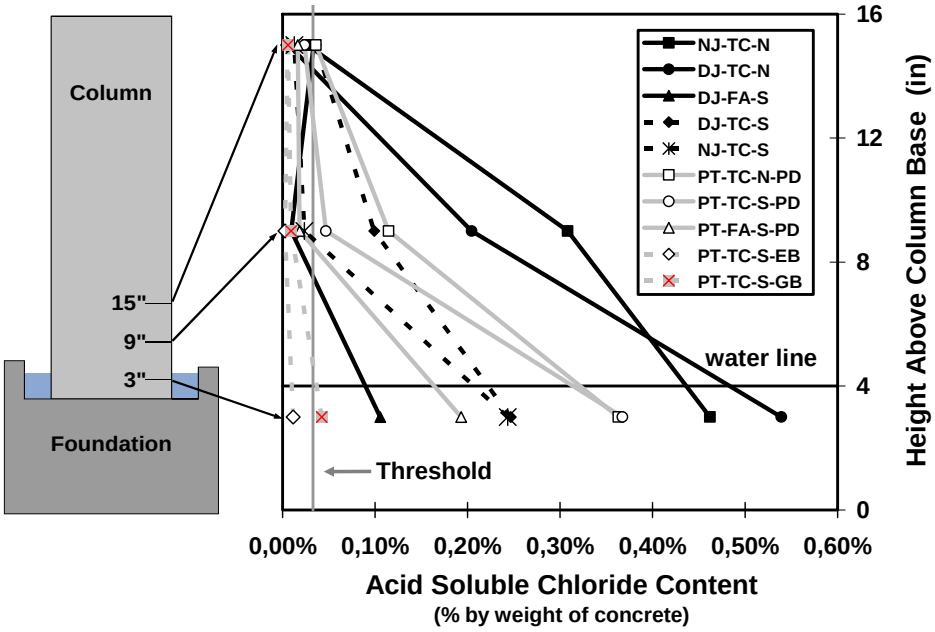

Figure 3.21 Concrete Chloride Penetration at 2.0 inches for All Columns in Non-Dripper Side at End of Testing[1]

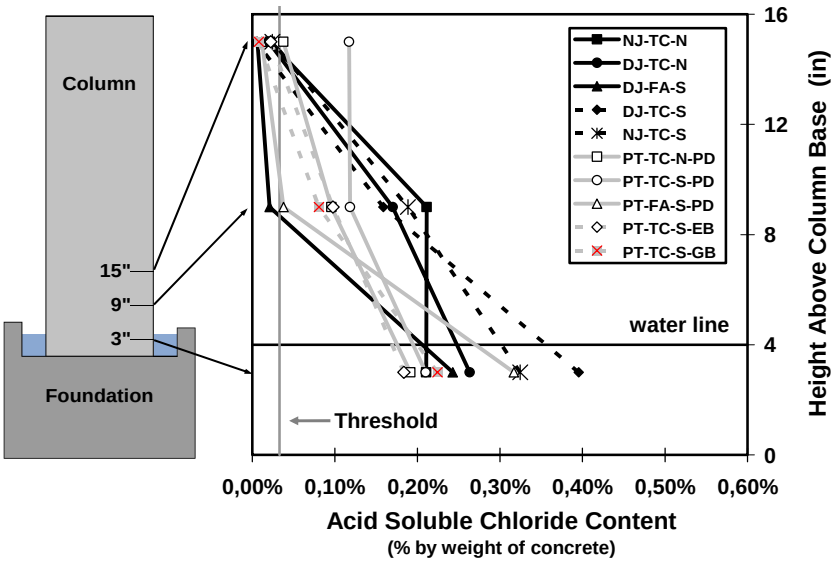

Figure 3.22 Concrete Chloride Penetration at 0.5 inches for All Columns in Dripper Side at End of Testing[1]

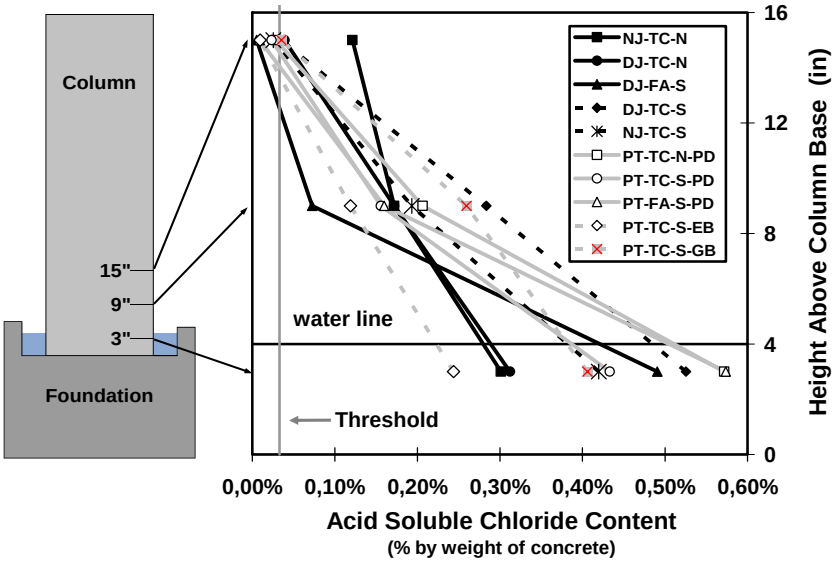

Figure 3.23 Concrete Chloride Penetration at 1.0 inches for All Columns in Dripper Side at End of Testing[1]

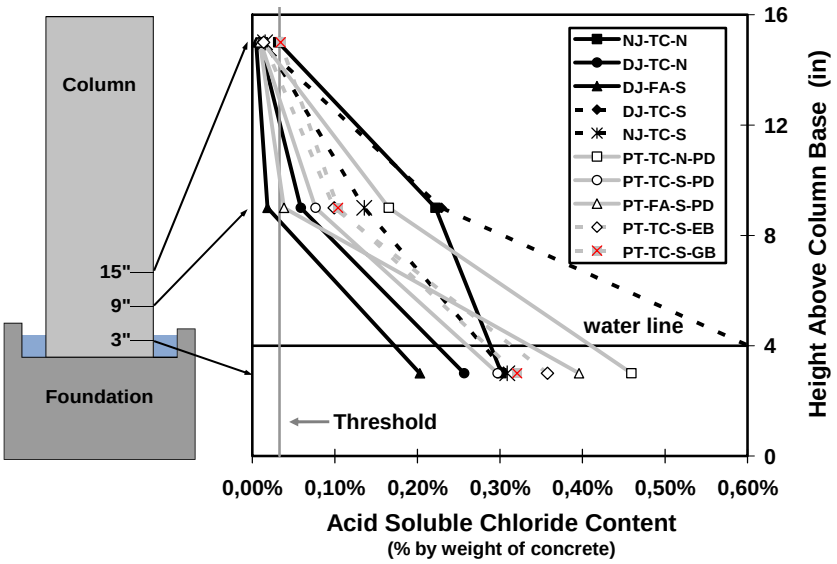

Figure 3.24 Concrete Chloride Penetration at 2.0 inches for All Columns in Dripper Side at End of Testing[1]

3.3 PREDICTION OF SPECIMEN PERFORMANCE USING HALF-CELL POTENTIAL DATA

The higher probability of corrosion using half-cell potential readings was found at the base of the column specimens. There was not a distinct trend with respect to dripper and non – dripper sides. The poorest performance was found for unloaded non-prestressed specimens and specimens with no-joint.

There was not a distinct trend between post-tensioned and non-prestressed columns. Only specimen NJ-TC-S showed slightly higher probability of corrosion than other specimens, when analyzing absolute values.

Only specimens NJ-TC-N, NJ-TC-S, PT-TC-N-PD (Rebar and PT Bars), PT-FA-S-PD (PT Bars), and PT-TC-S-EB (Rebar) showed some indication of corrosion activity over time, when analyzing trends over the total exposure period.

There was not a distinct trend with respect to post-tensioned bars in plastic ducts or galvanized ducts. Neither, was there any distinction between galvanized or epoxy-coated bars, compared to plain PT-Bars.

CHAPTER 4: FORENSIC EXAMINATION

4.1 PROCEDURE

4.1.1 Specimen Condition at End of Testing

Specimens were evaluated at the end of testing for signs of cracking or distress and corrosion stains.

4.1.2 Foundation Saw Cuts

Prior to concrete removal, column specimens sharing the same foundation were separated by saw cutting as shown in Figure 4.1. Due to special saw cutting equipment requirements, saw cutting had to be contracted with an external concrete demolition company.

Figure 4.1 Saw Cutting of Column Foundation[1]

4.1.3 Concrete Removal

Concrete in column specimens was carefully removed using pneumatic equipment, as shown in Figure 4.2. Care was exercised to ensure total exposure and removal of spiral and longitudinal mild steel reinforcement and post-tensioning duct/PT bar systems. Reinforcement was immediately inspected for any color changes due to drying of the corroded steel surfaces, if any. Reinforcement cages were dismantled for careful reinforcement inspection and rating.

4.2 AUTOPSY PROGRAM

All specimens (ten in total) were autopsied at the end of six and a half years of continuous exposure testing. After concrete was removed from each column, mild steel reinforcement, post-tensioning ducts and high-strength post-tensioning bars were carefully inspected and rated according to the corrosion rating scheme explained in the following section. During autopsy, ducts were cut open in half longitudinally, and grout samples were taken at different locations to investigate chloride ingress to the post-tensioning bar level. Anchorages and bar splices were also inspected for signs of corrosion in the areas exposed to concrete and at the crevices, where steel pieces in the post-tensioning system were in contact.

Figure 4.2 Concrete Removal and Reinforcement Dismantling[1]

4.3 EVALUATION AND CORROSION RATING USED DURING FORENSIC EXAMINATION

To maintain consistency in the corrosion ratings among the different series in the durability project, the same generalized evaluation and rating system previously used in the macrocell and beam corrosion tests, was used in the column series with only minor changes due to the specific specimen characteristics. The length of reinforcing bar, post-tensioning bar and post-tensioning duct in the column was subdivided into 34 two-inch increments. In addition, the post-tensioning bar length within the foundation was subdivided into seven two-inch increments. Dowels were subdivided into 26 two-inch increments and spirals were subdivided into 11 two-inch increments for every spiral step in the column North side and 11 two-inch increments for every step in the column South side. At each increment, the steel was examined and a rating was assigned to describe the corrosion severity within that increment. The ratings for all increments were summed to give a total corrosion rating for the element that could be compared for different specimens. This method allowed evaluation of corrosion extent and severity.

4.3.1 Mild Steel Reinforcement (Spirals, longitudinal Steel and dowels)

Mild steel reinforcement was examined at the intervals described above, which is also illustrated in Figure 4.3.

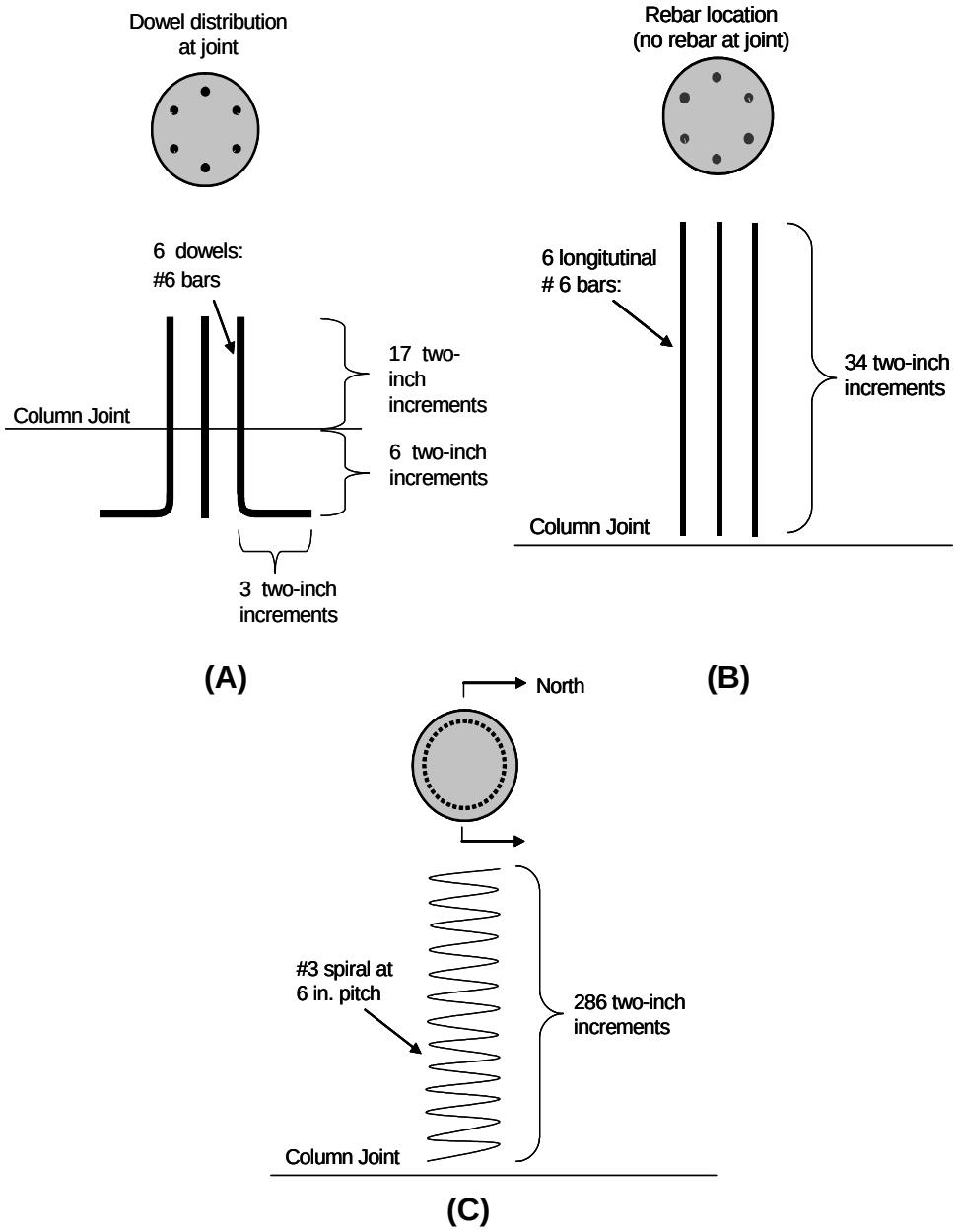

Figure 4.3 Intervals for Corrosion Ratings on (A) dowels, (B) mild steel longitudinal bars, and (C) spiral[1]

Corrosion ratings were assigned to indicate corrosion severity for each interval (considering top and bottom surfaces in the same corrosion rating). This procedure differs from that used in the beam and macrocell corrosion series, where the horizontal rebar top and bottom surfaces were rated separately. However, it was found that one corrosion rating was enough to adequately determine extent and severity of corrosion in these vertical bars. The total bar corrosion rating was calculated as indicated in the following equations.

Mild steel longitudinal bars:

$$\text{Bar Corrosion Rating} = \sum_{i=1}^{34}\sum_{j=1}^{6} R_{\text{Barj, Segmenti}} \qquad \textit{Eq. 3}$$

Mild steel dowels:

$$\text{Dowel Corrosion Rating} = \sum_{i=1}^{26}\sum_{j=1}^{6} R_{\text{Dowelj, Segmenti}} \qquad \textit{Eq. 4}$$

Spiral reinforcement: ***Eq. 5***

$$\text{Spiral Corrosion Rating} = \sum_{i=1}^{13}\sum_{j=1}^{11} R_{\text{North Segmentj,Spiral Stepi}} + \sum_{i=1}^{13}\sum_{j=1}^{11} R_{\text{Sourth Segmentj,Spiral Stepi}}$$

The reason for having distinctive totals for the North and South spiral sides was intended to identify any difference in spiral corrosion condition between the dripper and the non-dripper sides.

The corrosion rating system used is described in Table 4.1.

Table 4.1 Evaluation and Rating System for Corrosion Found on Mild Steel Bars[14]

Code	Meaning	Description	Rating
NC	No Corrosion	No evidence of corrosion	0
D	Discoloration	No evidence of corrosion, but some discoloration from original color	1
L	Light	Surface corrosion on less than one half of the interval, no pitting. Surface corrosion can be removed using cleaning pad.	2
M	Moderate	Surface corrosion on more than one half of the interval, no pitting. **and/or** Corrosion can not be completely removed using cleaning pad.	4
P	Pitting	Pits visible to unaided eye.	8
AR	Area Reduction	Measurable reduction in bar cross-sectional area due to corrosion	R^2

R = Estimated cross-sectional area reduction in percent.

4.3.2 Post-Tensioning Ducts

Post-Tensioning ducts were examined over 34 two-inch intervals, as indicated in Figure 4.4. At each location, corrosion ratings are assigned to indicate the severity of corrosion on the top and bottom surfaces of the inside and outside of each duct to reflect the possibility of different corrosion severity and extent. The corrosion rating system is described in Table 4.2. The total duct corrosion rating was calculated as follows:

$$\text{Duct Corrosion Rating} = \sum_{i=1}^{34}\left(R_{\text{TopOuter},i} + R_{\text{BotOuter},i} + R_{\text{TopInner},i} + R_{\text{BotInner},i}\right) \qquad \textit{Eq.6}$$

where, $R_{\text{TopOuter},i}$ = top outer surface corrosion rating, interval i

$R_{\text{BotOuter},i}$ = bottom outer surface corrosion rating, interval i

$R_{\text{TopInner},i}$ = top inner surface corrosion rating, interval i

$R_{\text{BotInner},i}$ = bottom inner surface corrosion rating, interval i.

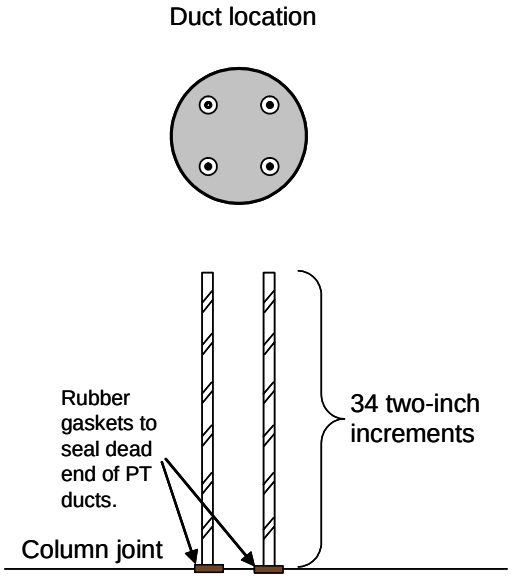

Figure 4.4 Intervals for Corrosion Ratings on PT Ducts[1]

Table 4.2 Evaluation and Rating System for Corrosion Found on Post-Tensioning Duct[14]

Code	Meaning	Description	Rating
NC	No Corrosion	No evidence of corrosion	0
D	Discoloration	No evidence of corrosion, but some discoloration from original color	1
L	Light	Surface corrosion on less than one half of the interval, no pitting.	2
M	Moderate	Surface corrosion on more than one half of the interval, no pitting.	4
S	Severe	Corrosion completely covers the interval. **and/or** Presence of pitting.	8
H	Hole Through Duct	Hole corroded through duct. Used in conjunction with ratings D, L, M and S.	$32 + A_h$

A_h = Area of hole(s) in mm^2

4.3.3 Post-tensioning Bars

Post-tensioning bars were examined at 34 intervals inside the column element and at seven two-inch increments in the short length of bar embedded in the foundation with bearing plate and nut as shown in Figure 4.5.

The total corrosion rating was calculated as follows:

$$\text{PT Bar Corrosion Rating} = \sum_{i=1}^{34}\sum_{j=1}^{4} R_{\text{PT Barj, Segment i}} + \sum_{k=1}^{7}\sum_{j=1}^{4} R_{\text{PT Barj, Segment k}} \qquad \textit{Eq. 7}$$

where, $R_{\text{PT Bar j, Segment i...}}$ = PT Bar j corrosion rating, interval i

(PT bar portion located inside column element).

$R_{\text{PT Bar j, Segment k...}}$ = PT Bar j Corrosion rating, interval k

(PT bar portion inside foundation).

The evaluation and rating system used for PT bars was the same system used for mild steel bars, as shown in Table 4.1.

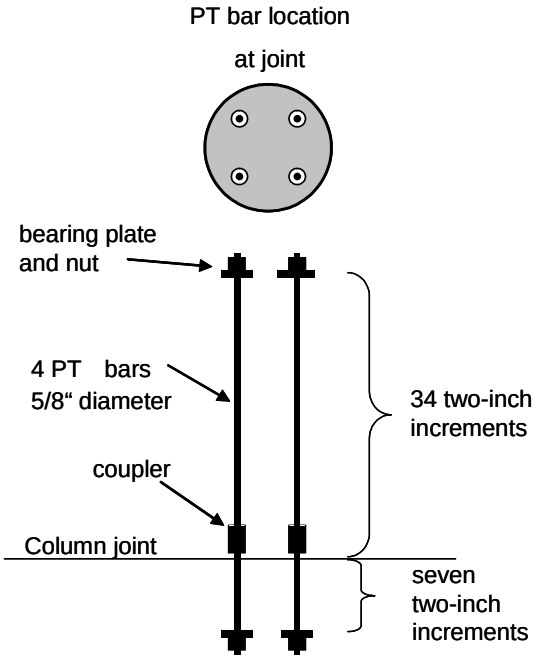

Figure 4.5 Intervals for Corrosion Ratings on PT Bars[1]

4.4 FORENSIC EXAMINATION RESULTS

4.4.1 Detailed Visual Inspection

A brief summary of forensic examination results after six and a half years of exposure is provided for each column specimen in the following sections. In general, at the end of testing rust stains were only visible in the base of the columns, in the bottom12 inches. No signs of cracking were observed in the column surfaces. Figure 4.6 shows the condition of the specimens after unloading and tie down bar cutting.

Tie down bars had uniform corrosion at the column base level, which stained the foundation, but no severe pitting was observed on these high-strength bars.

Figure 4.6 Specimen Condition at the End of Testing[1]

4.4.1.1 Specimen NJ-TC-N (No dowel, Class C Concrete, No load)

No signs of cracking were visible in the column surfaces and no corrosion stains were present at the column base, as observed in Figure 4.7.

Corrosion in the spiral was mostly concentrated at the spiral base (first 18 inches). In this region light corrosion was observed in a few segments with only two two-inch segments in the North side (dripper side) showing severe corrosion and pitting. The rest of the spiral had some discoloration from the original bar color with no signs of corrosion. See Figure 4.8.

Reinforcing bars were in excellent condition. Only rebar #2 showed light corrosion in one of the two inch segments as shown in Figure 4.8.

Corrosion Rating:

Specimen	NJ-TC-N
Autopsy after 6.5 years	
Spiral	532
Rebar	2
Dowel	NA
Duct #1	NA
Duct #2	NA
Duct #3	NA
Duct #4	NA
PT-Bar	NA

Figure 4.7 Condition of Specimen NJ-TC-N at the End of Testing[1]

Complete Cage

Spiral

Rebar #2

Figure 4.8 Reinforcement Condition for Specimen NJ-TC-N[1]

4.4.1.2 Specimen DJ-TC-N (Doweled Joint, Class C Concrete, No Load)

Only very few corrosion stains were visible at the base of the column. The rest of the specimen had no signs of cracking or corrosion stains.

Spiral reinforcement had pitting in the North side at the base of the column in the center three two-inch segments, as shown in Figure 4.9. Light to moderate corrosion extended up to a height of 14 inches from the column base, in both the North and the South sides. In the dripper side, light corrosion was concentrated in the center six inches of the total height of the spiral. In the non-dripper side, only discoloration and few areas of light corrosion were visible in the total spiral height.

The six reinforcing bars showed only light corrosion and discoloration in the first eight inches from the column base. The rest of the bar lengths were in excellent condition.

All six dowels showed severe corrosion and pitting at the column base (column-foundation interface). As shown in Figure 4.10, area reduction in the dowel bars was concentrated and severe, especially in Dowel #4 and Dowel #5.

Corrosion Rating:

Specimen	DJ-TC-N
Autopsy after 6.5 years	
Spiral	595
Rebar	35
Dowel	2704
Duct #1	NA
Duct #2	NA
Duct #3	NA
Duct #4	NA
PT-Bar	NA

Figure 4.9 Condition of Specimen DJ-TC-N at the End of Testing[1]

Complete Cage

Spiral

Rebar #3

Dowel #4

Figure 4.10 Reinforcement Condition for Specimen DJ-TC-N[1]

4.4.1.3 Specimen DJ-FA-S (Doweled Joint, Fly Ash Concrete, Service Load)

The specimen surface had no signs of corrosion stains or cracking. Concrete was in excellent condition at the end of testing. See Figure 4.11.

Spiral reinforcement had moderate corrosion in the North side (non-dripper side) at the four-inch level from the column base. Light corrosion was also concentrated in the spiral North side in the center four two-inch segments from the four-inch height up to a height of 30 inches.

Figure 4.11 Condition of Specimen DJ-FA-S at the End of Testing[1]

Corrosion Rating:

Specimen	DJ-FA-S
Autopsy after 6.5 years	
Spiral	360
Rebar	19
Dowel	619
Duct #1	NA
Duct #2	NA
Duct #3	NA
Duct #4	NA
PT-Bar	NA

The rest of the spiral in the north and south sides had from light corrosion to only discoloration.

Mild steel longitudinal reinforcement showed very few areas of light corrosion. Rebar #2 had light corrosion between the heights of 36 to 52 inches from the column base (with respect to the rebar analysis length of 68 inches). This bar was located in the dripper side.

Dowels showed in general light to moderate corrosion in the two-inch segment at the column base (joint location). Dowel #1 showed the heaviest corrosion and area loss in this region, as shown in Figure 4.12.

Complete Cage

Spiral

Rebar #1

Dowel #1

Figure 4.12 Reinforcement Condition for Specimen DJ-FA-S[1]

4.4.1.4 Specimen DJ-TC-S (Doweled Joint, Class C Concrete, Service Load)

No signs of corrosion were observed in the column surfaces at the end of testing. Concrete was in excellent condition.

Spiral reinforcement showed very similar corrosion ratings in the non-dripper and dripper sides. Light to moderate corrosion was concentrated in the first 22 inches from the column base; and, also some areas of moderate corrosion were observed in a few segments at the 46-inch and 53-inch levels.

Rebar corrosion in all cases was reduced to only light corrosion and bar discoloration in the first six segments. Moderate corrosion was very localized as observed in Rebar #3 in Figure 4.14.

Dowels showed light pitting and moderate corrosion in the vicinity of the column joint. Section loss was not significant, as observed in Figure 4.14.

Corrosion Rating:

Specimen	DJ-TC-S
Autopsy after 6.5 years	
Spiral	458
Rebar	26
Dowel	86
Duct #1	NA
Duct #2	NA
Duct #3	NA
Duct #4	NA
PT-Bar	NA

Figure 4.13 Condition of Specimen DJ-TC-S at the End of Testing[1]

Complete Cage

Spiral

Rebar #3

Dowel #3

Figure 4.14 Reinforcement Condition for Specimen DJ-TC-S[1]

4.4.1.5 Specimen NJ-TC-S (No dowel, Class C Concrete, Service load)

No signs of cracking or spalling were visible on the column surfaces. Rust stains extended the first 5 inches, from the column base, as shown in Figure 4.15. No other signs of corrosion were visible in the specimen.

Corrosion Rating:

Specimen	NJ-TC-S
Autopsy after 6.5 years	
Spiral	10266
Rebar	32
Dowel	NA
Duct #1	NA
Duct #2	NA
Duct #3	NA
Duct #4	NA
PT-Bar	NA

Figure 4.15 Condition of Specimen NJ-TC-S at the End of Testing[1]

Extremely severe spiral corrosion was mostly located at the base, in the North side (Dripper side) in the first three spiral steps (see Figure 4.16).

Rebar corrosion was concentrated in the first four inches from the column base. Rebar #1 showed the most severe corrosion with light pitting, while the other bars only had light to moderate corrosion. See Figure 4.16. The specimen did not have dowels.

Complete Cage

Spiral

Rebar #1

Figure 4.16 Reinforcement Condition for Specimen NJ-TC-S[1]

4.4.1.6 Specimen PT-TC-N-PD (Post-Tensioned, Class C Concrete, No Load, Plastic Duct)

As shown in Figure 4.17, the concrete surface was in excellent condition at the end of testing. No signs of corrosion stains or cracking were visible.

As shown in Figure 4.18, the spiral reinforcement showed light to moderate uniform corrosion in the first two steps (up to a height of nine inches). From this level to the top of the spiral (corresponding to the top of the column), the reinforcement only showed discoloration. Rebar corrosion was negligible.

Corrosion Rating:

Specimen	PT-TC-N-PD
Autopsy after 6.5 years	
Spiral	351
Rebar	9
Dowel	NA
Duct #1	Plastic
Duct #2	Plastic
Duct #3	276
Duct #4	4
PT-Bar	673

Figure 4.17 Condition of Specimen PT-TC-N-PD at the End of Testing[1]

Complete Cage

Spiral

Rebar #1

Figure 4.18 Reinforcement Condition for Specimen PT-TC-N-PD[1]

As shown in Figure 4.20, plastic ducts were in good condition with no signs of damage. One galvanized steel duct (Duct #3) showed moderate corrosion in the first 10 inches from the column base. This duct was located in the dripper side. Severe corrosion was found on this duct in the first two inches, in the area were the rubber gasket was located. Duct #4 in the non-dripper side showed negligible corrosion at the base.

The anchorage plate in the top of the column, below the pour-back, was found with moderate to severe corrosion, as shown in Figure 4.19. This finding was typical for all Post-Tensioned specimens.

Post-tensioned bars showed severe corrosion and section loss at the column-foundation joint section, as shown in Figure 4.20. PT bar localized corrosion was observed in both post-tensioned bars in the dripper side, in both plastic and galvanized steel duct.

Figure 4.19 PT Bar Top Anchorage Condition for Specimen PT-TC-N-PD[1]

4.4.1.7 Specimen PT-TC-S-PD (Post-Tensioned, Class C Concrete, Service Load, Plastic Duct)

As shown in Figure 4.21, no signs of corrosion or cracking were present in the concrete surfaces at the end of testing.

As shown in Figure 4.22, spiral reinforcement was found in very good condition at the end of testing. There was light corrosion up to a level of 9 inches in both dripper and non-dripper sides.

Rebar corrosion was negligible.

Figure 4.23 indicates that plastic ducts were in good condition, while galvanized steel ducts showed substantial area loss (approximately 260 mm^2 for Duct #3 and 1400 m^2 for Duct #4) in the first two inches from the column base, behind the rubber gasket. Post-tensioned bars showed moderate corrosion in the vicinity of the joint section and light to negligible corrosion in the other areas.

Corrosion Rating:

Specimen	PT-TC-S-PD
Autopsy after 6.5 years	
Spiral	339
Rebar	3
Dowel	NA
Duct #1	Plastic
Duct #2	Plastic
Duct #3	312
Duct #4	1461
PT-Bar	146

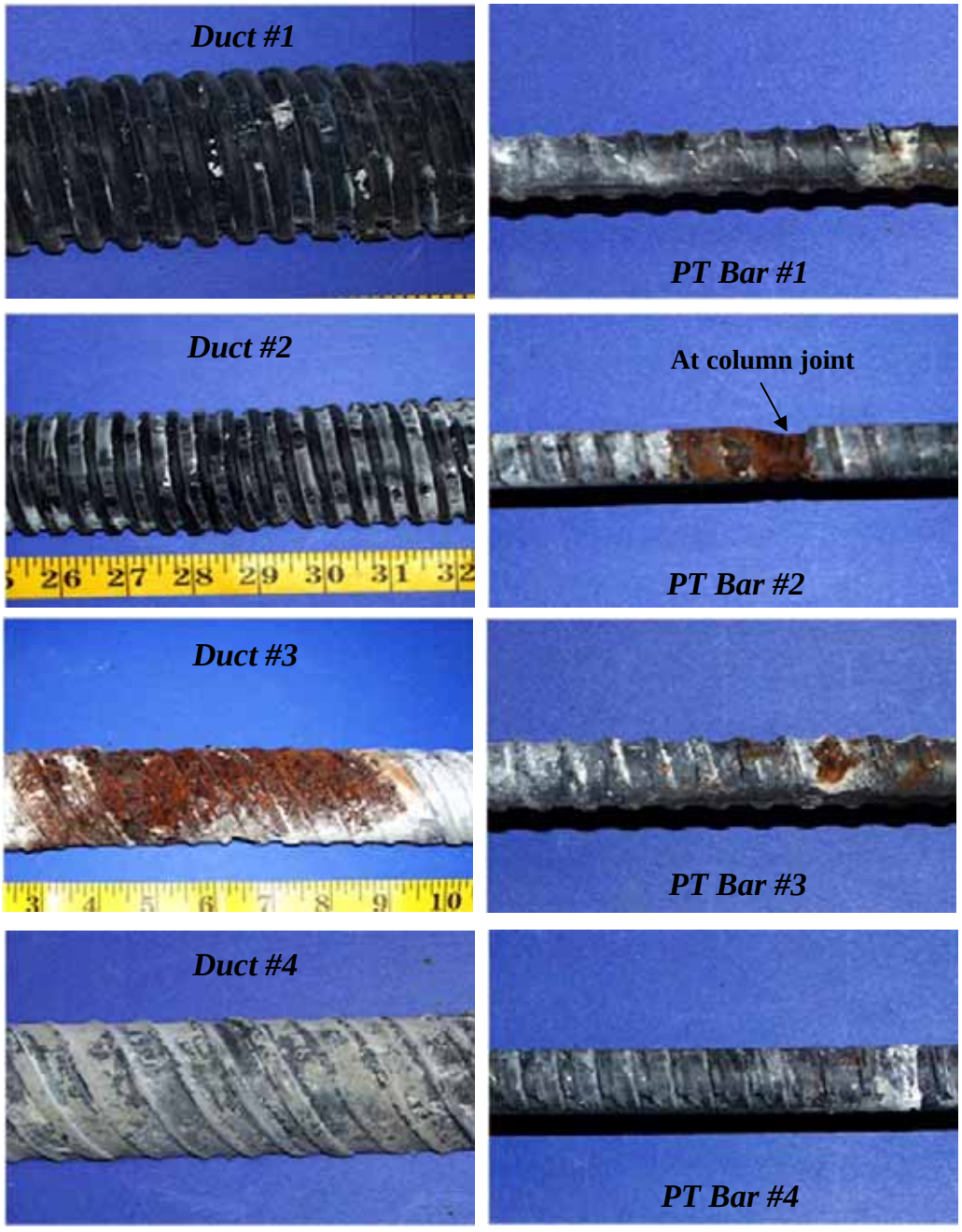

Figure 4.20 Reinforcement Condition for Specimen PT-TC-N-PD[1]

Figure 4.21 Condition of Specimen PT-TC-S-PD at the End of Testing[1]

Complete Cage

Spiral

Rebar #4

Figure 4.22 Reinforcement Condition for Specimen PT-TC-S-PD[1]

Duct #1

Duct #4

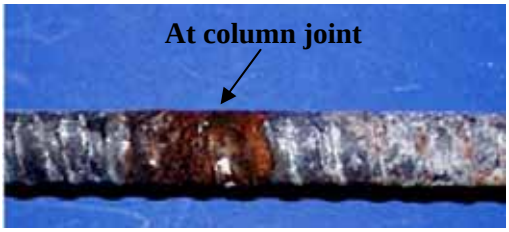

PT Bar #1

Figure 4.23 Duct and PT Bar Condition for Specimen PT-TC-S-PD[1]

4.4.1.8 Specimen PT-FA-S-PD (Post-Tensioned, Fly Ash Concrete, Service Load, Plastic Duct)

The concrete surface was in excellent condition at the end of testing as shown in Figure 4.24.

Figure 4.25 indicates that spiral reinforcement showed light corrosion and discoloration in approximately the first 23 inches from the column base level. No distinction was observed between the dripper and non-dripper sides. Rebar reinforcement corrosion was negligible.

Plastic ducts were in good condition and galvanized steel ducts showed moderate to severe corrosion in the first two inches from the column base level, in the rubber gasket location, as shown in Figure 4.26. Post-tensioned bars also showed moderated corrosion concentrated around the column-foundation joint section.

Corrosion Rating:

Specimen	PT-FA-S-PD
Autopsy after 6.5 years	
Spiral	337
Rebar	12
Dowel	NA
Duct #1	Plastic
Duct #2	Plastic
Duct #3	12
Duct #4	12
PT-Bar	95

Figure 4.24 Condition of Specimen PT-FA-S-PD at the End of Testing[1]

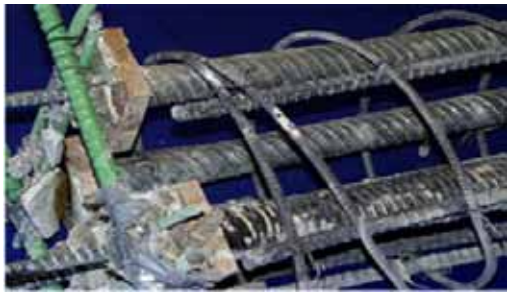

Complete Cage

Spiral

Rebar #6

Figure 4.25 Reinforcement Condition for Specimen PT-FA-S-PD[1]

Duct #1

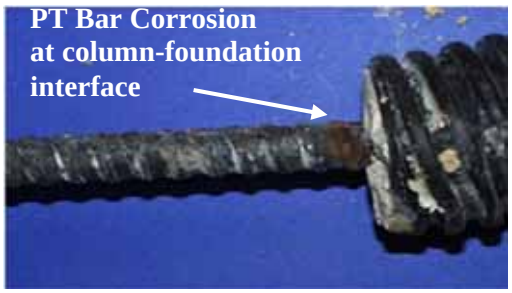

PT Bar #2 and Duct #2

PT Bar #3 and Duct #3

Figure 4.26 Duct and PT Bar Condition for Specimen PT-FA-S-PD[1]

4.4.1.9 Specimen PT-TC-S-EB (Post-Tensioned, Class C Concrete, Service Load, Epoxy-Coated PT Bar)

Few corrosion stains were visible at the end of testing in the base of the column, as shown in Figure 4.27.

Figure 4.28 shows that spiral reinforcement corrosion was limited to discoloration in the whole spiral length and mild steel longitudinal reinforcement had negligible corrosion.

Figure 4.29 showed ducts had very severe corrosion and extensive area loss in the first two to three inches from the column base level, behind the rubber gasket location.

Epoxy-coated post-tensioning bars (PT Bars #3 and #4) showed localized corrosion at the column-foundation joint section. The other areas of bar were in excellent condition. Regular black steel bars (PT Bars #1 and #2) had light to moderate corrosion in the vicinity (+/-10 inches) of the column base.

Corrosion Rating:

Specimen	PT-TC-S-EB
Autopsy after 6.5 years	
Spiral	291
Rebar	6
Dowel	NA
Duct #1	1740
Duct #2	16
Duct #3	2590
Duct #4	440
PT-Bar #1,#2	42
PT-Bar #3,#4	10

Figure 4.27 Condition of Specimen PT-TC-S-EB at the End of Testing[1]

Spiral

Rebar #3

Figure 4.28 Reinforcement Condition for Specimen PT-TC-S-EB[1]

Duct #4

PT Bar #3

PT Bar #1

Figure 4.29 Duct and PT Bar Condition for Specimen PT-TC-S-EB[1]

4.4.1.10 Specimen PT-TC-S-GB (Post-Tensioned, Class C Concrete, Service Load, Galvanized PT Bar)

Figure 4.30 showed that at the end of testing, no cracking or other signs of distress were observed.

Figure 4.31 indicates that the spiral reinforcement in the dripper side had only light corrosion at a level of three inches from the column base, and light corrosion in the center region from a height of 53 inches to 64 inches. In the non-dripper side, no corrosion was found in the spiral steel. No corrosion was found on mild steel longitudinal reinforcement.

Figure 4.32 shows that ducts were corroded with extensive area loss in the first two inches from the column base level, at the rubber gasket location.

Corrosion Rating:

Specimen	PT-TC-S-GB
Autopsy after 6.5 years	
Spiral	331
Rebar	0
Dowel	NA
Duct #1	2174
Duct #2	1810
Duct #3	2664
Duct #4	2665
PT-Bar #1,#2	39
PT-Bar #3,#3	21

Figure 4.30 Condition of Specimen PT-TC-S-GB at the End of Testing[1]

Complete Cage

Spiral

Rebar #3

Figure 4.31 Reinforcement Condition for Specimen PT-TC-S-GB[1]

Duct *PT Bar #4*

Figure 4.32 Reinforcement Condition for Specimen PT-TC-S-GB[1]

Galvanized PT bars (PT Bars #3 and #4) showed localized corrosion and pitting at the column base level. Black steel bars showed a more uniform corrosion in the vicinity of the joint section (the region defined between 12 inches at each side of the joint).

4.4.2 Corrosion Rating Summary

Spiral, longitudinal mild steel, dowel, duct and post-tensioning bar ratings are listed in Tables 4.3 through 4.13, and plotted in Figure 4.33 through Figure 4.42. Average, standard deviation and median values are listed at the bottom of the total corrosion tables. All these results correspond to the autopsy performed at six and a half years of exposure testing.

Data is presented in two analysis scenarios:

- Maximum corrosion rating in any two-inch increment
- Total corrosion rating in the complete element, adding corrosion rating for all increments

Specimen notation from Table 2.4 is repeated herein, in Table 4.3, to assist the reader:

Table 4.3 Specimen Notation[2]

Connection Type	Loading	Concrete type	PT Protection
DJ: Doweled Joint	**N:** No Load	**TC:** TxDOT Class C	**PD:** Plastic Duct
PT: Post-Tensioned Joint			**EB:** Epoxy-Coated PT Bar**
NJ: No dowel	**S:**Service Load	**FA:** 35% Fly Ash	**GB:** Galvanized PT Bar**
			Blank: Not applicable (i.e., no PT)
Example: PT-TC-S-PD			

* plastic ducts used for bars 1 and 2, galvanized steel ducts used for bars 3 and 4
** epoxy-coated or galvanized bars used for bars 3 and 4, uncoated bars used for bars 1 and 2

Table 4.4 Maximum Spiral Corrosion Rating in any two-inch increment for All Specimens[1]

Specimen Name	Maximum Spiral Corrosion Rating	
	Dripper side	Non-Dripper side
NJ-TC-N	100	2
DJ-TC-N	62	4
DJ-FA-S	8	4
DJ-TC-S	8	4
NJ-TC-S	3470	1
PT-TC-N-PD	8	4
PT-TC-S-PD	2	2
PT-FA-S-PD	2	2
PT-TC-S-EB	1	1
PT-TC-S-GB	2	2

Table 4.5 Total Spiral Corrosion Rating for All Specimens[1]

Specimen Name	Total Spiral Corrosion Rating		
	Dripper side	Non-Dripper side	Total
NJ-TC-N	322	210	532
DJ-TC-N	367	228	595
DJ-FA-S	175	185	360
DJ-TC-S	216	242	458
NJ-TC-S	10123	143	10266
PT-TC-N-PD	177	174	351
PT-TC-S-PD	169	170	339
PT-FA-S-PD	159	178	337
PT-TC-S-EB	148	143	291
PT-TC-S-GB	177	154	331
Average	1203.3	182.7	1386
Std. Dev.	2974.1	32.5	2961.5
Median	177	176	355.5

Table 4.6 Maximum Rebar Corrosion Rating in any two-inch Increment for All Specimens[1]

Specimen Name	Maximum Rebar Corrosion Rating
NJ-TC-N	2
DJ-TC-N	2
DJ-FA-S	1
DJ-TC-S	2
NJ-TC-S	8
PT-TC-N-PD	2
PT-TC-S-PD	2
PT-FA-S-PD	2
PT-TC-S-EB	2
PT-TC-S-GB	0

Table 4.7 Total Rebar Corrosion Rating for All Specimens[1]

Specimen Name	Total Rebar Corrosion Rating						
	Bar #1	Bar #2	Bar #3	Bar #4	Bar #5	Bar #6	Total
NJ-TC-N	0	2	0	0	0	0	2
DJ-TC-N	3	7	4	8	9	4	35
DJ-FA-S	4	13	0	0	2	0	19
DJ-TC-S	9	2	9	3	0	3	26
NJ-TC-S	16	10	0	0	0	6	32
PT-TC-N-PD	0	0	6	0	0	3	9
PT-TC-S-PD	0	0	0	0	3	0	3
PT-FA-S-PD	0	0	0	3	3	6	12
PT-TC-S-EB	2	4	0	0	0	0	6
PT-TC-S-GB	0	0	0	0	0	0	0
Average	3.4	3.8	1.9	1.4	1.7	2.2	14.4
Std. Dev.	5.0	4.4	3.1	2.5	2.7	2.4	12.2
Median	1	2	0	0	0	1.5	10.5

Table 4.8 Maximum Dowel Corrosion Rating in any two-inch Increment for All Specimens[1]

Specimen Name	Maximum Dowel Corrosion Rating
NJ-TC-N	NA
DJ-TC-N	2276
DJ-FA-S	591
DJ-TC-S	8
NJ-TC-S	NA
PT-TC-N-PD	NA
PT-TC-S-PD	NA
PT-FA-S-PD	NA
PT-TC-S-EB	NA
PT-TC-S-GB	NA

NA: NON APPLICABLE

Table 4.9 Total Dowel Corrosion Rating for All Specimens[1]

Specimen Name	Total Dowel Corrosion Rating						
	Dowel #1	Dowel #2	Dowel #3	Dowel #4	Dowel #5	Dowel #6	Total
NJ-TC-N	NA	NA	NA	NA	NA	NA	NA
DJ-TC-N	24	8	15	2284	365	8	2704
DJ-FA-S	603	4	0	4	4	4	619
DJ-TC-S	20	26	25	1	6	8	86
NJ-TC-S	NA	NA	NA	NA	NA	NA	NA
PT-TC-N-PD	NA	NA	NA	NA	NA	NA	NA
PT-TC-S-PD	NA	NA	NA	NA	NA	NA	NA
PT-FA-S-PD	NA	NA	NA	NA	NA	NA	NA
PT-TC-S-EB	NA	NA	NA	NA	NA	NA	NA
PT-TC-S-GB	NA	NA	NA	NA	NA	NA	NA
Average	216	13	13	763	125	7	1136
Std. Dev.	273.9	9.6	10.3	1075.5	169.7	1.9	1129.7
Median	24	8	15	4	6	8	619

NA: NON APPLICABLE

Table 4.10 Maximum Duct Corrosion Rating in any two-inch Increment for All Specimens[1]

Specimen	Maximum Duct Corrosion Rating			
Name	Duct #1	Duct #2	Duct #3	Duct #4
NJ-TC-N	NA	NA	NA	NA
DJ-TC-N	NA	NA	NA	NA
DJ-FA-S	NA	NA	NA	NA
DJ-TC-S	NA	NA	NA	NA
NJ-TC-S	NA	NA	NA	NA
PT-TC-N-PD	Plastic	Plastic	232	2
PT-TC-S-PD	Plastic	Plastic	292	1446
PT-FA-S-PD	Plastic	Plastic	8	8
PT-TC-S-EB	1732	8	2582	432
PT-TC-S-GB	2166	1802	2656	2657

NA: NON APPLICABLE

Table 4.11 Total Duct Corrosion Rating for All Specimens[1]

Specimen	Total Duct Corrosion Rating			
Name	Duct #1	Duct #2	Duct #3	Duct #4
NJ-TC-N	NA	NA	NA	NA
DJ-TC-N	NA	NA	NA	NA
DJ-FA-S	NA	NA	NA	NA
DJ-TC-S	NA	NA	NA	NA
NJ-TC-S	NA	NA	NA	NA
PT-TC-N-PD	Plastic	Plastic	276	4
PT-TC-S-PD	Plastic	Plastic	312	1461
PT-FA-S-PD	Plastic	Plastic	12	12
PT-TC-S-EB	1740	16	2590	440
PT-TC-S-GB	2174	1810	2664	2665
Average	1957	913	1171	916
Std. Dev.	217.0	897.0	1193.7	1022.9
Median	1957	913	312	440

NA: NON APPLICABLE

Table 4.12 Maximum PT-Bar Corrosion Rating in any two-inch Increment for All Specimens[1]

Specimen Name	Maximum PT-Bar Corrosion Rating
NJ-TC-N	NA
DJ-TC-N	NA
DJ-FA-S	NA
DJ-TC-S	NA
NJ-TC-S	NA
PT-TC-N-PD	608
PT-TC-S-PD	4
PT-FA-S-PD	4
PT-TC-S-EB	4
PT-TC-S-GB	4

NA: NON APPLICABLE

Table 4.13 Total PT-Bar Corrosion Rating for All Specimens[1]

Specimen Name	Total PT-Bar Corrosion Rating				
	Bar #1	Bar #2	Bar #3	Bar #4	Total
NJ-TC-N	NA	NA	NA	NA	NA
DJ-TC-N	NA	NA	NA	NA	NA
DJ-FA-S	NA	NA	NA	NA	NA
DJ-TC-S	NA	NA	NA	NA	NA
NJ-TC-S	NA	NA	NA	NA	NA
PT-TC-N-PD	15	626	16	16	673
PT-TC-S-PD	16	22	27	81	146
PT-FA-S-PD	37	15	12	31	95
PT-TC-S-EB	27	15	4	6	52
PT-TC-S-GB	18	21	12	9	60
Average	23	140	14	29	205
Std. Dev.	8.4	243.1	7.5	27.6	236.2
Median	18	21	12	16	95

NA: NON APPLICABLE

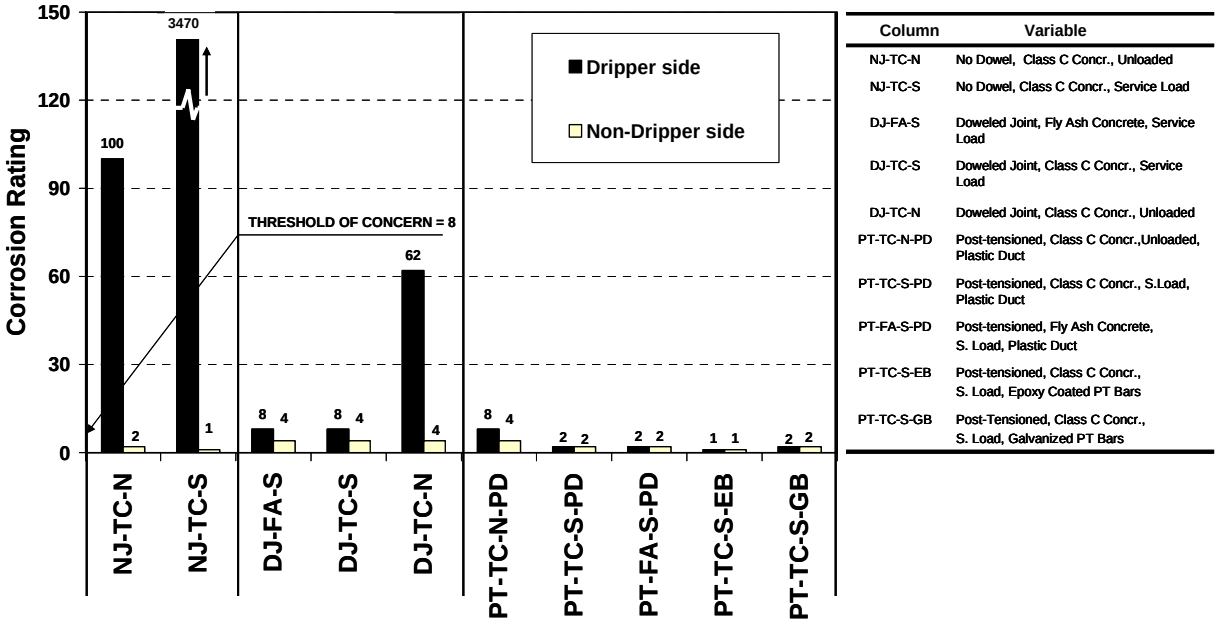

Figure 4.33 Maximum Spiral Corrosion Rating in any two-inch Increment for All Specimens[1]

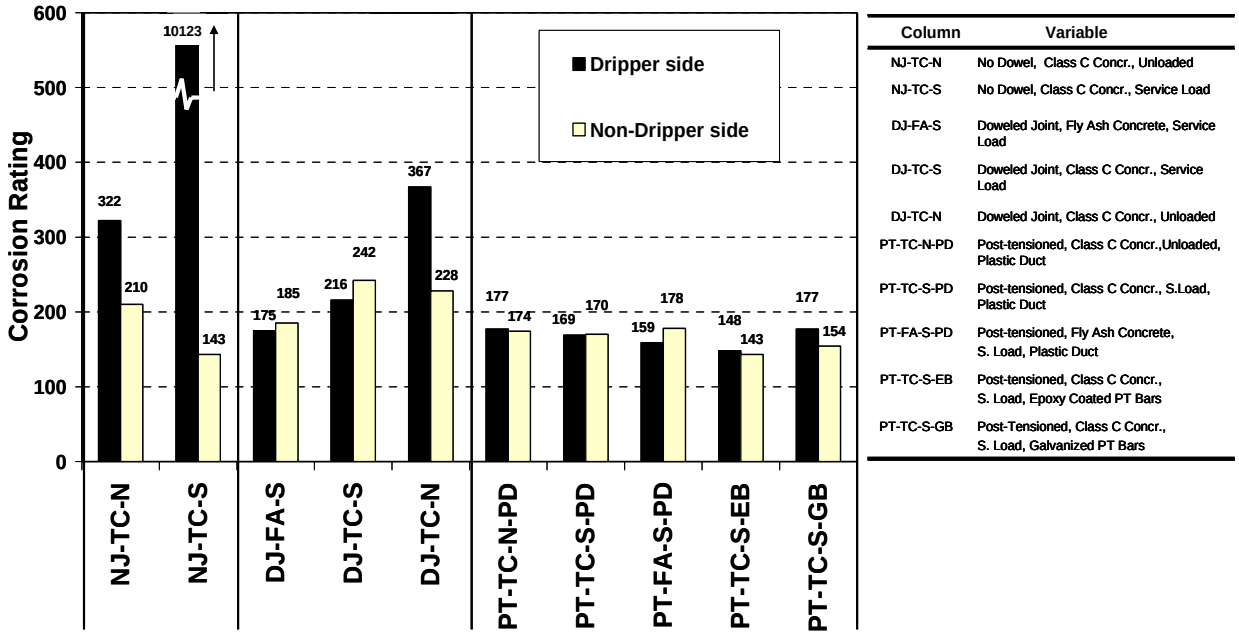

Column	Variable
NJ-TC-N	No Dowel, Class C Concr., Unloaded
NJ-TC-S	No Dowel, Class C Concr., Service Load
DJ-FA-S	Doweled Joint, Fly Ash Concrete, Service Load
DJ-TC-S	Doweled Joint, Class C Concr., Service Load
DJ-TC-N	Doweled Joint, Class C Concr., Unloaded
PT-TC-N-PD	Post-tensioned, Class C Concr.,Unloaded, Plastic Duct
PT-TC-S-PD	Post-tensioned, Class C Concr., S.Load, Plastic Duct
PT-FA-S-PD	Post-tensioned, Fly Ash Concrete, S. Load, Plastic Duct
PT-TC-S-EB	Post-tensioned, Class C Concr., S. Load, Epoxy Coated PT Bars
PT-TC-S-GB	Post-Tensioned, Class C Concr., S. Load, Galvanized PT Bars

Figure 4.34 Total Spiral Corrosion Rating for All Specimens[1]

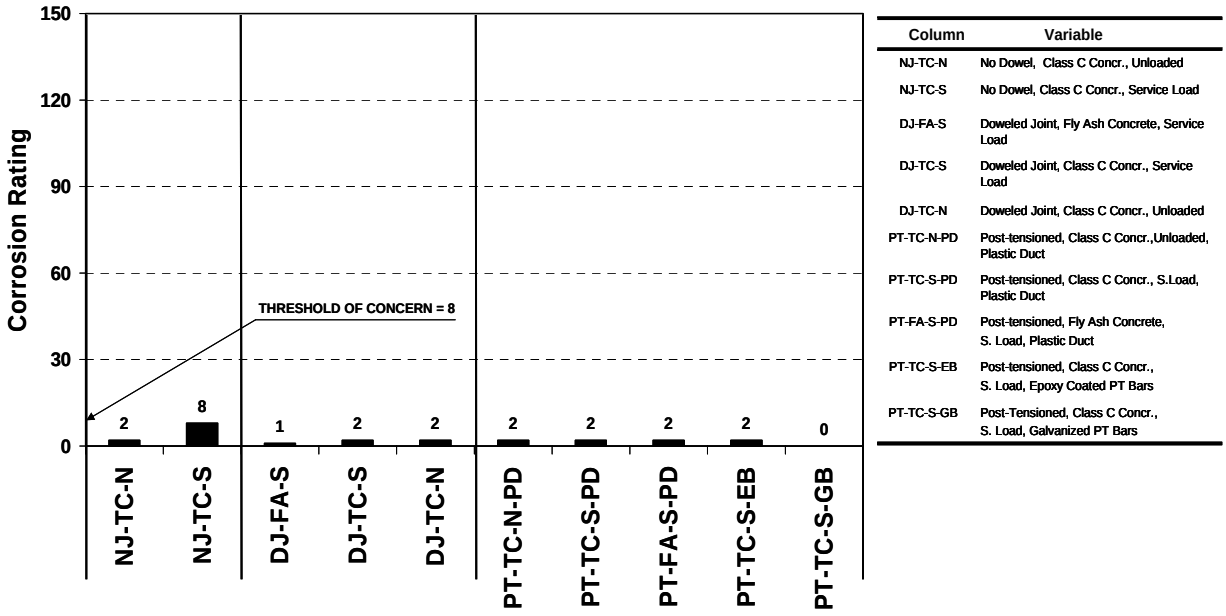

Column	Variable
NJ-TC-N	No Dowel, Class C Concr., Unloaded
NJ-TC-S	No Dowel, Class C Concr., Service Load
DJ-FA-S	Doweled Joint, Fly Ash Concrete, Service Load
DJ-TC-S	Doweled Joint, Class C Concr., Service Load
DJ-TC-N	Doweled Joint, Class C Concr., Unloaded
PT-TC-N-PD	Post-tensioned, Class C Concr.,Unloaded, Plastic Duct
PT-TC-S-PD	Post-tensioned, Class C Concr., S.Load, Plastic Duct
PT-FA-S-PD	Post-tensioned, Fly Ash Concrete, S. Load, Plastic Duct
PT-TC-S-EB	Post-tensioned, Class C Concr., S. Load, Epoxy Coated PT Bars
PT-TC-S-GB	Post-Tensioned, Class C Concr., S. Load, Galvanized PT Bars

Figure 4.35 Maximum Rebar Corrosion Rating in any two-inch Increment for All Specimens[1]

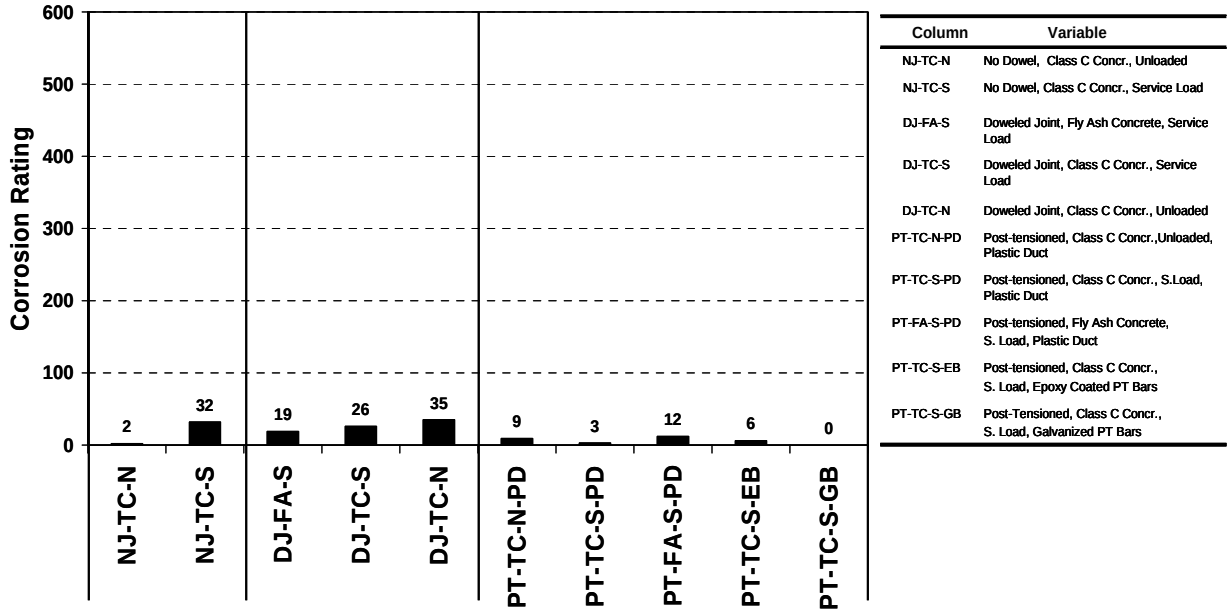

Figure 4.36 Total Rebar Corrosion Rating for All Specimens[1]

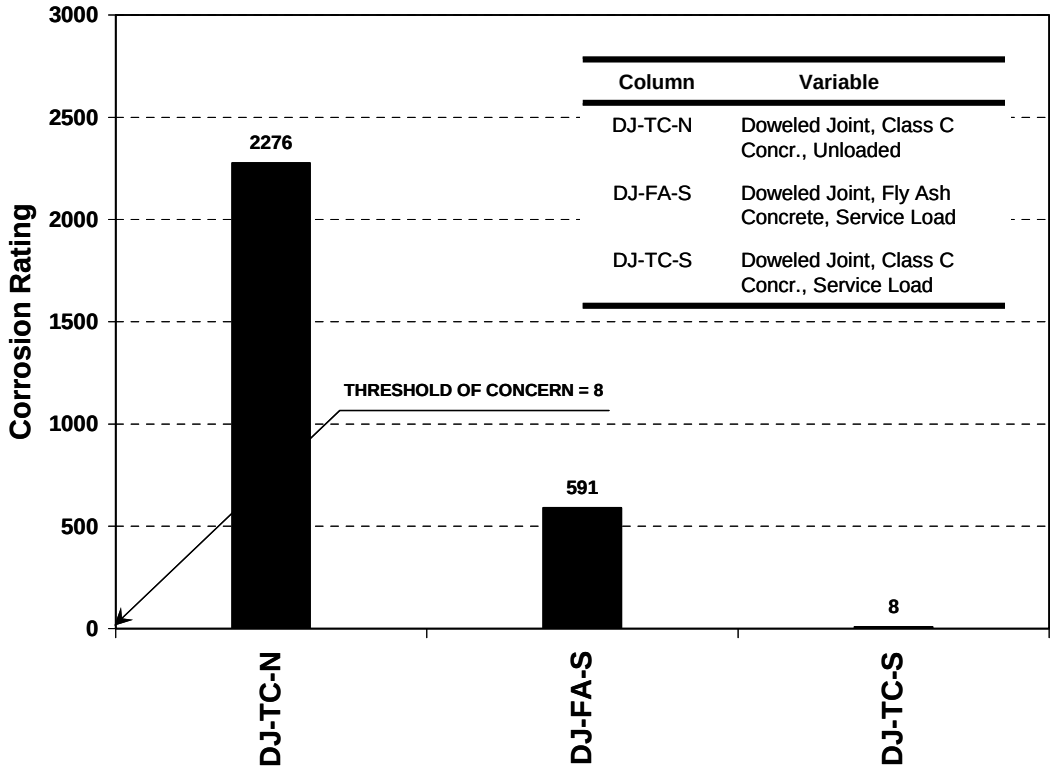

Figure 4.37 Maximum Dowel Corrosion Rating in any two-inch Increment for All Specimens[1]

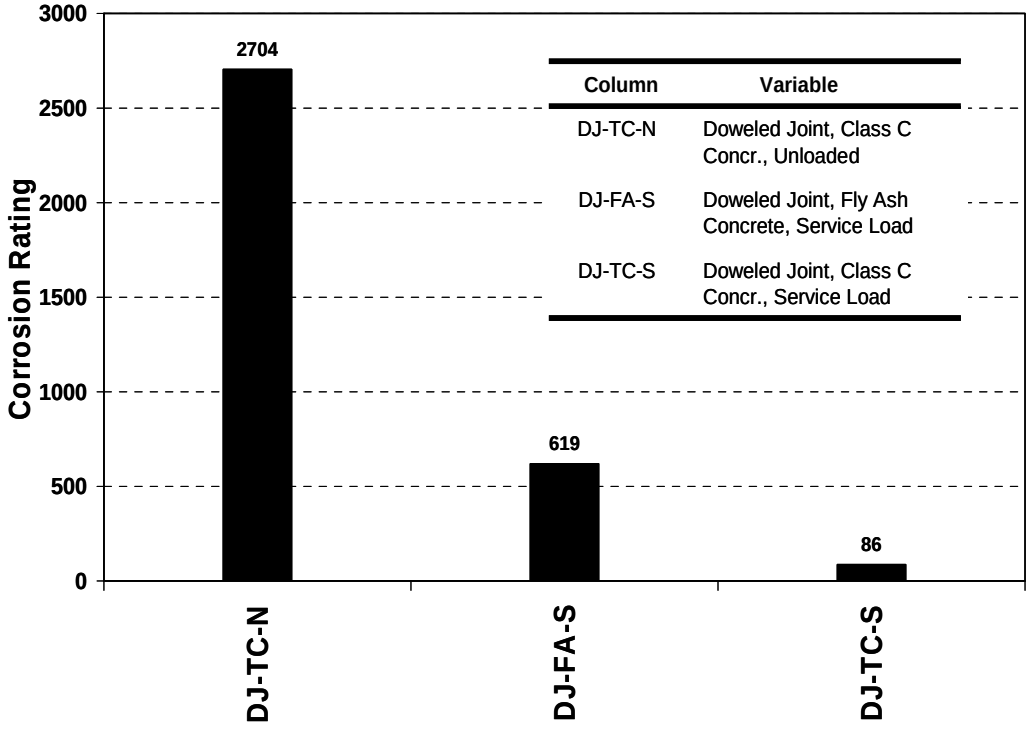

Figure 4.38 Total Dowel Corrosion Rating for All Specimens[1]

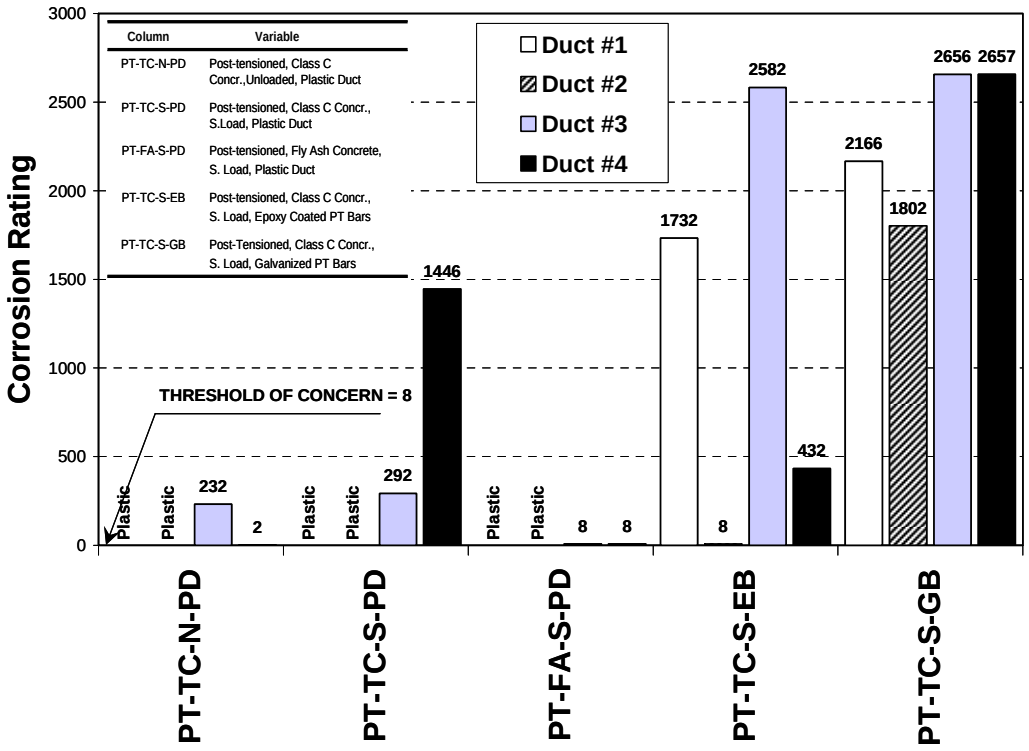

Figure 4.39 Maximum Duct Corrosion Rating in any two-inch Increment for All Specimens[1]

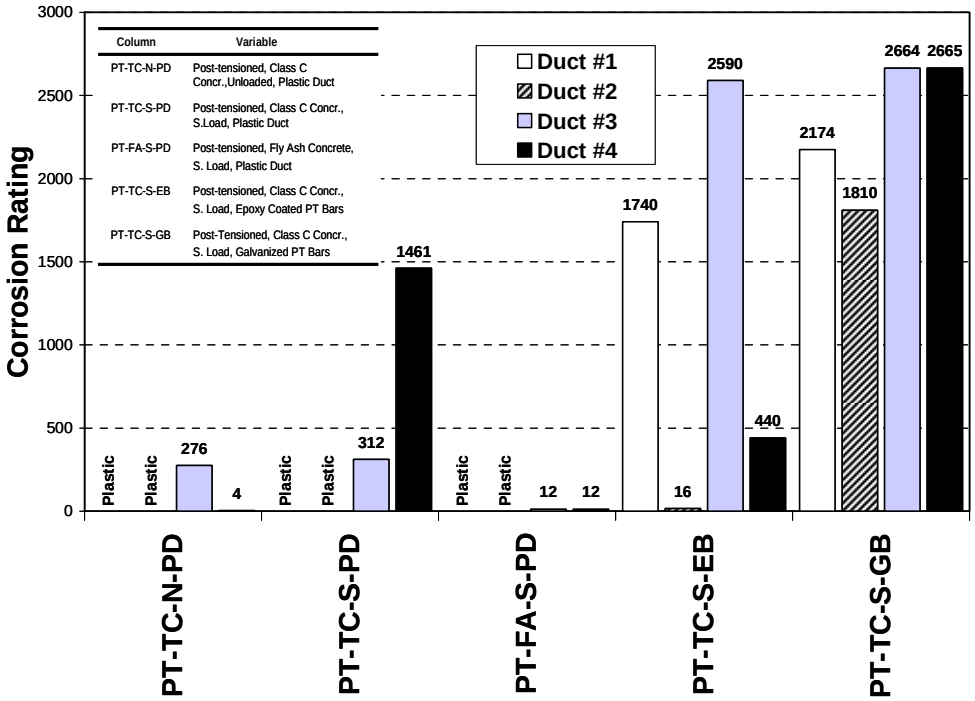

Figure 4.40 Total Duct Corrosion Rating for All Specimens[1]

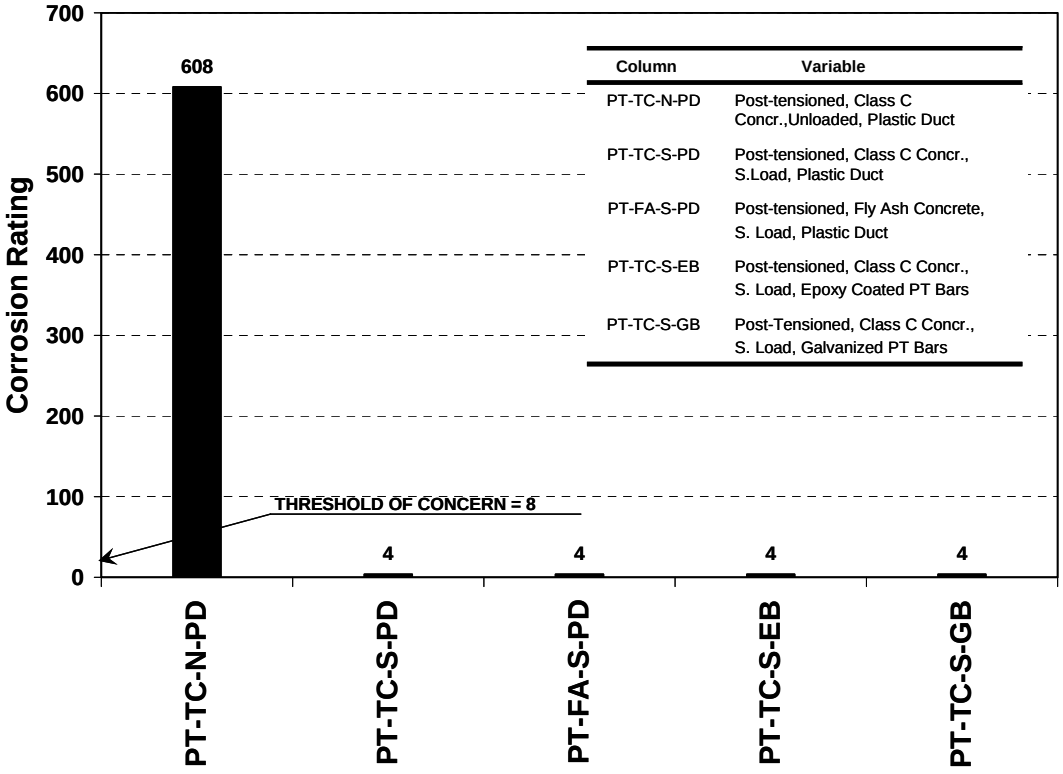

Figure 4.41 Maximum PT-Bar Corrosion Rating in any two-inch Increment for All Specimens[1]

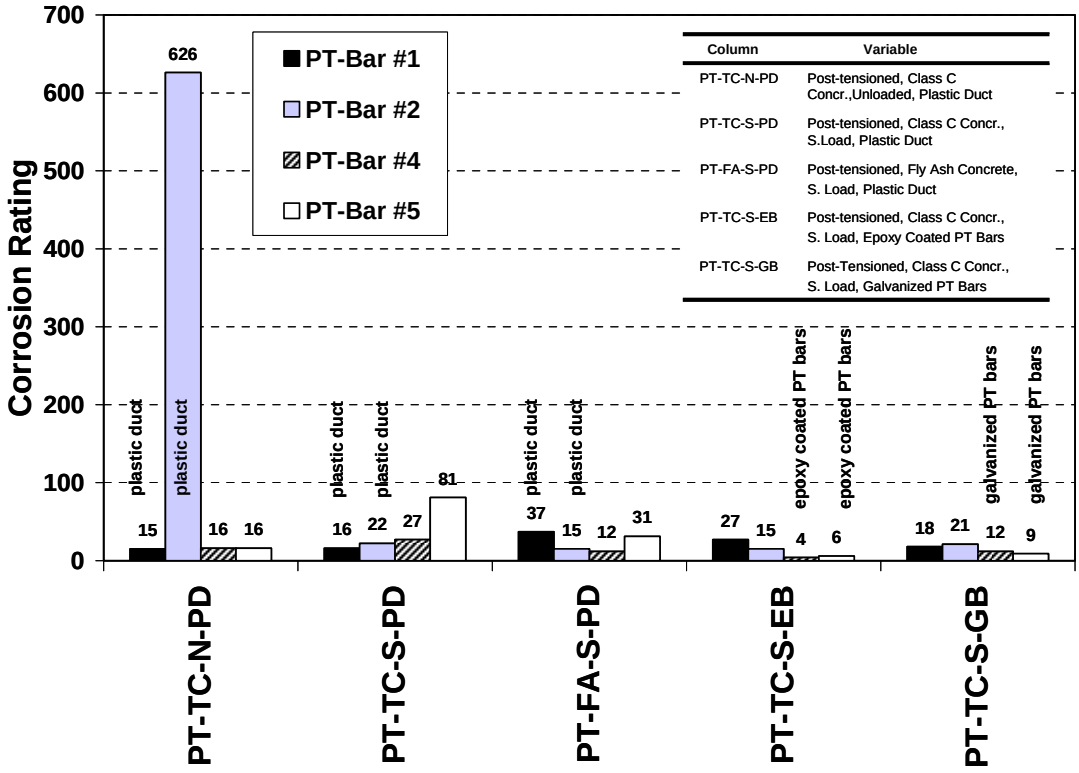

Figure 4.42 Total PT-Bar Corrosion Rating for All Specimens[1]

Based on the pitting values of Tables 4.1 and 4.2, and to put corrosion ratings in perspective, a "threshold value of concern" was assigned at the corrosion rating of 8, for the maximum (rebar, PT bars, and duct) corrosion rating found in any two-inch interval. A corrosion rating of 8 corresponds to pitting visible to the unaided eye in rebar or PT bars and pitting and severe corrosion found on the duct surface. Above this threshold value, severe pitting, and section loss is expected.

A threshold value is not indicated in the total corrosion ratings, since it could be misleading. However, by comparing maximum corrosion ratings with total corrosion rating, it is possible to gain a sense of corrosion severity and extent in the element.

After six and a half years of exposure, Figure 4.33 shows that in the dripper side, specimen NJ-TC-S (No dowel, type C concrete, service load) showed extremely severe spiral corrosion rating, over 400 times the threshold value. With applied loading the epoxy joint used in non-joint specimens could have opened up in the North side (refer to applied moment direction in Figure 2.11) and moisture and chlorides could have been able to penetrate the joint (see Figure 4.15). In addition, it appears that the concrete cover was between half to one inch at the base of the column, instead of the design value of two inches, and therefore moisture could have penetrated rapidly to the spiral level.

Specimen NJ-TC-N and DJ-TC-N also showed very high maximum spiral corrosion ratings. Specimens DJ-FA-S, DJ-TC-S, and all post-tensioned specimens showed essentially negligible maximum spiral corrosion ratings at or below the threshold value. In the non-dripper side, all specimens showed maximum corrosion ratings below the threshold value.

Spiral corrosion in all specimens was mostly concentrated in the bottom 18 inches. Total spiral corrosion was higher in specimen NJ-TC-S, the same specimen that showed maximum spiral corrosion in any two-inch increment. The worst performance of this specimen was followed by moderately elevated readings for specimens NT-TC-N and DJ-TC-N. For all other specimens, (DJ-FA-S, DJ-TC-S, and all PT

specimens) total spiral corrosion rating is similar and there is not a clear distinction between the dripper and the non-dripper sides.

Maximum rebar corrosion rating as shows in Figure 4.35 was in all cases below the threshold value, at levels of very light corrosion, except specimen NJ-TC-S that had a rating of 8, just at the threshold value, meaning some pitting visible with the unaided eye. Using maximum corrosion ratings no clear distinction exists, between post-tensioned and non post-tensioned specimens, and between specimens with Fly Ash concrete and Class C concrete.

Total rebar corrosion ratings of Figure 4.36 suggest a better performance of PT specimens. However, the exception was specimen NJ-TC-N (No dowel, class C concrete, no load), which showed very low total corrosion rating, only surpassed by specimen PT-TC-S-GB.

Dowel corrosion was mostly concentrated at the column-foundation interface. At this cold joint localized corrosion was extremely severe. Figure 4.37 indicated that specimens DJ-TC-N and DJ-FA-S showed very large dowel section loss. Specimens DJ-TC-S showed a maximum corrosion rating equal to the threshold value, representing some pitting in the bar surface. Total dowel corrosion ratings were very similar to the maximum dowel corrosion ratings since corrosion was localized. Dowel joints did not have an epoxy bonding agent at the joint, as with the no-joint specimens, and therefore, moisture and chlorides found an easy path towards the dowel location. The loaded specimen with Standard Concrete may have been benefited from the precompression applied to the joint. It is not clear the reason why Specimen DJ-FA-S showed more dowel corrosion than Specimen DJ-TC-S. One possibility is to consider that loading was able to open up a larger opening at the joint in the South side, allowing for moisture to penetrate more easily.

Figure 4.39 showed that specimen PT-TC-S-GB had the most extensive maximum duct corrosion rating; however this corrosion was mostly concentrated in the first two-inch increment, and was mostly due to the negative conditions given by the use of the rubber gasket at the column-foundation interface. The rubber gaskets were found to be detrimental for the performance of galvanized ducts, since moisture was trapped in the inner gasket faces and corrosion was accelerated. This result shows that a better splicing method is required. For the same reasons, specimens PT-TC-S-EB and PT-TC-S-PD showed high duct corrosion ratings in the first and second two-inch increments. Specimen PT-FA-S-PD showed maximum duct corrosion ratings equal to the threshold value; however this specimen was also starting to have severe localized corrosion due to the use of the gasket. Figure 4.26 (PT bar #3 and duct #3) clearly shows this situation.

Since corrosion of galvanized steel ducts was mostly concentrated underneath the rubber gasket, total duct corrosion ratings are very similar to maximum duct corrosion rating.

Figure 4.41 shows that PT bar maximum corrosion rating was generally below the threshold value of concern, meaning only moderate surface corrosion in the most damaged two-inch increment. The only exception was specimen PT-TC-N-PD (post-tensioned, class C concrete, no load, plastic duct) that showed very severe pitting in PT bar #2, as was shown in Figure 4.20. This PT bar showed this high corrosion at the column-foundation interface, where the plastic duct was interrupted. This shows the serious error made at the specimen definition, not adequately splicing ducts to the foundation.

Corrosion on PT bars extended a few inches up from the column base section, resulting in the total corrosion ratings shown in Figure 4.42. However, the corrosion was low in most specimens.

Epoxy-coated and galvanized PT bars showed somewhat lower total corrosion rating than plain bars, and corrosion on these bars was more concentrated around the column-foundation interface.

4.4.3 Chloride Content in Grout

Grout chloride content profiles are shown in Figure 4.43 through Figure 4.47. Grout samples were taken at 3, 15, 30 and 50 inches from the column base.

The acid soluble chloride threshold value of concern is shown in the figures at 0.14% assuming chloride threshold of 0.2% by weight of cement and a water cement ratio of 0.44.

As observed in the figures, grout chloride contents at 30 and 50 inches are in all cases lower than the threshold value. At 15 inches, only the grout for PT bar #3 (galvanized) in specimen PT-TC-S-GB showed chloride contents in excess of the threshold value. It exceeded the threshold by 80%. At 3 inches (submerged zone) specimens showed grout acid soluble-chloride contents higher than the threshold value in five PT bars: PT bar #1 and #3 in specimen PT-TC-N-PD, PT bar #1 in specimen PT-TC-S-PD, PT bar #1 in specimen PT-TC-S-EB; and, PT bar #3 in specimen PT-TC-S-GB.

After autopsy very high porosity was observed in grouts for specimens PT-TC-S-EB and PT-TC-S-GB. As explained in Section 2.6, the constructors of the specimens were concerned that during construction and grout injection, it was possible that incorrectly labeled cement barrels may have resulted in partial or complete cement replacement with Class F Fly Ash, with the most likely columns affected by this error being specimens PT-TC-S-EB and PT-TC-S-GB. The resulting porosity could be the reason for the high chloride content observed at 15 inches.

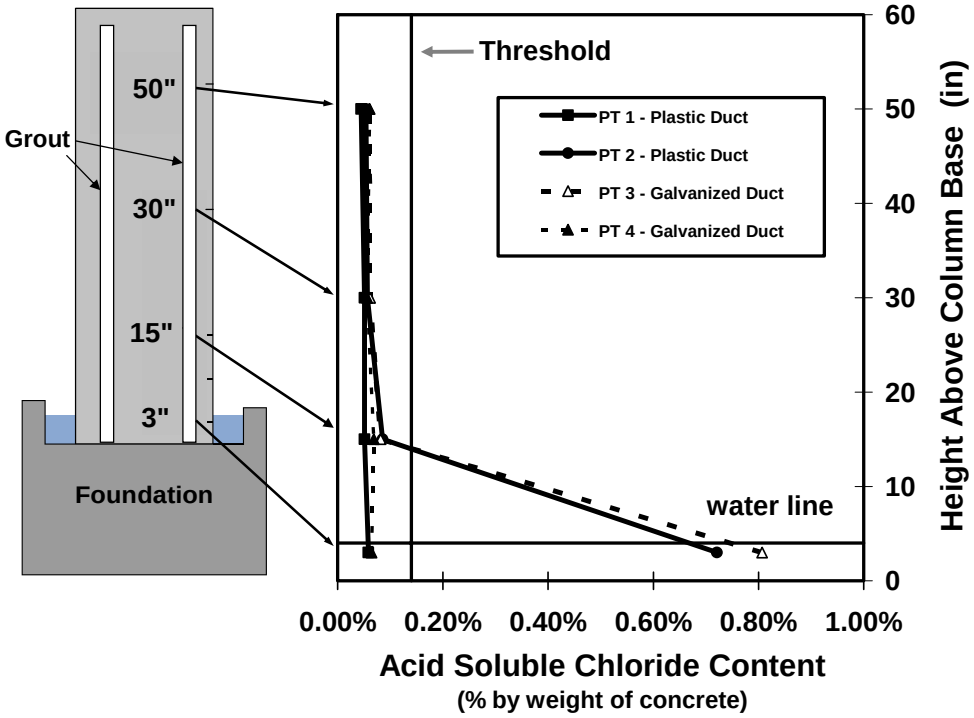

Figure 4.43 Grout Chloride Penetration for Column PT-TC-N-PD at End of Testing[1]

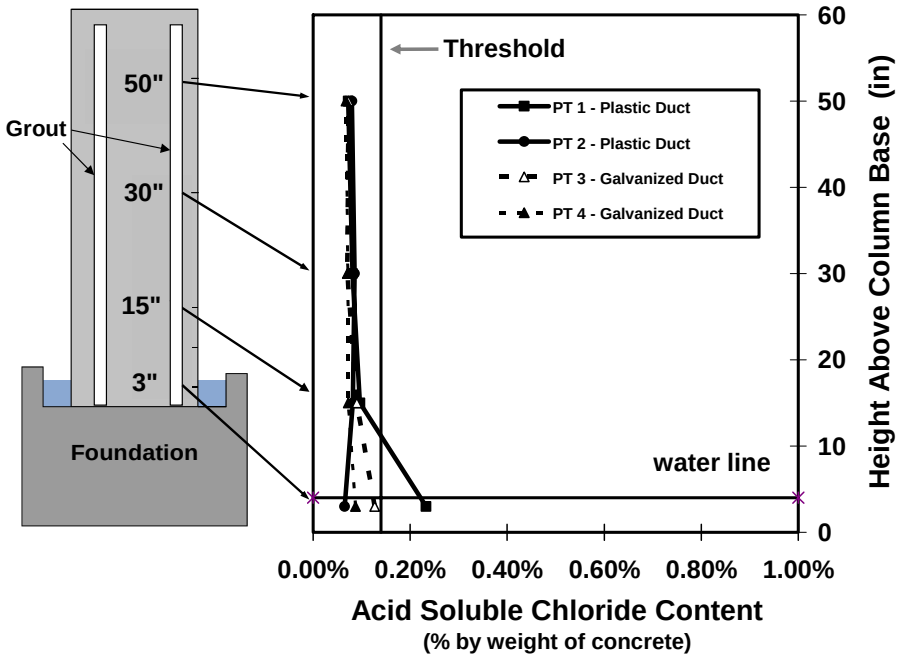

Figure 4.44 Grout Chloride Penetration for Column PT-TC-S-PD at End of Testing[1]

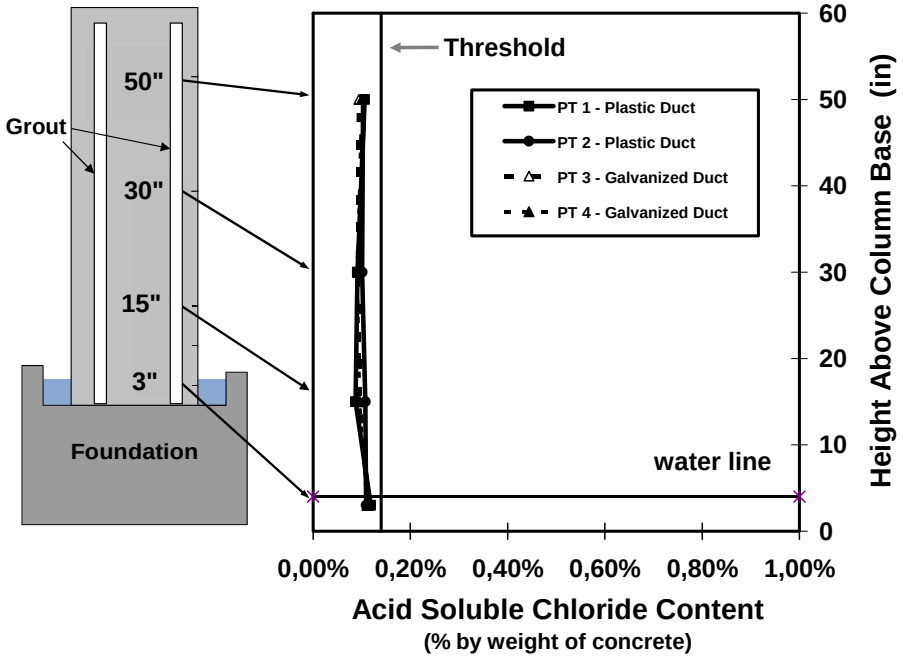

Figure 4.45 Grout Chloride Penetration for Column PT-FA-S-PD at End of Testing[1]

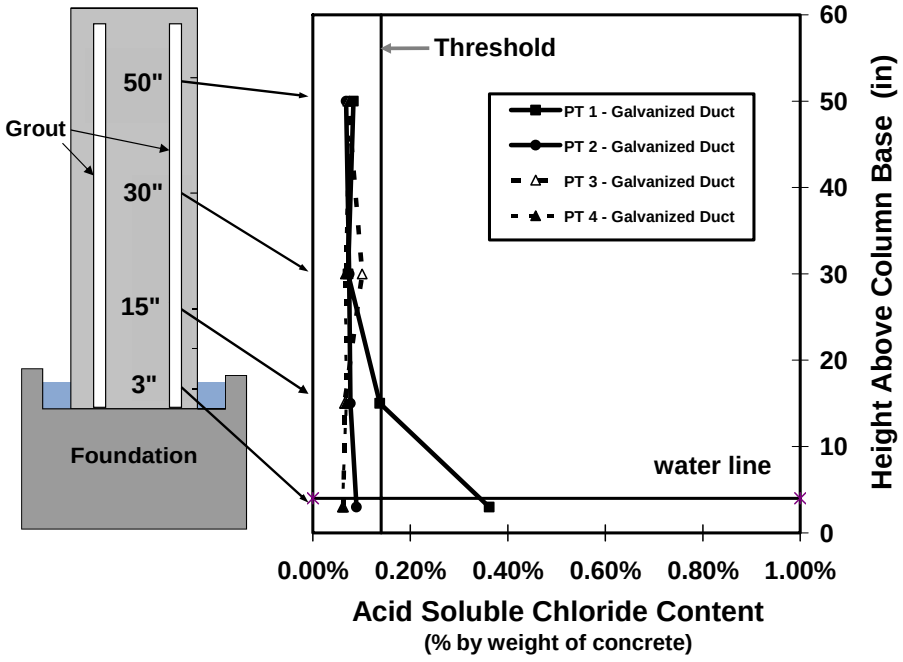

Figure 4.46 Grout Chloride Penetration for Column PT-TC-S-EB at End of Testing[1]

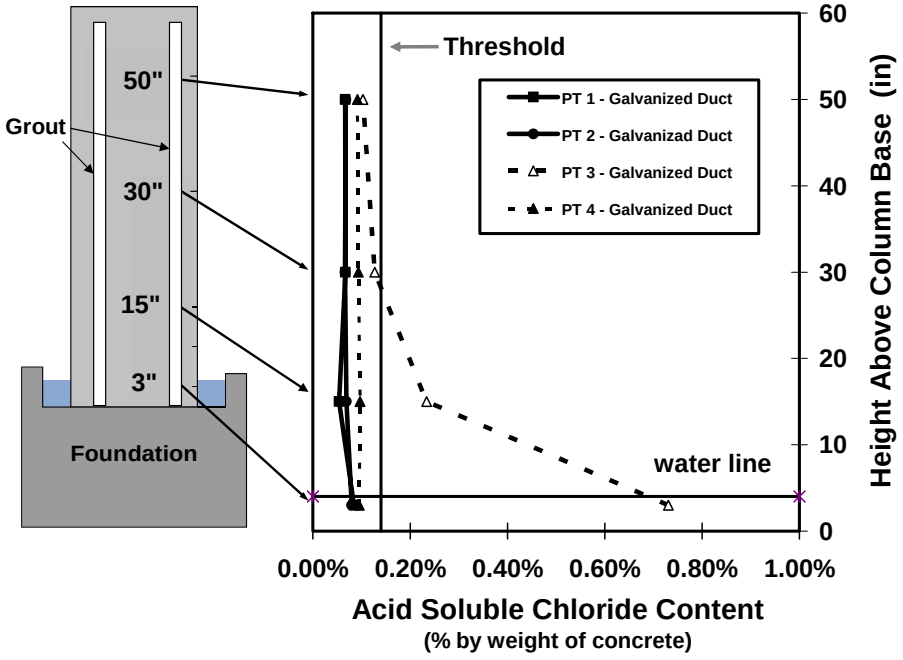

Figure 4.47 Grout Chloride Penetration for Column PT-TC-S-GB at End of Testing[1]

CHAPTER 5: ANALYSIS AND DISCUSSION OF RESULTS

After full autopsy had been performed on the column specimens at six and a half years of accelerated exposure testing, the effect of all variables involved in this testing program could be analyzed and compared. Limited autopsy results performed at the end of 1998 for specimens DJ-TC-N (doweled joint - Class C concrete - unloaded) and PT-TC-S-PD (post-tensioned – Class C concrete – service load – plastic duct) were described in Reference 2.

5.1 OVERALL PERFORMANCE

One of the objectives for this research program was to investigate the effect of the typical cold joint between foundation and columns on chloride ion movement and corrosion activity. After autopsy, corrosion in dowels, ducts and post-tensioning bars was mostly found concentrated at the column-foundation interface. The joint acted as a weak link in corrosion protection, behaving as a pre-formed crack, which could have opened under loading. Specimen NJ-TC-N (No dowel-Class C concrete – unloaded) showed very low spiral and rebar corrosion with respect to the other specimens, which could be explained by the epoxy bonding agent used to prepare the foundation surface on no-joint specimens prior to casting. Figure 5.1 shows the severe section loss due to corrosion in a dowel crossing a typical joint location.

The wicking effect (migration of chlorides upward in the concrete from ponded base) was typically observed in the first 18 inches from the base of the columns. Spiral, rebar, duct dowel and post-tensioned bar corrosion was very severe at or near the column-foundation interface and decreased with increasing column height.

Figure 5.1 Typical Corrosion and Section Loss Found on Dowels at the Column-Foundation Interface[1]

As shown in Figure 5.2, galvanized steel ducts were found severely corroded inside the rubber gaskets that were supposed to seal the "dead end" of these ducts. The use of these gaskets was found to be detrimental for the performance of galvanized ducts, since moisture was trapped and corrosion was accelerated. A better splicing method is required.

Epoxy-coated bars and galvanized post-tensioned bars showed localized corrosion at the column-foundation interface, but negligible occurrence of corrosion away from the interface.

The relative performance of the column specimens is better described by organizing the corrosion ratings according to performance. Figure 5.3 through Figure 5.6 show the results for spiral, rebar, dowel and PT-bars. Ducts have not been included, since some specimens have plastic ducts and others only galvanized ducts, which makes it difficult to compare the specimens with average values. Duct performance can be analyzed with the use of Figure 4.39 and Figure 4.40.

Figure 5.2 Duct Corrosion Found Inside Rubber Gaskets[1]

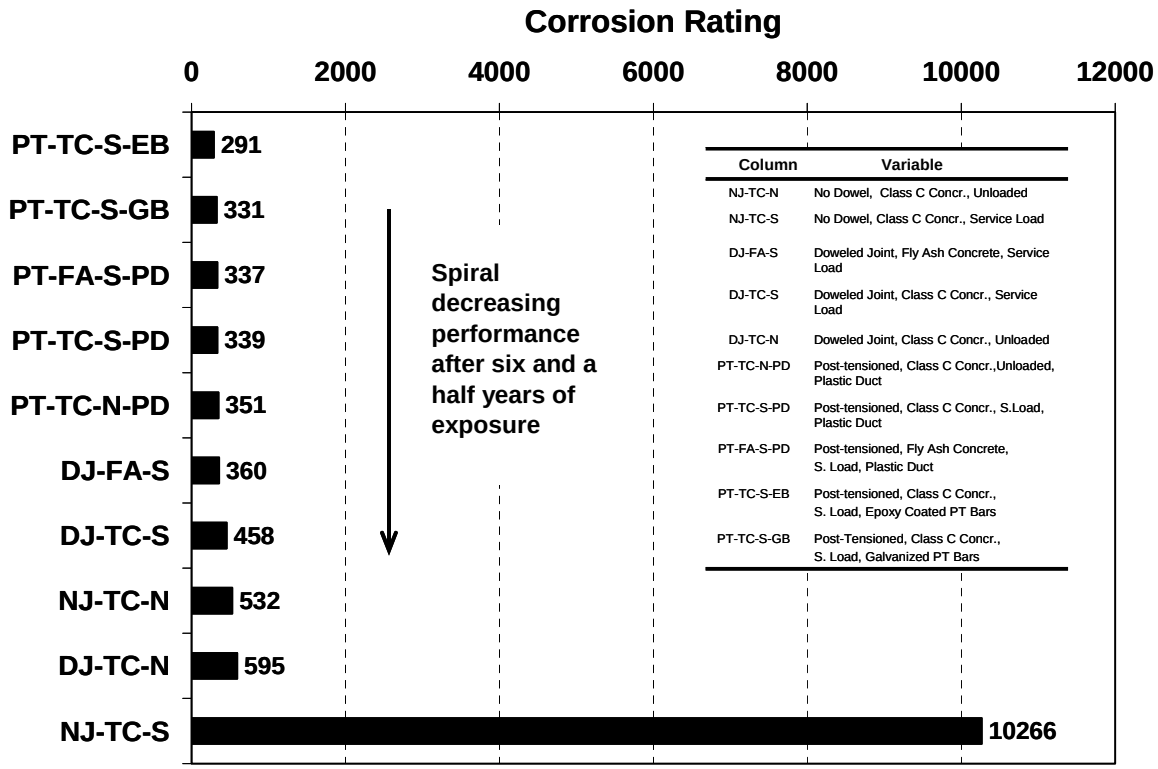

Figure 5.3 Total Spiral Corrosion Rating Ordered According to Performance[1]

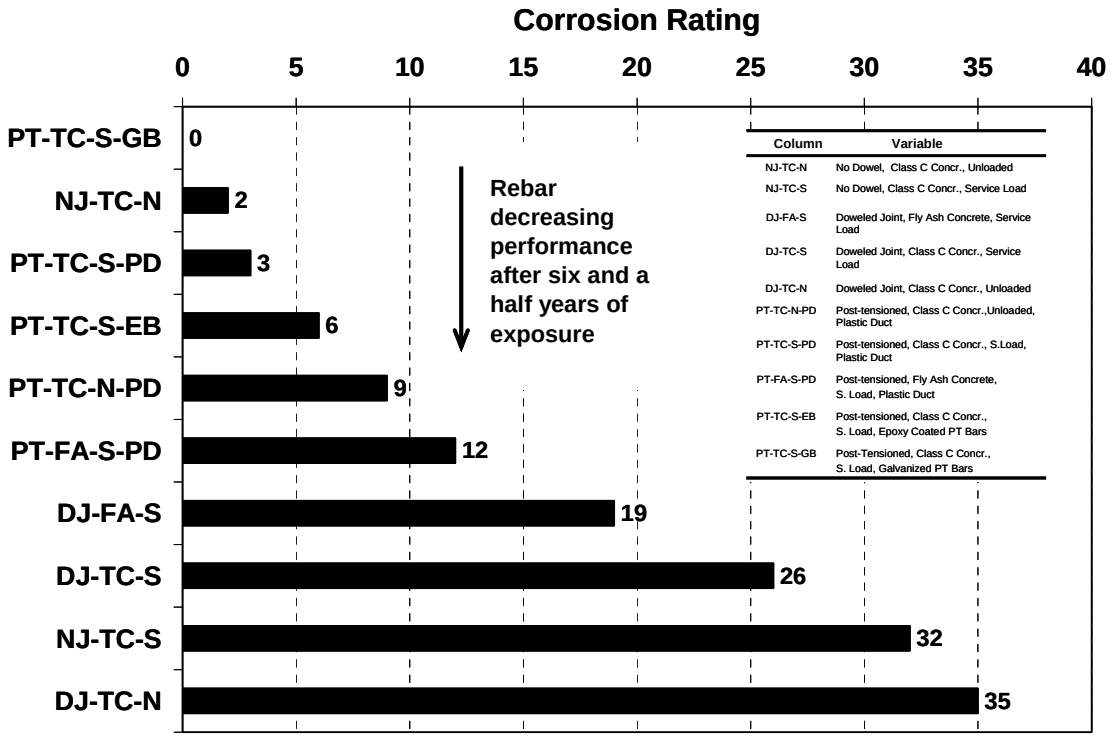

Figure 5.4 Total Rebar Corrosion Rating Ordered According to Performance[1]

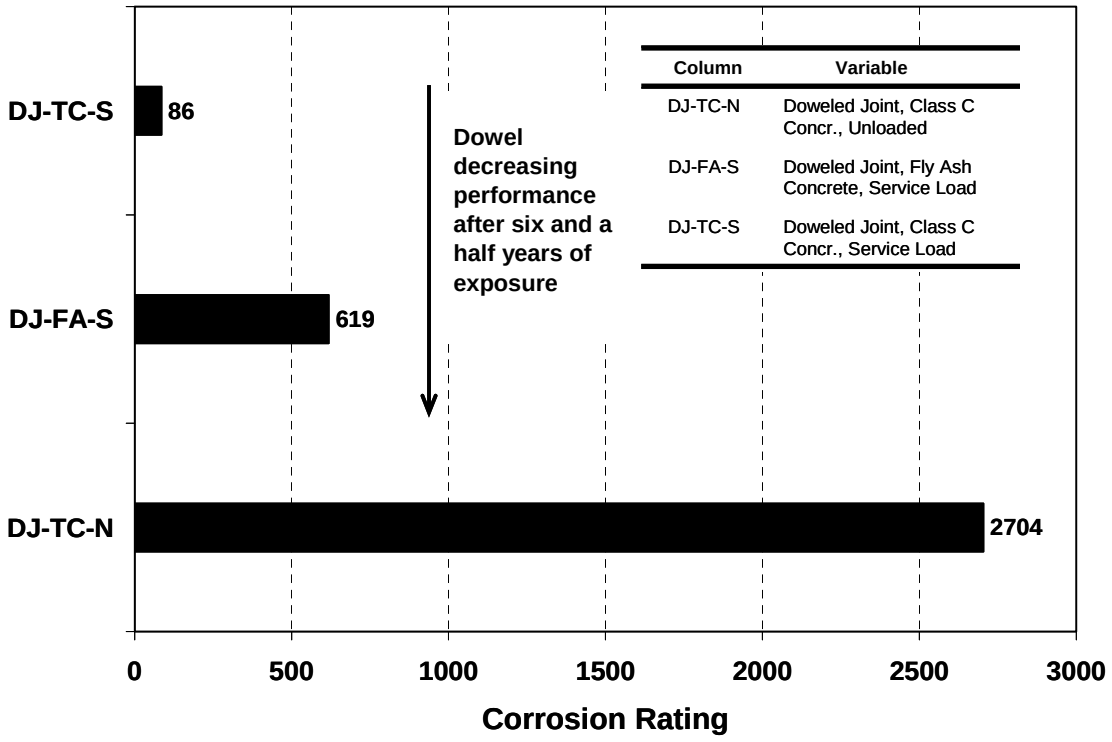

Figure 5.5 Total Dowel Corrosion Rating Ordered According to Performance[1]

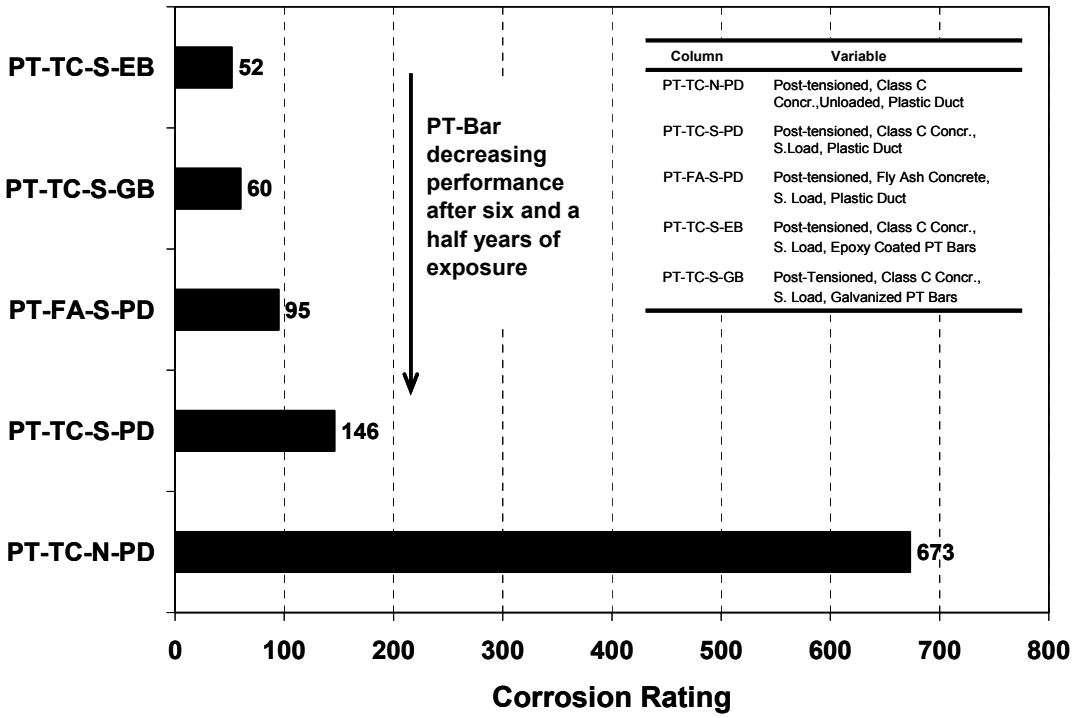

Figure 5.6 Total PT-Bar Corrosion Rating Ordered According to Performance[1]

Specimen NJ-TC-S shows the worst spiral corrosion rating. The reason appears to be the effect of loading on the epoxy joint on this specimen, slightly opening the North joint side and allowing moisture and chlorides to penetrate the joint. In addition, concrete over the spiral at the bottom of the column seems to have been somewhat smaller than the 2-inch design cover, allowing for moisture and chlorides to easily penetrate the concrete up to the spiral level. Post-tensioned columns show lesser spiral corrosion, showing the positive effect of concrete and joint precompression.

The better rebar performance was shown for post-tensioned columns, except for Specimen NJ-TC-N. This no-joint specimen was unloaded and epoxy jointed. The worst rebar performance was shown on Specimen DJ-TC-N, since this specimen did not have any epoxy bonding agent between the column and the foundation, which allowed the joint to act as a pre-formed crack. This specimen was unloaded, which could have played an important role. There was not a distinct trend among specimens with fly ash and standard concrete. Fly ash non-post-tensioned specimen DJ-FA-S (doweled, fly ash concrete, service load) showed only a slight decrease in rebar corrosion with respect to Specimen DJ-TC-S (doweled specimen with standard concrete and service load).

Specimen DJ-TC-N (doweled joint, standard concrete, unloaded) showed the worst dowel performance. The reason is associated with the joint not being epoxy sealed, serving as a preset crack. The dowel performance of fly ash concrete specimen DJ-FA-S was worse than Specimen DJ-TC-S. This result is explained by the fact that corrosion mostly occurred at the column-foundation interface, and therefore the concrete in the column did not play an important role.

Post-tensioned bar corrosion was mostly concentrated at the column-foundation interface, as in the previous case for the dowels. For this reason, concrete type did not play an important role. The worst performance was observed in Specimen PT-TC-N-PD (post-tensioned column, standard Class C concrete, unloaded, plastic duct). However it is not clear why this performance is worse than Specimen PT-TC-S-PD (post-tensioned column, standard Class C concrete, service load, plastic duct). The best performance was observed in galvanized and epoxy coated post-tensioning bars, although in both cases corrosion had started.

5.2 COMPARISON BETWEEN HALF-CELL POTENTIALS AND CORROSION RATINGS

At the end of testing, half-cell potential readings were compared with corrosion found during autopsies on specimen reinforcement. In general, half-cell potentials were able to detect the higher probability of corrosion occurring at the base of the column, and low to negligible probability of corrosion above column mid-height. However, since dowel bars, post-tensioning bars and ducts all showed severe corrosion at the joint area, it is difficult to determine which source of corrosion potential was being detected by the half-cell readings. The post-tensioning bar may have been in electrical contact with the mild steel reinforcement, and therefore, half-cell potential measurements may have been a combination of active corrosion sources.

5.3 EFFECT OF LOADING

The effect of loading on spiral corrosion is not clear when looking at the non-prestressed specimen corrosion rating data, Figure 5.3. Specimen NJ-TC-S (No dowel-Class C concrete – service load) showed very high corrosion ratings when compared to specimen NJ-TC-N (No dowel-Class C concrete-no load); however, the trend was reversed for specimen DJ-TC-S (doweled – Class C concrete – service load) that showed less corrosion rating than specimen DJ-TC-N (doweled – Class C concrete – no load). In the post-tensioned specimens spiral corrosion rating was of the same magnitude in both the non-loaded specimen and the specimens continuously subjected to service load. Similar results were obtained for rebar corrosion (see Figure 5.4).

Dowels and post-tensioned bars (see Figures 5.5 and Figure 5.6) were found to corrode more at the column-foundation interface in non-loaded specimens. However, the contradiction between dowel and duct corrosion, makes it difficult to draw any definite conclusions.

5.4 EFFECT OF TRICKLE SALTWATER

The trickle system on one face of the columns did produce a clear increase in spiral corrosion in non-prestressed specimens, as shown in Table 4.4. The trend was not shown in post-tensioned specimens, where spiral corrosion ratings were very similar in both column faces. Rebar, duct or post-tensioned bars did not show any distinct corrosion trend with respect to dripper and non-dripper sides (see Figure 2.11 for dripper and element location, and corrosion rating data on Tables 4.7, 4.11 and 4.13).

5.5 EFFECT OF JOINT TYPE

Corrosion was mostly concentrated at the column-foundation interface (see examples in Figures 4.8 and 4.12 (complete cage)). At this section, doweled and post-tensioned specimens showed very severe section loss, with less corrosion observed in galvanized and epoxy coated PT-bars, as shown in Figure 5.6.

There was not a distinct trend with respect to the use of post-tensioned joints versus doweled joints. The doweled joint would be expected to provide the least corrosion protection since the joint is not precompressed. However, this behavior was not clearly shown after autopsy.

As shown in Figure 5.3 and 5.4, the use of post-tensioning did provide enhanced spiral and rebar corrosion protection, compared to non-post-tensioned specimens. In the case of the spirals, the effect of post-tensioning was dramatic, since very severe section loss and pitting in the stirrup in non-prestressed specimens was reduced to light to moderate surface corrosion in post-tensioned specimens.

The use of post-tensioned joints also provided better resistance to the wicking effect, when acid-soluble chloride contents were compared to doweled and no-joint specimens, see Figure 3.21.

5.6 EFFECT OF CONCRETE TYPE

As shown in Figure 5.5 and Figure 5.6, the effect of concrete type was not clearly shown in dowel and PT-bar performance since the corrosion in these specimens was mainly at the column-foundation interface, and therefore, chloride penetration through concrete had little effect. On the contrary, as shown in Figures 4.39 and 4.40, duct corrosion – even when it was mostly concentrated at the column base – was lower in Fly Ash specimens.

As shown in Figures 5.3 and 5.4, spiral and rebar corrosion in non-prestressed specimens showed a better performance in Fly Ash concrete than in Class C concrete specimens. This trend was not clearly shown in post-tensioned specimens.

5.7 EFFECT OF DUCT TYPE

Since post-tensioning bar corrosion was mostly concentrated at the column-foundation interface, where ducts were interrupted, the duct type had little influence on PT-bar performance. However, advanced galvanized steel duct corrosion inside the rubber gasket, suggested a significant superiority of plastic duct. The use of the rubber gaskets was a serious error. Instead of gaskets, the ducts must have been adequately spliced at the column-foundation interface to avoid moisture and chlorides to penetrate at the joint section.

5.8 EFFECT OF POST-TENSIONING BAR COATINGS

As shown in Figure 5.6, PT bar coatings, either epoxy or galvanized (which showed very similar results) improved the performance of post-tensioning bars, when compared to plain post-tensioning bars. From Figures 4.29 and 4.32 it is shown that the PT-bar coatings were not sufficient to stop corrosion from occurring at the column-foundation interface, but corrosion was limited to moderate surface corrosion in a few inches around the joint area.

When drawing conclusions from these observations, care must be exercised, since localized corrosion in the black steel, once it has started, could grow rapidly underneath the coatings and bar capacity could be threatened, specially when corrosion is not extended in a large bar area.

CHAPTER 6: SUMMARY AND CONCLUSIONS

Five non-prestressed and five post-tensioned columns specimens were used to investigate corrosion mechanisms and chloride ion transport ("wicking effect") in various column connection configurations and to evaluate column corrosion protection measures. Variables included column to foundation connection (no dowel joint, doweled joint and post-tensioned joint), loading (no loading and service load – with combined moment and axial load), concrete type (TxDOT Class C concrete, and Class C Fly Ash concrete – 35% replacement by volume), prestressing bar coatings (uncoated, galvanized PT-bars, and epoxy coated PT-bars), and post-tensioning ducts (plastic and galvanized steel). Trickle water was used on one face of each column to determine the effect of salt water spray or dripping. Test specimen exposure started in July of 1996 and ended in January of 2003, after six and a half years. Full autopsies were performed at the end of testing, and conclusions are as follows.

6.1 POST-TENSIONING TO IMPROVE CORROSION PROTECTION

The possible weak link in corrosion protection at the column-foundation interface was studied with three different configurations: no dowel joint, doweled joint and post-tensioning joint. Determination of the effect of post-tensioning on durability through precompression of the concrete and precompression of construction joints was one of the main objectives of this research series. The conclusions are as follows:

- Post-tensioned specimens did not show any distinct improvement in specimen performance at the column foundation interface, when compared to doweled specimens.
- Post-tensioning dramatically reduced the corrosion found on spiral reinforcement in the first 18 inches from the column base.
- Post-tensioned specimens under loading showed an increase in spiral and mild steel reinforcement corrosion protection when compared to non-loaded specimens.
- Post-tensioning reduced the risk of spiral corrosion due to saltwater dripping.
- Post-tensioning provided better resistance to the wicking effect, when acid-soluble chloride contents were compared to doweled and no-dowel specimens.

6.2 FLY ASH AS PARTIAL CEMENT REPLACEMENT IN CONCRETE

TxDOT standard concrete mix Class C concrete was used in eight specimens (w/c = 0.45, type I/II Cement, f´c=3600). In two columns, 35% of cement by volume (31% by weight) was replaced with Class C Fly Ash, with no other significant changes to the concrete mix. After autopsy, the following conclusions are drawn:

- Fly ash concrete did seem to provide enhanced corrosion protection to galvanized steel ducts.
- Spiral and mild steel reinforcement corrosion in non-prestressed specimens showed a better performance in Fly Ash concrete than in Class C concrete specimens. This trend was not clearly shown in post-tensioned specimens.
- Post-tensioned bar corrosion did not show any distinct trend with respect to the type of concrete in the specimen.

6.3 PLASTIC DUCTS FOR POST-TENSIONING

Standard galvanized steel ducts were compared to impermeable plastic ducts in three post-tensioned specimens: Class C concrete (unloaded and service load) and Fly Ash concrete under service load. In all cases uncoated post-tensioning bars were used. The conclusions are as follows:

- Although results are very limited, advanced galvanized steel duct corrosion at the column base, inside the rubber gasket, show the superiority of using plastic ducts.
- Corrosion in post-tensioned bars in plastic ducts and galvanized ducts was always at the column-foundation interface, where the plastic or galvanized duct was interrupted. Therefore, conclusions regarding duct performance based on post-tensioning bar corrosion are not possible. The ducts need an effective splice seal at all joints.

6.4 POST-TENSIONING BAR COATINGS

Two prestressing bar coatings were investigated: epoxy-coated (according to ASTM A775-97) and zinc galvanized prestressing bars. The coated bars were compared directly to uncoated bars within individual specimens. In both cases, anchorage hardware was either epoxy coated or galvanized. The following conclusions are drawn:

- Epoxy coating or galvanized post-tensioning bars showed enhanced corrosion protection, with respect to plain post-tensioning bars.
- Coatings were not sufficient to stop corrosion from occurring at the column-foundation interface. Corrosion was very localized.
- Superiority of coated bars should not be concluded, since localized corrosion may accelerate deterioration at the local level, which in turn may result in unexpected failure.

CHAPTER 7: IMPLEMENTATION OF RESULTS

After full autopsy of all ten column specimens, research results generated the following findings to be implemented for partially submerged columns or columns exposed to saltwater runoff:

Substructure Prestressing

- Column elements should be prestressed, to improve spiral and rebar corrosion protection. However, designers should not rely entirely on post-tensioning to provide adequate corrosion protection at the cold joint. Other protection measures should be investigated.

Concrete Type

- Fly Ash concrete may be used to provide enhanced spiral, rebar and duct corrosion protection.

Duct Types

- Plastic ducts should be used to better protect post-tensioning bars. However, better sealing materials or splices should be used or developed, to seal the duct "dead" ends and protect the post-tensioning bar.

Gaskets

- Rubber gaskets are not effective to seal the duct "dead" ends and should not be used.

Post-tensioning Bar Coatings

- Galvanized steel bars or epoxy-coated bars provide enhanced protection against uniform corrosion, but are susceptible to severe localized corrosion.

Appendix
Supplementary Material

A. HALF-CELL POTENTIAL PLOTS

The following Half-Cell potential plots complement those contained in Figure 5.22 through Figure 5.25. "All" Half-Cell Potential Readings are followed by "Average" Half-Cell Potential readings.

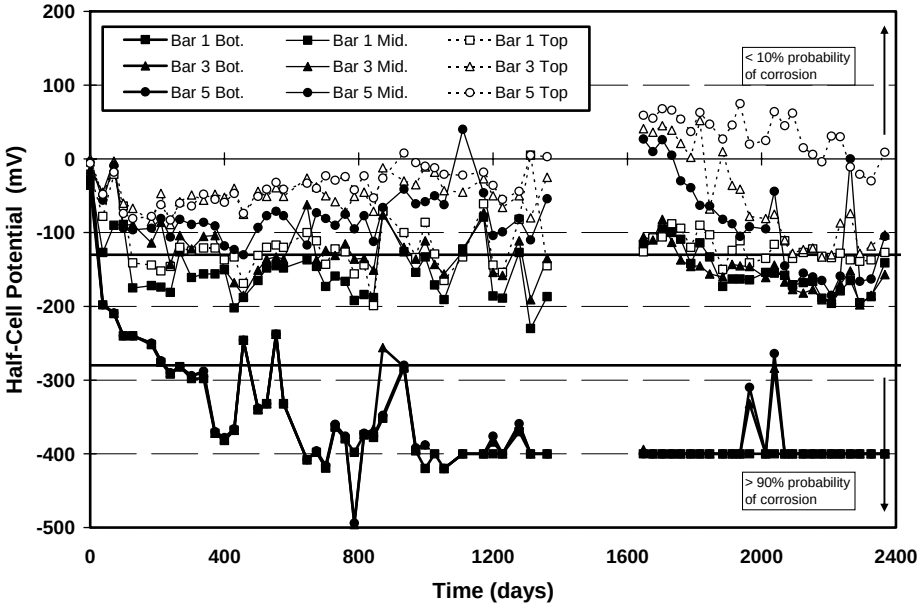

Figure A.1 All Half-Cell Potential Readings for Column NJ-TC-S[1]

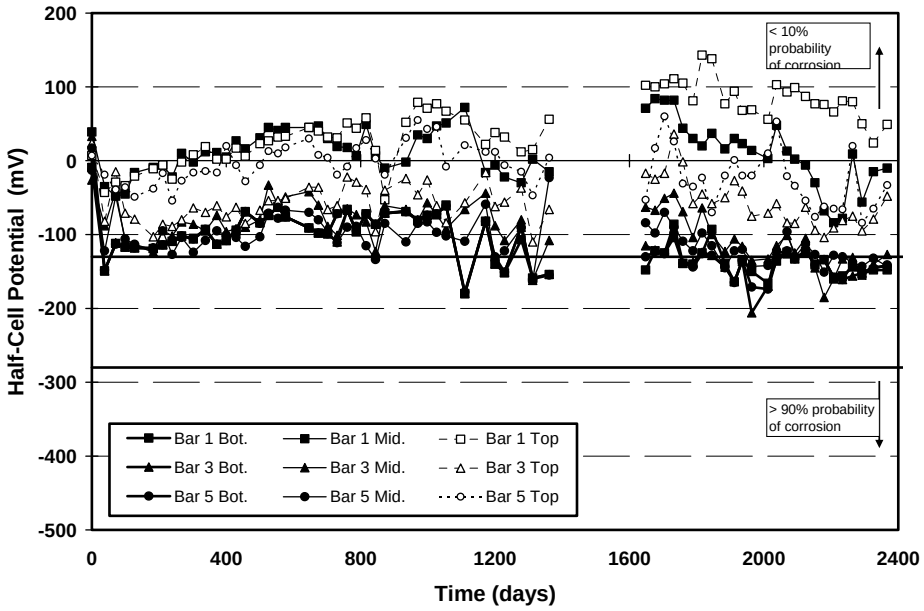

Figure A.2 All Half-Cell Potential Readings for Column DJ-TC-S[1]

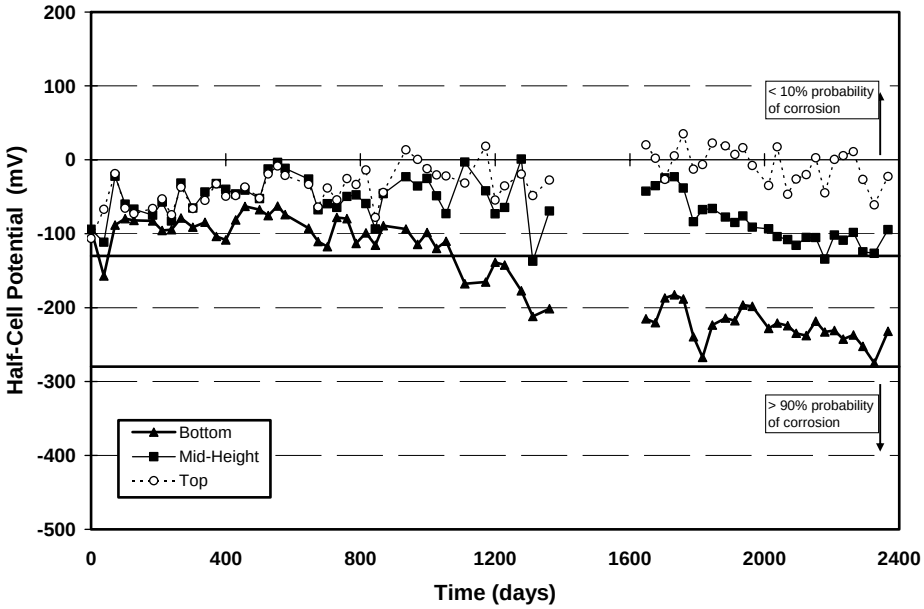

Figure A.3 All Half-Cell Potential Readings for Column PT-TC-S-PD – Rebar[1]

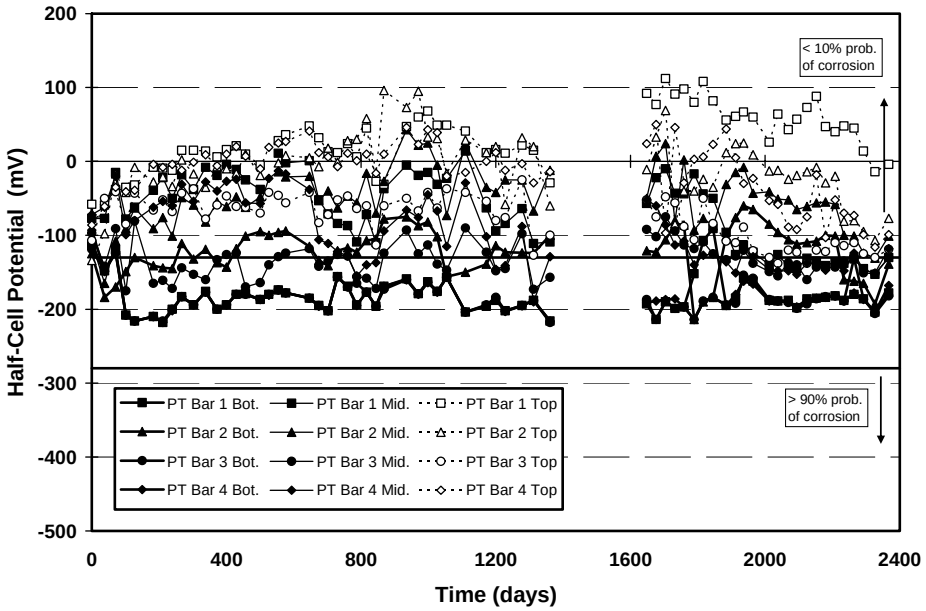

Figure A.4 All Half-Cell Potential Readings for Column PT-TC-S-PD – PT Bars[1]

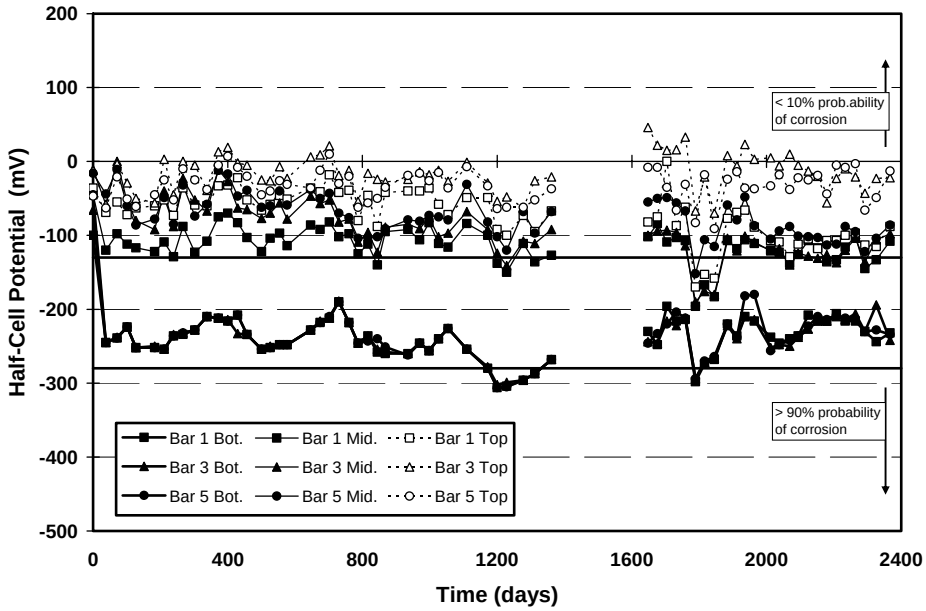

Figure A.5 All Half-Cell Potential Readings for Column PT-FA-S-PD – Rebar[1]

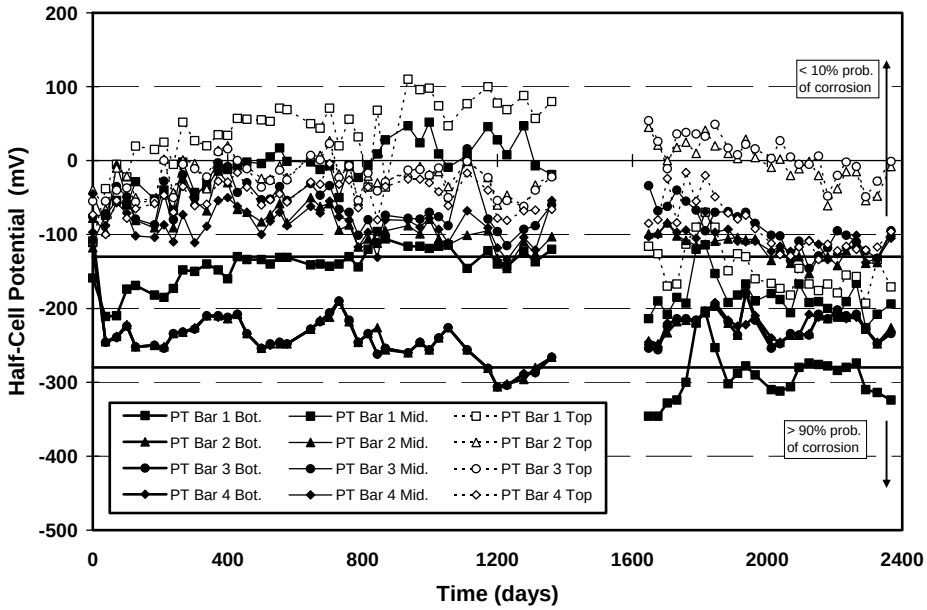

Figure A.6 All Half-Cell Potential Readings for Column PT-FA-S-PD – PT Bars[1]

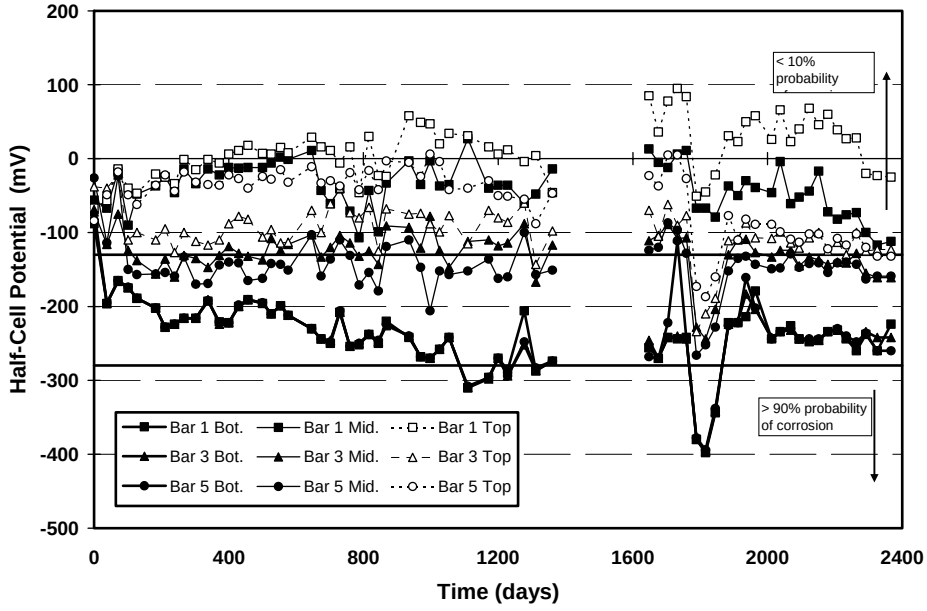

Figure A.7 All Half-Cell Potential Readings for Column PT-TC-S-EB – Rebar[1]

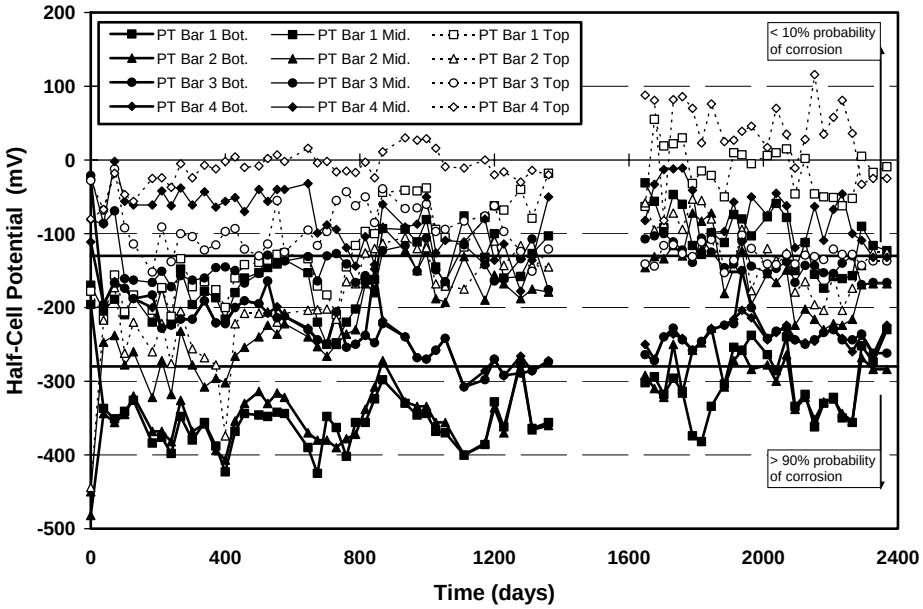

Figure A.8 All Half-Cell Potential Readings for Column PT-TC-S-EB – PT Bars[1]

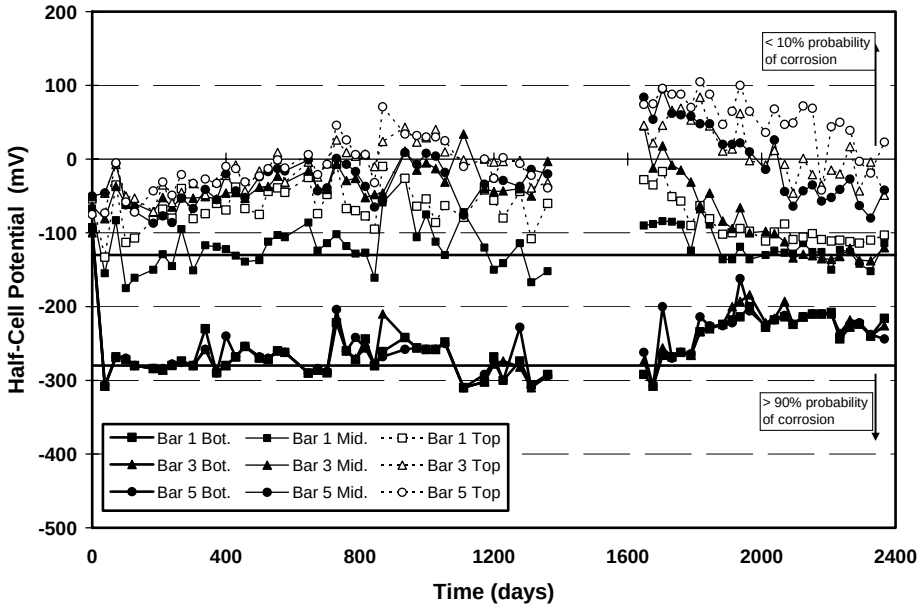

Figure A.9 All Half-Cell Potential Readings for Column PT-TC-S-GB – Rebar[1]

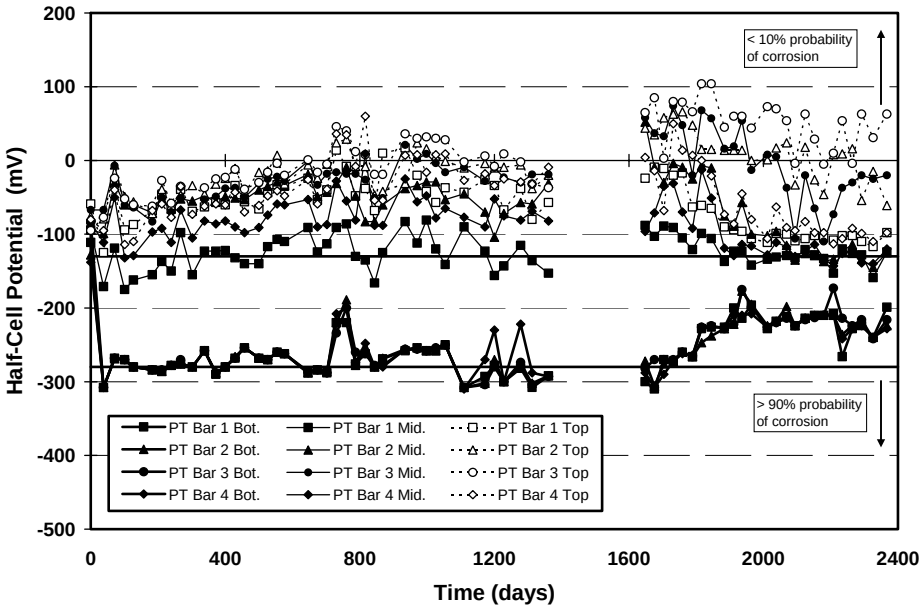

Figure A.10 All Half-Cell Potential Readings for Column PT-TC-S-GB – PT Bars[1]

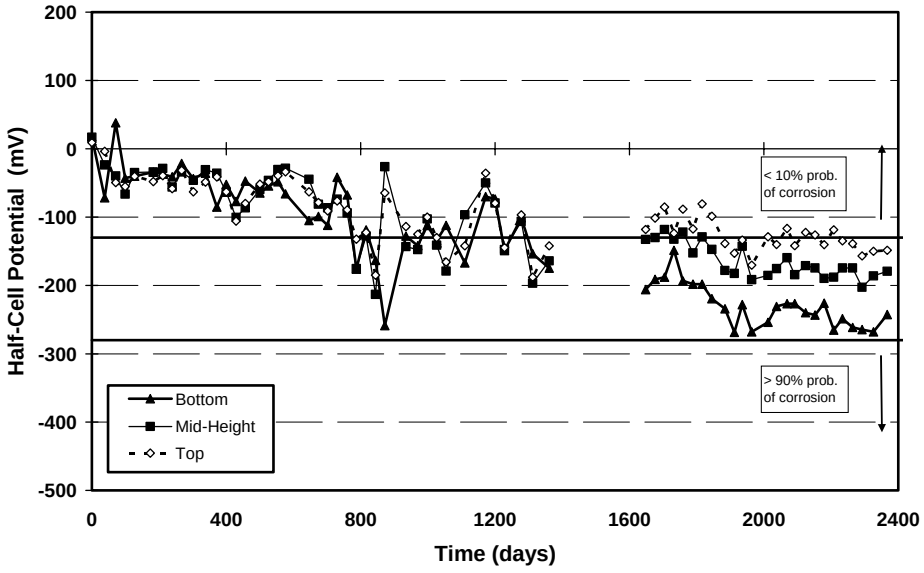

Figure A.11 Average Half-Cell Potential Readings for Column NJ-TC-N[1]

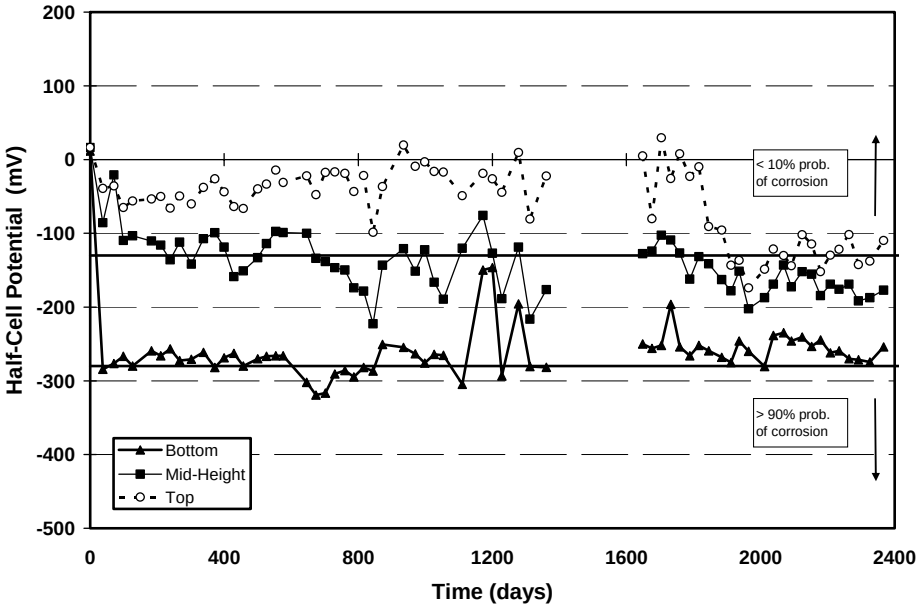

Figure A.12 Average Half-Cell Potential Readings for Column DJ-TC-N[1]

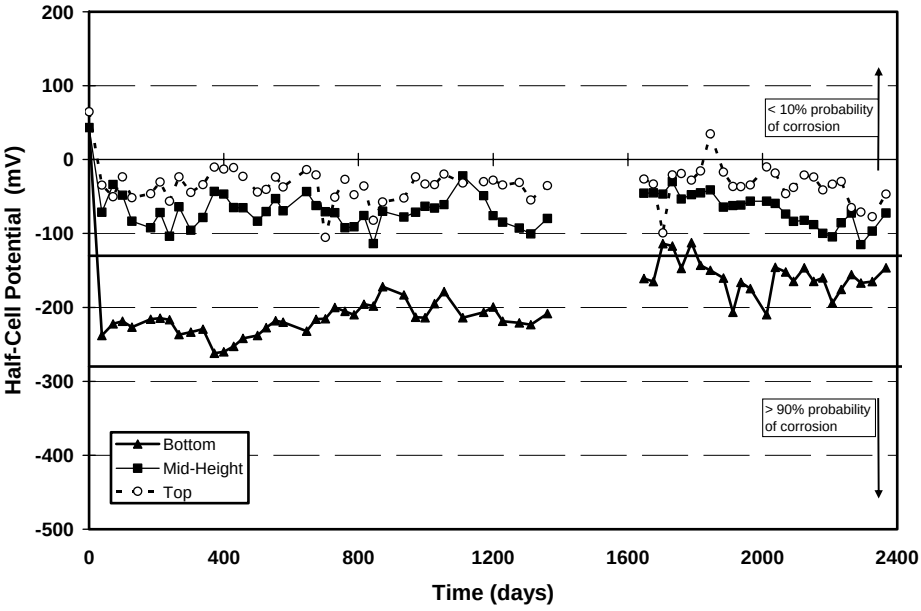

Figure A.13 Average Half-Cell Potential Readings for Column DJ-FA-S[1]

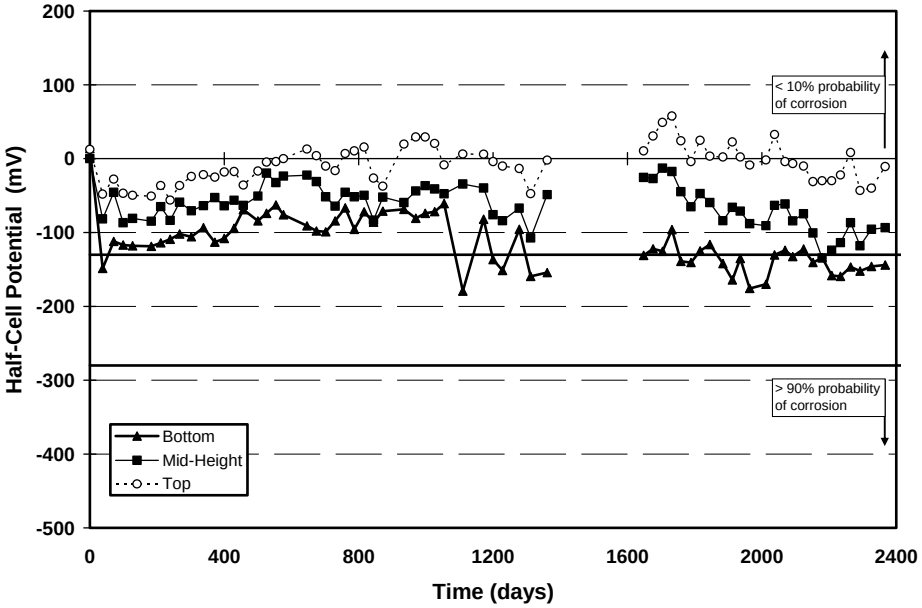

Figure A.14 Average Half-Cell Potential Readings for Column DJ-TC-S[1]

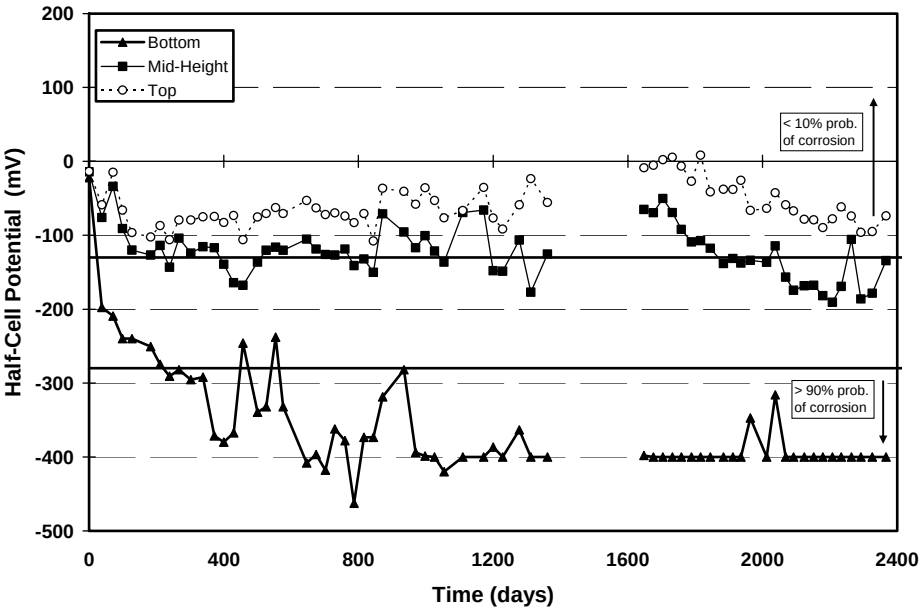

Figure A.15 Average Half-Cell Potential Readings for Column NJ-TC-S[1]

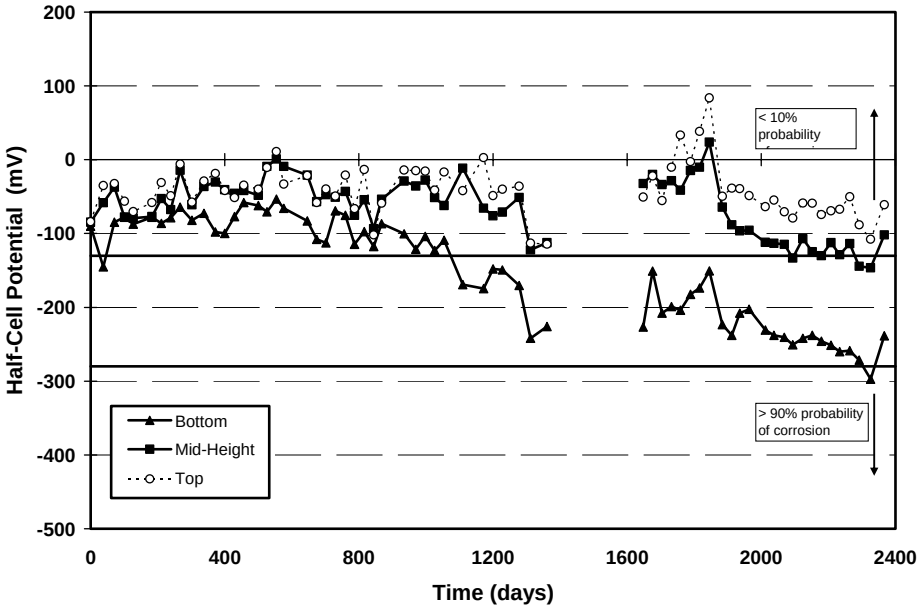

Figure A.16 Average Half-Cell Potential Readings for Column PT-TC-N-PD – Rebar[1]

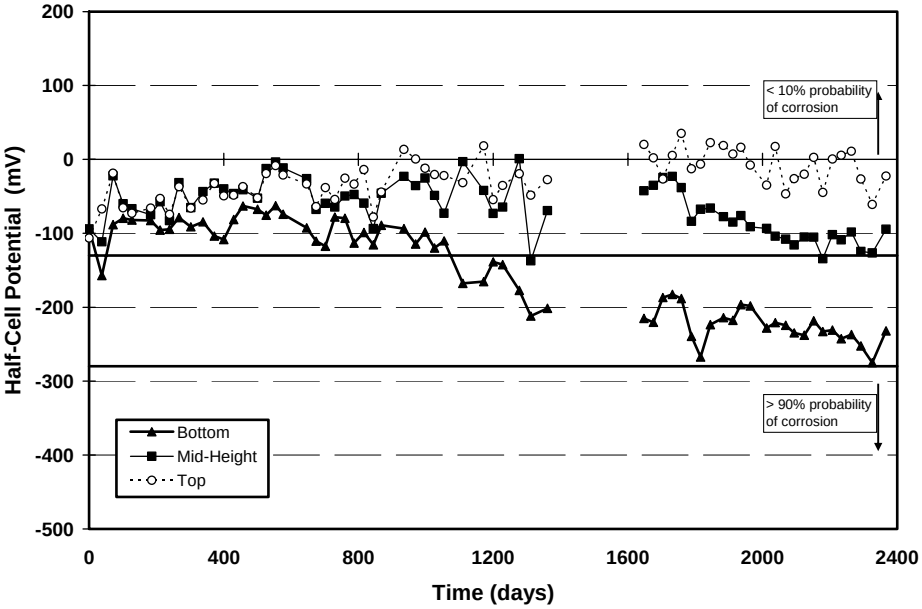

Figure A.17 Average Half-Cell Potential Readings for Column PT-TC-N-PD – PT Bars[1]

B. CONCRETE CHLORIDE CONTENT PLOTS

The following Acid-Soluble Chloride Content Plots complement those contained in Figure 5.36 through Figure 5.45. Chloride Threshold value is indicated in the figures at 0.033%. This value, intended only as a guide, is based on the widely accepted chloride threshold value of 0.2% of the weight of cement.[5.5]

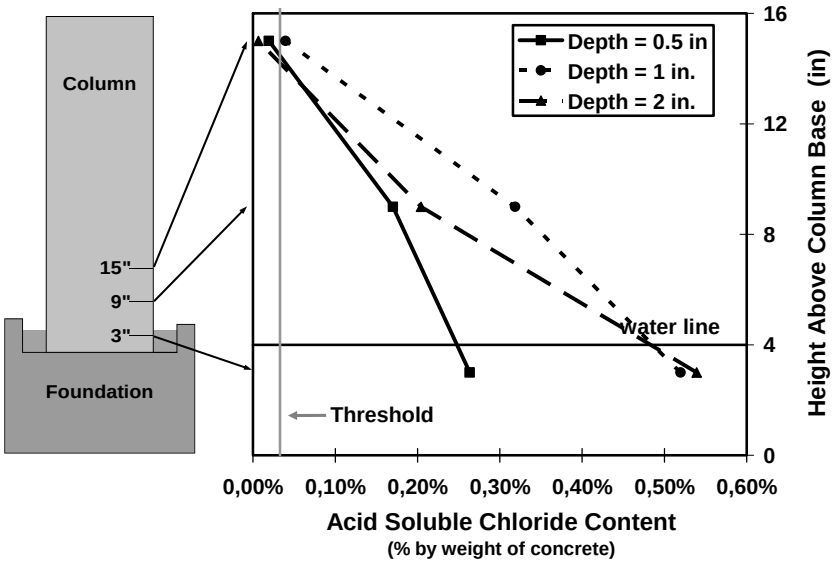

Figure B.1 Concrete Chloride Penetration for Column DJ-TC-N in Non-Dripper Side at End of Testing[1]

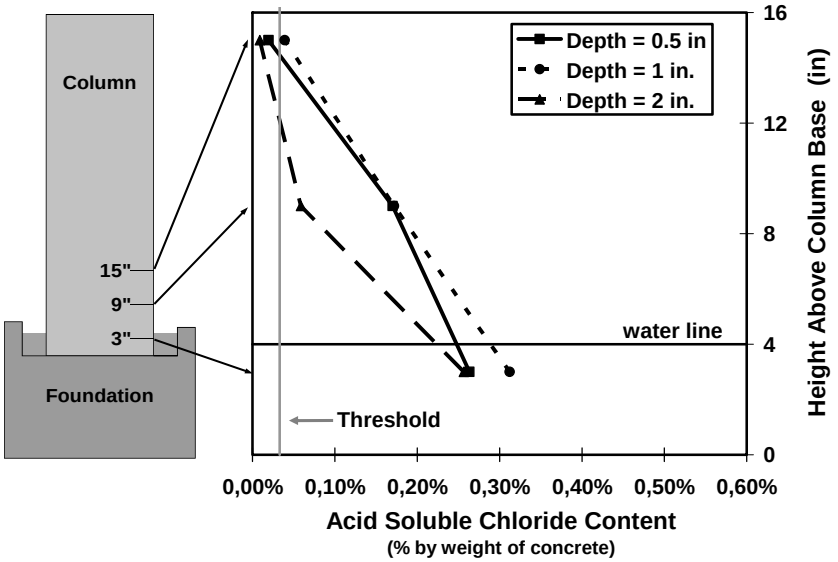

Figure B.2 Concrete Chloride Penetration for Column DJ-TC-N in Dripper Side at End of Testing[1]

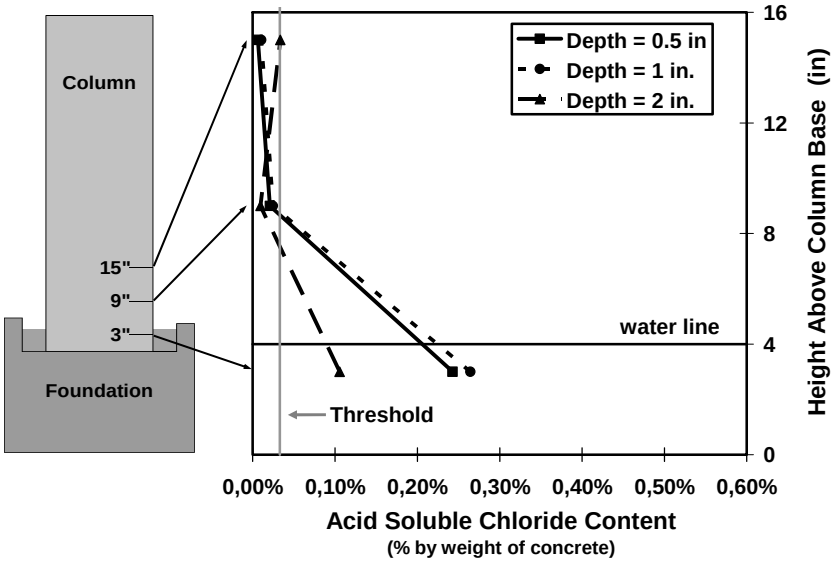

Figure B.3 Concrete Chloride Penetration for Column DJ-FA-S in Non-Dripper Side at End of Testing[1]

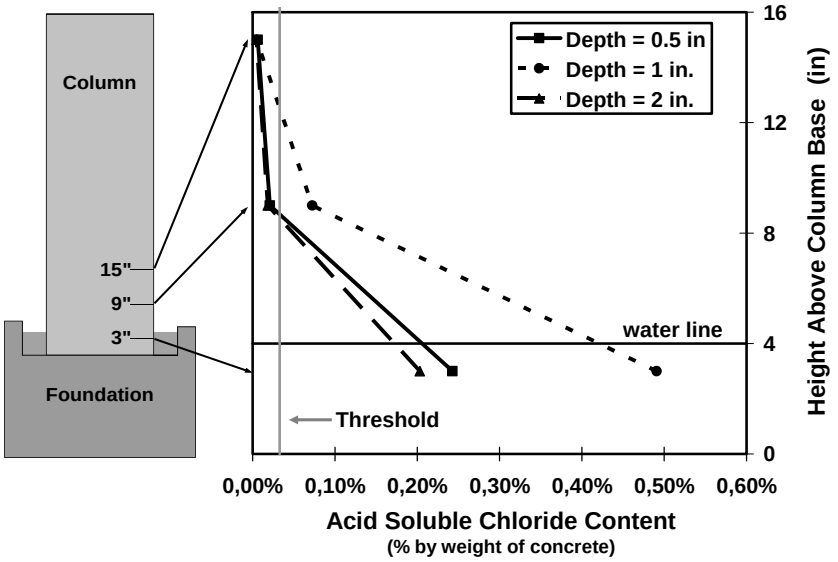

Figure B.4 Concrete Chloride Penetration for Column DJ-FA-S in Dripper Side at End of Testing[1]

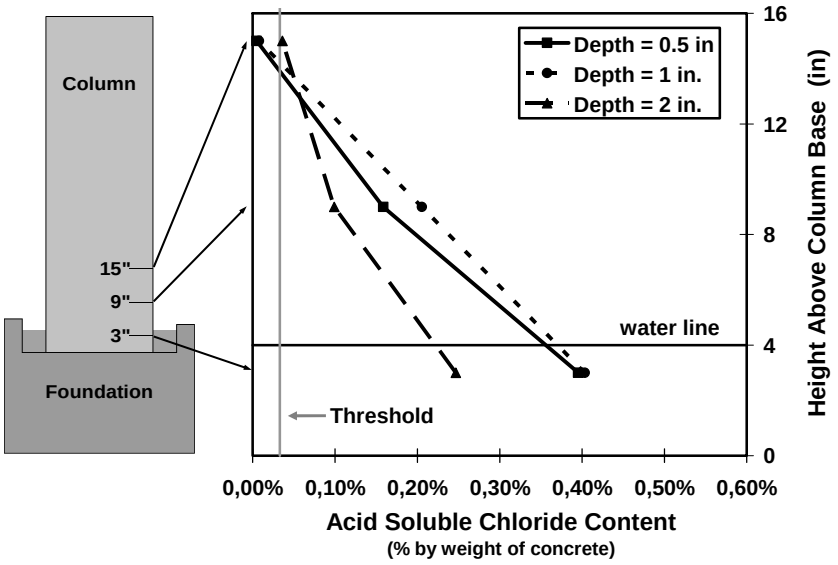

Figure B.5 Concrete Chloride Penetration for Column DJ-TC-S in Non-Dripper Side at End of Testing[1]

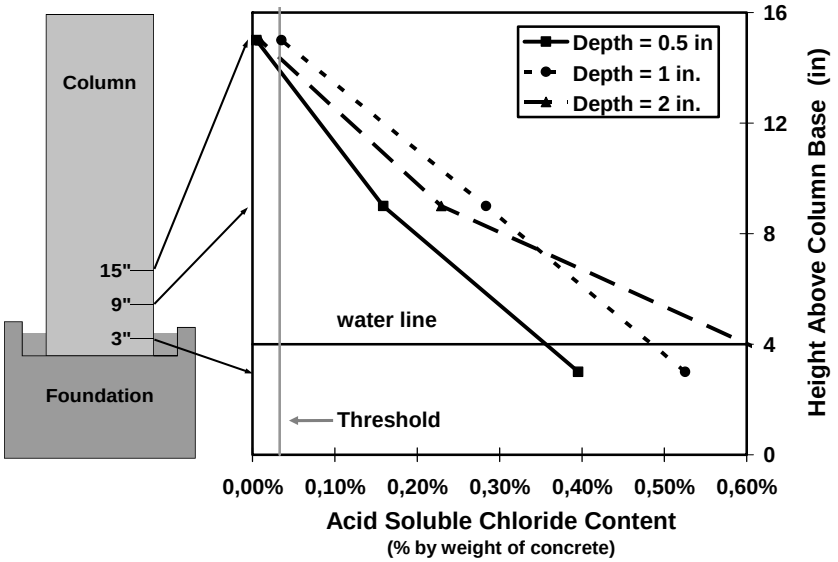

Figure B.6 Concrete Chloride Penetration for Column DJ-TC-S in Dripper Side at End of Testing[1]

.

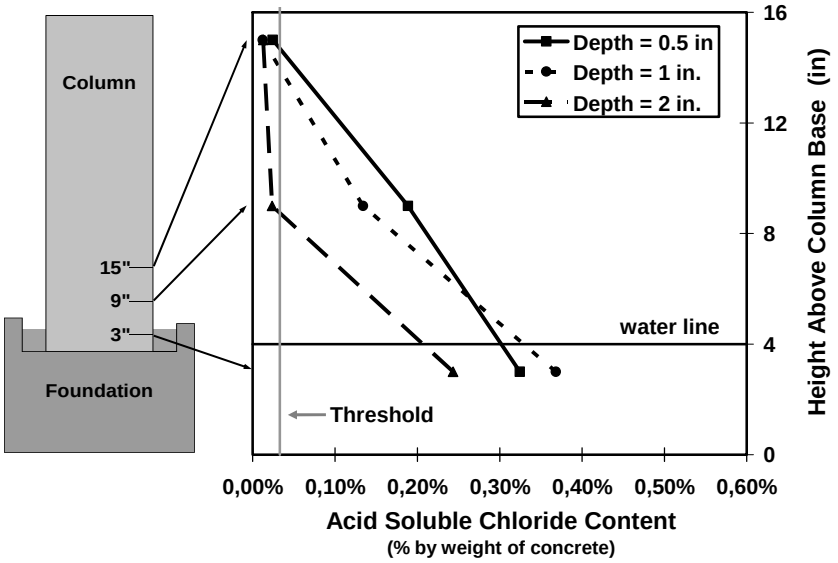

Figure B.7 Concrete Chloride Penetration for Column NJ-TC-S in Non-Dripper Side at End of Testing[1]

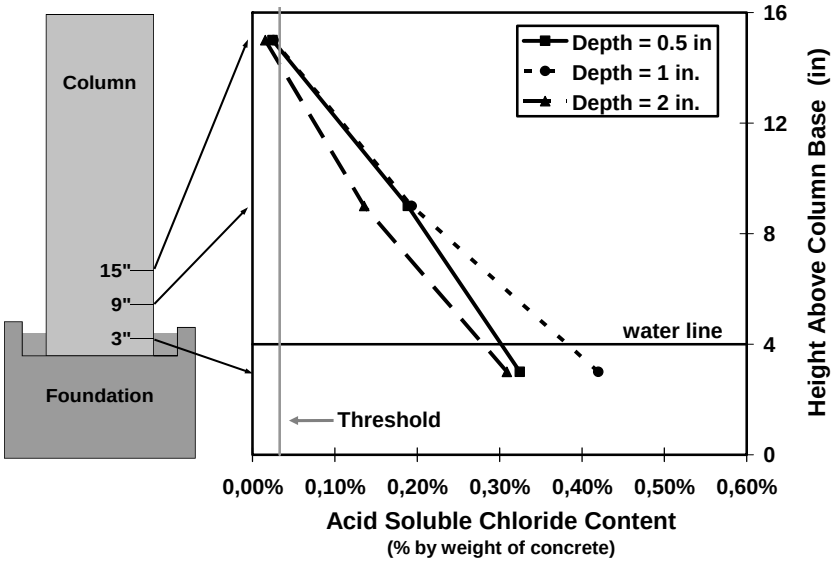

Figure B.8 Concrete Chloride Penetration for Column NJ-TC-S in Dripper Side at End of Testing[1]

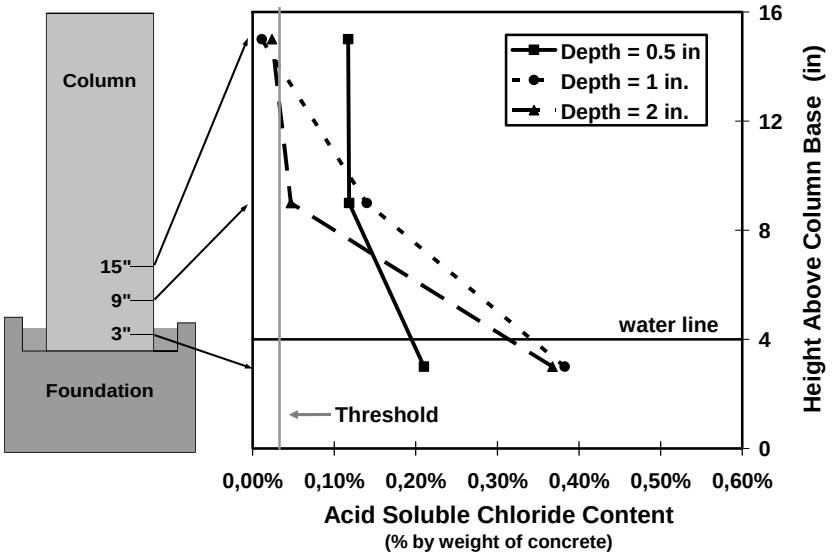

Figure B.9 Concrete Chloride Penetration for Column PT-TC-S-PD in Non-Dripper Side at End of Testing[1]

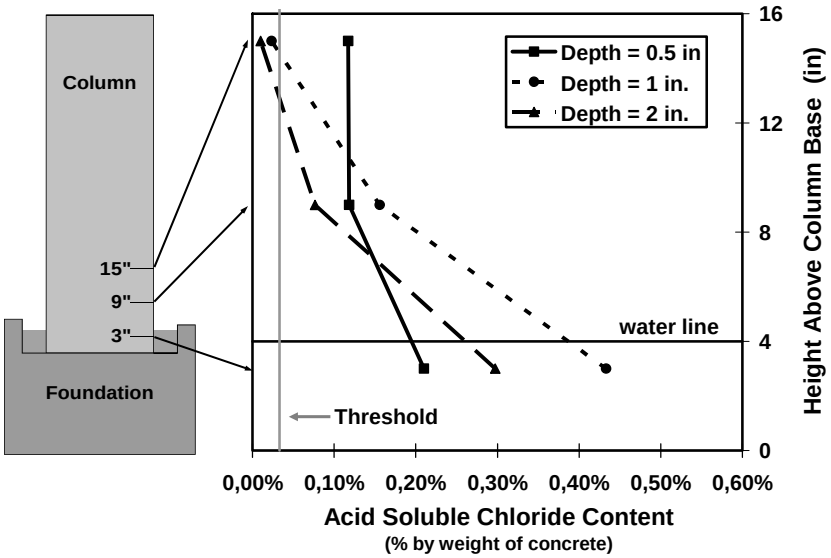

Figure B.10 Concrete Chloride Penetration for Column PT-TC-S-PD in Dripper Side at End of Testing[1]

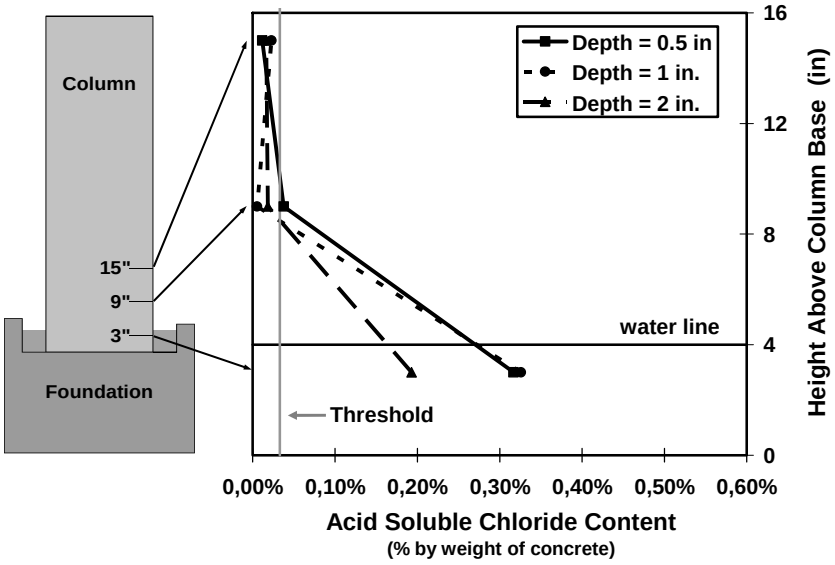

Figure B.11 Concrete Chloride Penetration for Column PT-FA-S-PD in Non-Dripper Side at End of Testing[1]

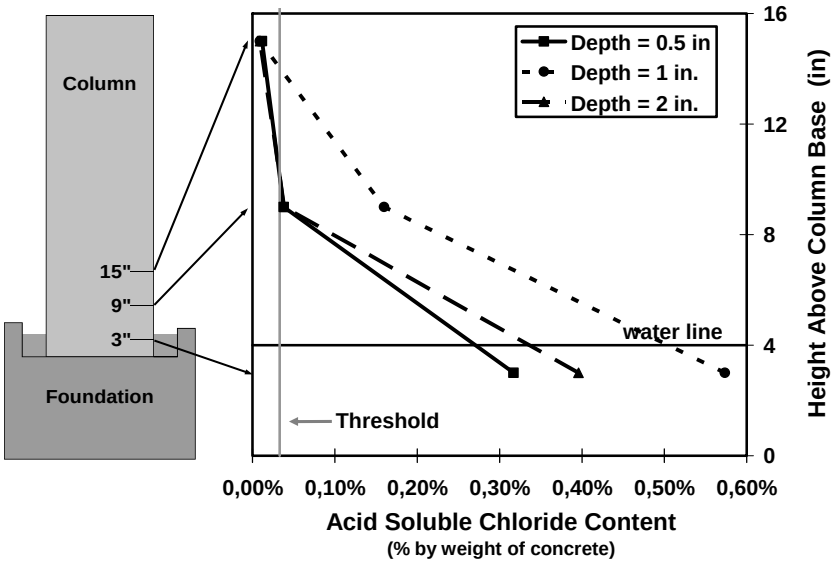

Figure B.12 Concrete Chloride Penetration for Column PT-FA-S-PD in Dripper Side at End of Testing[1]

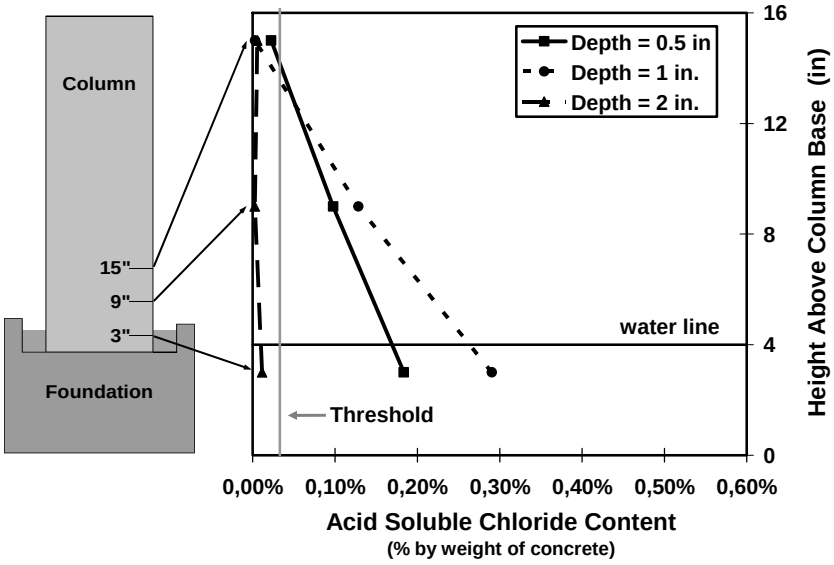

Figure B.13 Concrete Chloride Penetration for Column PT-TC-S-EB in Non-Dripper Side at End of Testing[1]

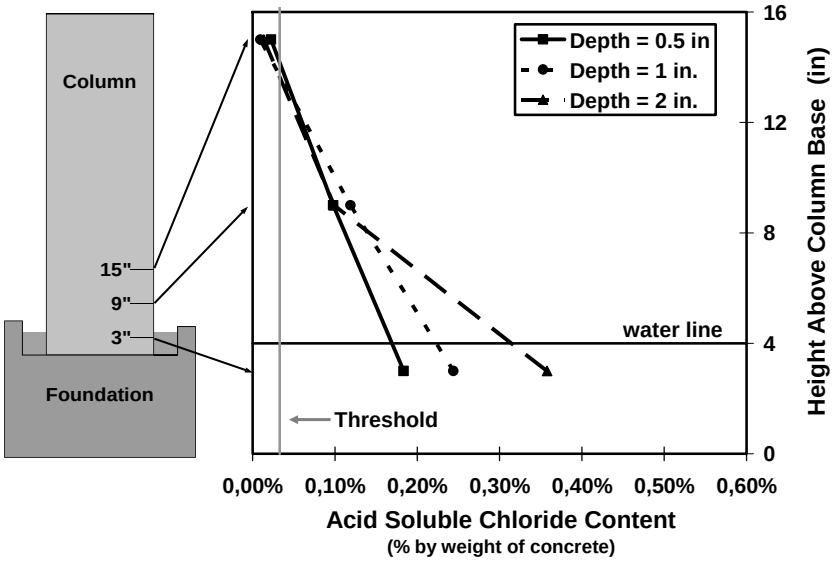

Figure B.14 Concrete Chloride Penetration for Column PT-TC-S-EB in Dripper Side at End of Testing[1]

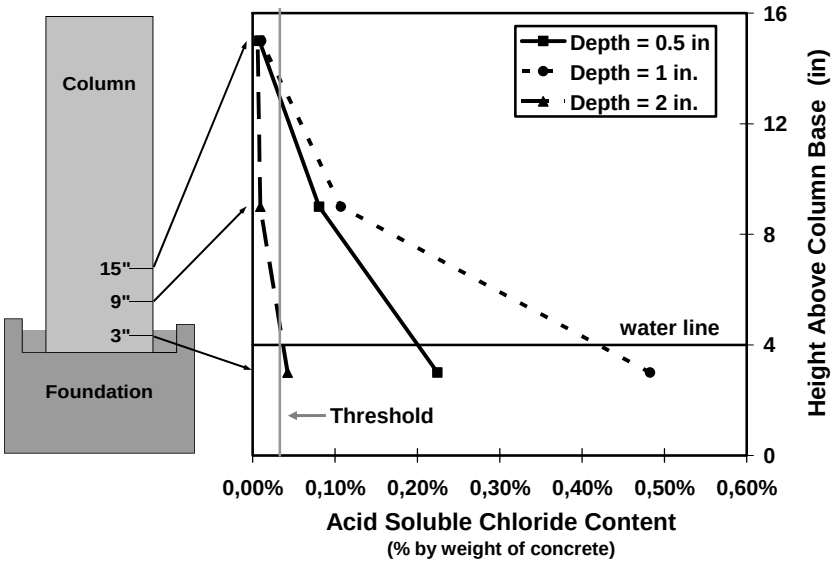

Figure B.15 Concrete Chloride Penetration for Column PT-TC-S-GB in Non-Dripper Side at End of Testing[1]

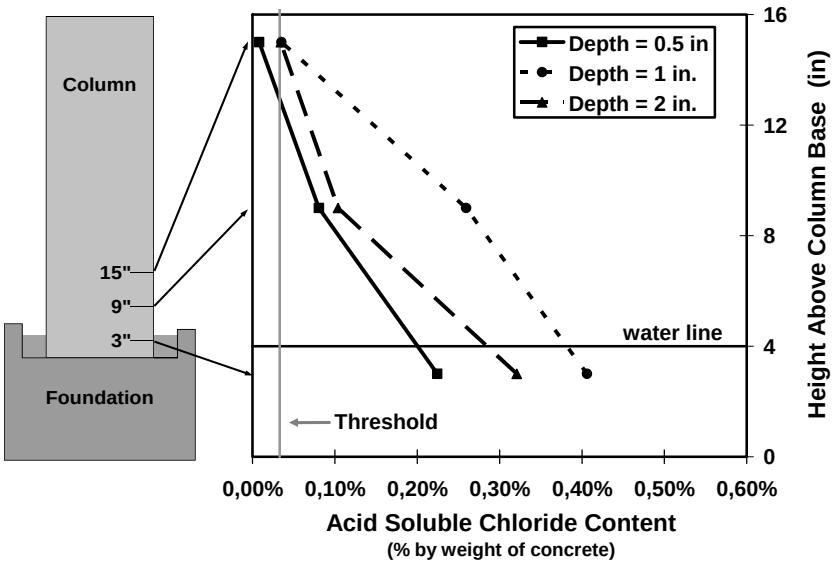

Figure B.16 Concrete Chloride Penetration for Column PT-TC-S-GB in Dripper Side at End of Testing[1]

References

1. **Salas, R.M.**, *"Accelerated Corrosion Testing, Evaluation and Durability Design of Bonded Post-Tensioned Concrete Tendons,"* Doctor of Philosophy Dissertation, The University of Texas at Austin, August 2003.

2. **West, J.S., (1999) "***Durability Design of Post-Tensioned Bridge Substructures,"* Doctor of Philosophy Dissertation, The University of Texas at Austin, May 1999.

3. **Schokker, A.J., (1999)** "*Improving Corrosion Resistance of Post-Tensioned Substructures Emphasizing High Performance Grouts,"* Doctor of Philosophy Dissertation, The University of Texas at Austin, May 1999.

4. **Koester, B.D. (1995)**, "*Evaluation of Cement Grouts for Strand Protection Using Accelerated Corrosion Tests*," Master of Science Thesis, the University of Texas at Austin, December 1995.

5. **Larosche, C.J. (1999),** "*Test Method for Evaluating Corrosion Mechanisms in Standard Bridge Columns*," Master of Science Thesis, The University of Texas at Austin, August 1999.

6. **Kotys, A.L. (2003)** "*Durability Examination of Bonded Tendons in Concrete Beams under Aggressive Corrosive Environment*," Unpublished Master of Science Thesis, The University of Texas at Austin. (under preparation), 2003.

7. **Vignos, R.P. (1994)**, "*Test Method for Evaluating the Corrosion Protection of Internal Tendons Across Segmental Bridge Joints*," Master of Science Thesis, The University of Texas at Austin, May 1994.

8. **Hamilton, H.R. (1995),** "*Investigation of Corrosion Protection Systems for Bridge Stay Cables*," Ph.D. Dissertation, The University of Texas at Austin, 1995.

9. **Schokker, A.J., Koester, B.D., Breen, J.E., Kreger, M.E. (1999)** "*Development of High Performance Grouts for Bonded Post-Tensioned Structures,"* Center for Transportation Research, Report 1405-2. The University of Texas at Austin, October 1999.

10. **Schokker, A.J., West, J.S., Breen, J.E., Kreger, M.E. (1999)** "*Interim Conclusions, Recommendations, and Design Guidelines for Durability of Post-Tensioned Bridge Substructures,"* Center for Transportation Research, Report 1405-5. The University of Texas at Austin, October 1999.

11. **West, J.S., Schokker, A.J., Larosche,C.J., Breen, J.E., Kreger, M.E. (1999)** "*Long-Term Post-Tensioned Beam and Column Exposure Test Specimens: Experimental Program,"* Center for Transportation Research, Report 1405-3. The University of Texas at Austin, October 1999.

12. **ASTM**, **(1991)** "*Standard Test Method for Half-Cell Potentials of Uncoated Reinforcing Steel in Concrete*," ASTM C876-91, American Society for Testing and Materials, Philadelphia, Pa., 1991.

13. **ACI Committee 222 (1996),** "*Corrosion of Metals in Concrete*," ACI 222 R-96, American Concrete Institute, Detroit, Michigan, 1996.

14. **West, J.S., Vignos, R.P., Breen, J.E., and Kreger, M.E. (1999),** "*Corrosion Protection for Bonded Internal Tendons in Precast Segmental Construction*," Research Report 1405-4, Center for Transportation Research, The University of Texas at Austin, Austin, Texas, October 1999.